Pharmacodynamics of therapeutic dose selenium compounds:

A determination study for dose/compound efficacy potential

A thesis

submitted in partial fulfilment

of the requirements for the degree

of

Master of Science (Research) in Cellular and Molecular Biology

at

The University of Waikato

by

Renëe Jo-Leigh Goodall

THE UNIVERSITY OF
WAIKATO
Te Whare Wānanga o Waikato

2025

Abstract

This research is a key part of a Phase 1(b) clinical trial that was designed to investigate a potential therapeutic dose of selenium (Se) in an oncology setting to aid in protection against toxicities caused by cancer therapies. The trial's primary objectives were to identify the most effective combination of Se dosage (1600 or 6400 µg/day) and compound using three forms of Se (Selenomethionine (SLM), methyl-selenocysteine (MSC), and Sodium selenite (SS). To achieve this, western blot methodologies were used to investigate the effect of the Se compounds on the protein expression. Three antibodies, HIF-1α, EGLN1 and EGLN3 were used to identify changes in the hypoxic pathway, CASPASE-8 was used for the apoptosis pathway and a singular GAPDH loading control was used to estimate regulation change. In addition, LORD-Q PCR was implemented to evaluate both the mitochondrial and nuclear DNA damage.

Nine patients who provided informed consent were recruited for the trial. The trial protocol involved seven visits in which blood and plasma samples, adverse events (AE) reporting, and other safety procedures were collected. Two baseline (at the pre-check visit and on day 1) samples were taken one to two weeks apart before dosing to assess intrapatient variability. Two samples for 1600 µg and 6400 µg and a singular post-trial sample over the course of the 12 week trial. Patients kept a diary to self-record any AEs experienced over the trial period. No AEs higher than grade 2 were reported during the trial, with the most common AE being gastrointestinal-related.

Western blot analysis showed minimal increase in expression for HIF-1α for four out of five patients with data, when compared to the baseline samples and showed an overall decreased protein expression when normalised against GAPDH. Except patient 29 who showed a distinct increase during the trial, peaking at 25 times the level of GAPDH. The

measurement of the apoptotic pathway using CASPASE-8 was used however, insufficient data was gained.

LORD-Q PCR data showed that damage sustained to mtDNA and ntDNA was not consistent between patients of a singular compound. Data from this trial demonstrate a potential protective effect on DNA damage at the nuclear and mitochondrial level at both 1600 μg/day and 6400 μg/day in all Se compounds. MSC and SS showed to be the least volatile compounds, indicating increased protective effects against DNA damage, which is supported by the western blots for hypoxia. SLM was volatile, showing higher mitochondrial damage and a slight upregulation in the minimal apoptosis data obtained.

The difference in in protective effects and pathway regulation was minimal; further investigation into the hypothesis that they are at the same level in the U-shaped tolerance that Se has in humans is advised. Future studies should further investigate the clinical significance and potential of Se as an adjuvant therapy alongside chemotherapy and radiotherapy in cancer patients.

Preface and Acknowledgements

This thesis was prepared as part of the requirements for the Master of Science (Research) in Molecular and Cellular Biology at The University of Waikato. The contents within, reflect the research and academic journey undertaken from March 2024 to September 2025. It highlights the skills, development and knowledge obtained throughout this time.

The work presented aims to explore the genotoxic potential of therapeutic doses of Selenium as a potential adjuvant with current therapies. In addition, it explores the molecular and cellular differences between different compounds and doses on cancer patients not currently undergoing chemo or radiotherapy.

I would like to acknowledge the unwavering help, guidance, and support of Dr. Linda Peters, my main supervisor. She was a wealth of understanding and assisted both with the work involved in this thesis and emotionally during the turbulent years leading up to it. I chose her as a supervisor because of her loyalty, compassion for students, and her enigmatic enthusiasm for research. She did not disappoint; in fact, she exceeded all expectations in relation to this project.

A personal and professional thank-you to Catherine Turnbull, my senior student supervisor, current PhD candidate, and friend. You have supported me throughout this journey, guided me, and shown me what it truly means to be a scientist. From learning how to label correctly and complete protocols to understanding when to give myself a break, you transformed me from an awkward lab chair into a functioning scientist. I will always be grateful for your unwavering love and support throughout this entire process.

To Craig Burns, my co-conspirator and fellow traveller on this project, you have undoubtedly shown me who I am as a scientist and person. You've been a rock, helping and supporting me every step of the way. From late-night texts about results, to picking up each other's slack, and sharing bacon and egg croissants, I wouldn't have achieved these milestones without doing it together.

To Dr. Michael Jameson, the trial co-ordinator, thank you sincerely for allowing me to be part of this incredible research. Your enthusiasm, zest for life, and optimism have made the whole process enjoyable. It was a pleasure working under you, learning your ways, and gaining insight from the professional and personal wisdom you've shared. To all the participants of the trial, this research and body of work would not exist with your co-operation and willingness. You are the backbone of science in general and providing this service in the pursuit of knowledge is admiring.

To Hunter, who has been with me through finishing my undergraduate degree, entering into Post-graduate studies and now finishing my masters; thank-you for your support and listening to my rants and rambles. Lastly, to my friends and family, this path has not been easy. Without late-night phone calls, coffee breaks, and sneaking into your homes for a moment of peace and quiet, none of this would have been possible.

Table of Contents

List of Figures

List of Tables

List of Abbreviations

ATCC	American Type Culture Collection
B2M	Beta-2-microglobulin
Bis-Tris	Bis-Tris methane (biochemical buffering agent)
BSA	Bovine Serum Albumin
BSC	basal cell carcinoma
CASP8	Cysteine-aspartic acid protease 8 (protein)
CI	Confidence interval
Cp_L	Crossover threshold Long primers (fluorescence)
Cps	Crossover threshold Short primers (fluorescence)
CT#	Catalogue number
DIO1	Iodothyronine Deiodinase type 1
DIO2	Iodothyronine Deiodinase type 2
DIO3	Iodothyronine Deiodinase type 3
DIOX	Iodothyronine Deiodinases
DISC	Death-induced signalling complex
DNA	Deoxyribose Nucleic Acid
EGLN1	Egl-9 Family Hypoxia Inducible Factor 1 (formerly PHD2)
EGLN3	Egl-9 Family Hypoxia Inducible Factor 3 (formerly PHD3)
EL	Efficiency of amplification for Long primer
EPAS	Endothelial PAS Domain Protein 1 formerly HIF-2α
ER	Endoplasmic reticulum
ES	Efficiency of amplification of short primer

GAPDH	Glyceraldehyde 3-phosphate dehydrogenase
GPX	Glutathione peroxidases
GPX1	Glutathione peroxidase 1
GPX2	Glutathione peroxidase 2
GPX4	Glutathione peroxidase 4
GPX6	Glutathione peroxidase 6
HDEC	Health and Disability Ethics Committee
HIF	Hypoxia-inducible factor
HIF-1α	Hypoxia-inducible factor 1 alpha
HIF-3α	Hypoxia-inducible factor 2 alpha
HR	Hazard ratio
HRP	Horseradish Peroxidase (Secondary antibody)
LORD-Q	Long run qPCR technique for DNA damage quantification
MSC	Methyl-selenocysteine
NaCl	Sodium chloride
NMSC	Nonmelanoma skin cancer
NPC	Nutritional Prevention of Cancer
PBMC	Peripheral blood mononuclear cell
PBS	Phosphate-buffered saline
PC2	Physical containment facility level II
PCR	Polymerase chain reaction
PD	Pharmacodynamics
PHDs	Prolyl hydroxylase domain enzymes
PVDF	Polyvinylidene difluoride
ROS	Reactive oxygen species

RT	Room Temperature
RT-qPCR	Real time quantitative PCR
SCC	Squamous cell carcinoma
SDS-PAGE	Sodium dodecyl sulfate–polyacrylamide gel electrophoresis
SELECT	Selenium & Vitamin E Cancer Prevention Trial
SELENOP	Selenoprotein P
SLM	Selenomethionine
SS	Sodium selenite
TAE	Tris-acetate-EDTA (Buffer)
TBS	Tris-buffered saline
TBST	Tris-buffered saline with tween
TXN	Thioredoxin
TXNRD 1/2/3	Thioredoxin-glutathione reductase 1/2/3
UoW	University of Waikato
UP-H_2O	Ultra-pure H_2O
UV	Ultraviolet
UV-C	Ultraviolet Type C
WB	Western Blotting
WHO	World Health Organisation

1 Literature Review

1.1 Introduction

This research project was conducted alongside the Phase 1b dose-escalation trial of selenium (Se) compounds in New Zealand cancer patients (registry number ACTRN12613000118707). The primary aim of this Phase 1b trial was to identify the safest and most effective Se compound and dose for future clinical trials by assessing the safety, pharmacodynamics, and pharmacokinetic properties of three Se compounds; methyl-selenocysteine (MSC), selenomethionine (SLM), and sodium selenite (SS), and two doses; 1600 µg/day and 6400 µg/day The focus of this thesis is on safety evaluations through adverse events (AEs), reported by the participants, and pharmacodynamics (PD), assessed using western blots to detect changes in regulation of protein pathways and long-run real-time (LORD-Q PCR) examining DNA damage. All three Se compounds used in the trial are commonly found in the diet or in Se/Se-containing supplements.

Se was chosen as an investigative subject because it is an essential element for humans, with a broad and diverse role in the body. Se-containing proteins play important roles such as acting as antioxidants, regulating low oxygen levels (hypoxia), and facilitating programmed cell death (apoptosis). Se has been shown to be vital for human health, as a deficiency can cause harmful effects like Keshan's disease, although a surplus of Se can also cause toxicity. Research into Se, its mechanisms, exposure levels, and routes has identified it as a potential agent for cancer prevention. Cancer is one of the leading causes of death worldwide and is characterised by tumours, which result from unregulated cell growth caused by downregulation of the apoptosis pathway. Tumours can cause and be caused by inflammation, which antioxidants help prevent, and most tumours are associated with hypoxic environments that support tumour proliferation. These cancer pathways are directly

linked with Se pathways, and potential manipulation of these pathways could aid in cancer prevention.

Recent explorative studies assessing the relationship between Se and cancer have shown changes to these pathways can benefit individuals who already have cancer and undergoing cancer treatments. Cancer treatments such as chemotherapy and/or radiation have seen a benefit with Se supplementation enhancing the Se pathways reducing normal tissue toxicity, which could prevent further tumours and enhance the effects of treatment. This Phase 1b trial investigates the potential dosage/compound combination that could be used as an adjuvant to already established therapies.

1.2 Research Methodology

The review of current literature was conducted using electronic databases via the University of Waikato (UoW) online library from 14th February 2024 until 29th June 2025. Systematic reviews, independent articles, and other materials were searched with the main focal words: selenium, CLL, prostate cancer, breast cancer, EGLN1, EGLN3, PHD2, PHD3, HIF-1α, CASPASE8, cancer, antioxidant, hypoxia, apoptosis, trial, review (or any combination of the aforementioned) using the UoW library. Higher consideration and weight were given to those with clinical or laboratory trials on Se and its compounds to give the most value and credibility as a comparison to this study. Articles not considered for this review were limited to those written in languages other than English and those specific to plants not involved in human intake and absorption, inorganic species involved in physical sciences such as geology.

1.3 Selenium and Cancer

1.3.1 Hallmarks of Cancer

In 2000, Douglas Hanahan and Robert A. Weinberg published a paper aimed to simplify the basics of cancer to give researchers and practitioners a building block for tackling this huge problem. The "Hallmarks of Cancer" identified six crucial alterations to basic cell physiology that are required for a cell to form tumours as well as the singular enabling characteristic of genome instability (Figure 1). These hallmarks include resisting cell death, sustaining proliferative signalling, evading growth suppressors, enabling replicative immortality, activating invasion and metastasis, and inducing or accessing vasculature.(Hanahan & Weinberg, 2000).

Ten years later, in 2011, a review paper was published by the duo which encompassed the previously published data and incorporated the current research, expanding the original hallmarks to eight to include deregulating cellular metabolism and avoiding immune destruction. The paper also formally identified two enabling characteristics, tumour-promoting inflammation and genome instability and mutation which are required for the cell hallmarks identified, all four of which have been universally accepted (Hanahan & Weinberg, 2011).

The most recent review in 2022 proposed an expansion to ten hallmarks and four characteristics to again bring the article in line with the new mass of oncology research developed. This paper included unlocking phenotypic plasticity and non-mutational epigenetic programming as hallmarks with polymorphic microbes and senescent cells being identified as enabling characteristics (Hanahan, 2022).

Figure 1: *The hallmarks of cancer. Figure adapted from Hallmarks of Cancer: New Dimensions (reproduced with permission available via license: Creative Commons Attribution 4.0 International). The 14 cancer hallmarks; original six represented in the green boxes, the four added in the 2011 review in the red boxes and the blue boxes showing the four new additions from the 2022 review.*

1.3.2 Common Cancers in New Zealand

The Global Cancer Observatory (GCO) was published by the International Agency for Research on Cancer (IARC), an agency of the World Health Organisation (WHO). The most recent publication from 2022 shows that the most common cancers in New Zealand were breast, colorectal, prostate, and lung cancer (Sung et al., 2021). Prostate cancer was the most prevalent among males (18.3%) and the third leading cause of overall mortality. Breast cancer was the most prevalent among females (21.7%) and the fourth in overall mortality. Together, prostate and breast cancer accounted for 9.9% and 10% of new cases, respectively. Colorectal cancer was the second most common in both sexes and the most frequent overall, with 10.7% of all new cases, and it also ranked second in overall mortality. Lung cancer was

the leading cause of death overall but was the third most common cancer for men and the fourth for women, and it ranked fourth overall (Sung et al., 2021).

1.3.3 Cancer and Selenium Deficiency

Current literature shows many observational studies and controlled trials that highlight the influence of Se on human diseases such as cancer. Cai et al., published a meta-analysis on the current literature in 2018 encompassing 69 studies that showed high Se exposure and high bodily Se (toenail, serum, and blood samples) were associated with lower overall cancer risk (Cai et al., 2016). Jenkins et., al from 2020 published another meta-analysis of 43 studies for Se supplementation which saw a decreased risk for all-cause mortality (Jenkins et al., 2020). A meta-meta-analysis was published in 2023 by Arayici et al., which pooled the data from 20 meta-analyses on the effects of Se exposure and cancer incidence which also showed an inverse relationship (Arayici et al., 2023).

The main mechanisms for these results discussed in literature are based on the mechanism of actions seen in selenoproteins and other pathways with selenocompounds. Selenoproteins are theorised to counteract cancer cell growth as they increase DNA stability, cell proliferation, regulate oxidative stress in cells and are a part of cell death cycles in both healthy and malignant cells. Selenoproteins and other selenocompound levels in the body are directly related to the Se levels as there is no free storage in the body. As such, it is theorised that the lower Se in the body, the less Se enzymes there are in the body which maintain homeostasis, whereas cancer is a result of disruption and dysregulation in the body (Vinceti et al., 2018).

1.3.4 Intervention Trials using Selenium for Cancer Prevention

Dietary factors and nutrition are active areas of research in carcinogenesis and the prevention of cancer; specifically, the optimisation of nutritional elements and dietary concentrations. Se is one of the nutritional factors of great interest due to its antioxidant properties as well as its role as an essential nutrient. There have been two notable large-scale studies in the United States of America: The Nutritional Prevention of Cancer (NPC) Trial and the Selenium & Vitamin E Cancer Prevention Trial (SELECT) that examined the effect of selenium supplementation for cancer prevention in individuals at high risk for prostate cancer.

The NPC trial was a double-blind, randomised trial conducted from 1983 to 1996, investigating the secondary chemo preventive effects of selenium in patients diagnosed with nonmelanoma skin cancer (NMSC) within the preceding year (Clark et al., 1996). In total, 1312 patients received 200 μg/day of selenised yeast, based on the rationale that this population faced elevated recurrence risks. The results for the entire blinded period showed that Se supplementation was not associated with a risk of basal cell carcinoma (BSC). BSC has a hazard ratio (HR) of 1.09 with a 95% confidence interval (CI) of 0.94 – 1.26. Conversely, Se supplementation showed a statistically significant risk increase with NMSC where HR = 1.17 and CI = 1.02 – 1.34 and squamous cell carcinoma (SCC) risk increase where HR = 1.25 and CI = 1.03 – 1.51; making the total increased risk of 20 – 40% (Duffield-Lillico et al., 2003) The NPC trial also showed Se supplementation to reduce total cancer incidence by 25% and overall mortality by 40%, with notable declines in prostate (50%), lung (30%), and colorectal cancer (54%) incidence, though the latter lacked statistical significance. Secondary analyses revealed that the beneficial effects were more pronounced in individuals with lower baseline Se plasma levels, whereas those with higher levels faced greater NMSC recurrence risks (Duffield-Lillico et al., 2002).

A second arm of the trial (1989 – 1996) assessed a 400 µg/day dose in 423 participants. Despite the smaller sample size, baseline characteristics matched the 200 µg/day group, enabling valid comparisons. At this higher dose, NMSC risk did not increase relative to the lower dose, nor did SCC or basal cell carcinoma (BCC) risks significantly differ from the other arm. Total cancer incidence trended lower but remained statistically nonsignificant, attributed to limited changes in risk. Notably, Se plasma levels stabilised at ~250 ng/mL (standard deviation = 24.3) after one year in the 400 µg/day group, compared to 115 – 200 ng/mL in the 200 µg/day group, with standard deviations of 20.9 and 23.2, respectively. These results aid in confirming the dose-dependent bioavailability of Se in the body increases with higher supplementation amounts (Reid, Duffield-Lillico, et al., 2008).

SELECT was a Phase 3 clinical prevention trial involving ~35,000 men from the United States of America, Canada, and Puerto Rico (Lippman et al., 2009). The study ran from 2001 to 2012 and was funded by the National Cancer Institute (NCI) with implementation and design by the Southwest Oncology Group (SWOG). The Se arm of the trial involved dosing healthy men with an elevated risk of prostate cancer, with a 200 µg daily dose of SLM which was chosen over sodium selenite (SS) used in the NPC trial due to problems in acquisition. It was hypothesised that with SS and SLM being the most common types found in diets that there would be minimal difference between the two for trial outcome comparison. It was also hypothesised that SLM may led to better outcomes as SS increases DNA single-stranded breaks and is linked to cell growth pathway (Klein et al., 2000).

The SELECT trial, like the NPC trial, showed no statistically significant reduction in incidence of prostate cancer for the treatment arms compared to the control arm. The authors note that both the dosage and type of selenium used were two possible major contributing factors in the failure to show cancer prevention. The dosage level was based on the same rationale as the NPC study, citing that Se administered at levels higher than the required dose for nutrition has shown carcinogenic repression in animal models but has been found

inconsistent in vivo; of which this study showed a null effect. This was compounded by the participants starting with a relatively optimal selenium status. In contrast, several studies (including European Prospective Investigation into Cancer and Nutrition (EPIC), and the Swedish Mammography Cohort) indicate that low Se status is associated with increased risk of cancer, and Se supplementation could be effective in persons with low Se levels and/or intake (Harris et al., 2012; Hughes, et al., 2015). The longevity of the study was able to definitively characterise the higher Se levels from baseline reflected from long-term Se supplementation (E.-H. Lee et al., 2011).

Both the NPC and SELECT trials represent some of the largest datasets accumulated on intervention trials with selenium and cancer incidence. An array of hypotheses have been generated from these trials which have been partially explored in follow-up studies. One of the prevailing hypotheses has been that the NPC and SELECT trial suggests that Se has a therapeutic effect on cancer pathways rather than preventative (Vinceti et al., 2018).

1.3.5 Cancer Therapy in Conjunction with Selenium

A 2024 systematic review by Krannich et al., investigated high-dose Se supplementation as a complementary therapy for cancer treatments. The review investigated 12 studies (2006 – 2023) across a range of cancer types, including breast, prostate, cervical, non-Hodgkins lymphoma and leukaemia. Findings indicated that patients with Se deficiency may experience therapeutic effects and/or reduction in toxicity compared to cancer treatment on its own (Krannich et al., 2024)

This review highlights the emerging evidence on high-dose Se supplementation's potential role in anti-cancer efficacy, toxicity reduction from treatment and as a complement to conventional cancer therapies. Some of these studies suggest that this high level of supplementation has the potential in reducing AE of chemotherapy and radiotherapy without compromising its effectiveness. Selenoproteins have impactful properties that reduce toxicity

and improve efficacy by four main mechanisms; 1) enhanced DNA repair in normal cells but not malignant cells, 2) promotion of malignant cell death via endoplasmic reticulum (ER) stress response, 3) inhibition of hypoxia-induced angiogenesis and 4) reversing cellular resistance to some cytotoxic drugs (Fernandes & Gandin, 2015).

1.4 General Overview of Selenium

1.4.1 Selenium and Human Health

Selenium was first detected in 1817 by Jöns Jakob Berzelius as a byproduct of sulphuric acid manufacturing in Switzerland ("The Discovery of Selenium," 2023). Se was given the atomic number 34 and noted to have similar characteristics to Sulphur, leading it to be labelled as a toxic element (Shamberger, 1984). The toxic element label for Se was changed in 1957 when Klaus Schwarz recognised Se as an essential part of the Factor 3 pathway in mice, which is crucial for the prevention of hepatic necrosis. This paved the way for further research into Se as an essential trace element and its potential role in disease prevention and human health (Brigelius-Flohé, 2018; Schwarz & Foltz, 1999).

The following 70 years of research proved that Se is necessary for important biological functions in humans, including key antioxidant roles, and aiding in immune system regulation, muscle function, fertility and reproduction, thyroid function, and brain function (Rayman, 2012). This further solidifies Se as an essential mineral for humans within the literature and highlights the biological pathways that humans have developed to maintain optimal Se levels. The element selenium has received considerable attention as a potential cancer preventive agent, at least in populations with low intake (*Dietary Reference Intakes for Vitamin C, Vitamin E, Selenium, and Carotenoids*, 2000). There is considerable variability in Se intake, exposure, forms of Se, levels in the body, and the functions and

pathways within the body, which can be attributed to geographic differences, cultural factors, age, and bodily responses.

1.4.2 Selenium Intake

The WHO recommends twenty-six micrograms of Se per day for women and thirty-four micrograms per day for men. However, this recommendation varies depending on the average selenium concentration found in different populations. Studies report total body Se values ranging from 3 mg in New Zealanders to 14 mg in Americans. New Zealand has some of the lowest selenium levels in the world, reflected in the NZ Nutrition Foundation's recommendation of 70 μg/day for men and 60 μg/day for women — almost double the WHO recommendations. (*Vitamin and Mineral Requirements in Human Nutrition*, 2005)

The main source of Se in the general population comes from food intake. The most common and highest sources of organic selenium are grains, nuts, cereals, meat, and fish. Other exposure routes include air, drinking water, and dietary supplements. However, Se levels in soil and consequently in food also change depending on the geographical area of production. Dietary selenium is absorbed in the gastrointestinal tract before being transported to the liver, where SELENOP is synthesised to regulate systemic selenium distribution. However, the absorption of selenium varies with each selenocompound. Selenomethionine is taken up via the gut and is not saturable, leading to high concentrations of total Se. Selenocysteine is taken up from intestinal transporters and selenite is absorbed directly from the gut but can be saturable (Schomburg, 2022a)

1.4.3 Safe Exposure Amounts

Selenium lacks universally defined thresholds but has a narrow safe exposure range that follows a U-shaped curve, with AE occurring when Se intake or levels are too low or too high (Figure 2). The amount of Se in the human body averages 3 – 20 mg, with skeletal muscle holding ~50% of total content. The most common indicator of Se status is its concentration in serum, typically between 60 – 120 µg/L. However, the optimal concentration and daily intake is heavily reliant on geographical and cultural factors. Se reserves in the body increase until reaching peak levels in adulthood and then gradually decline after the age of 60.

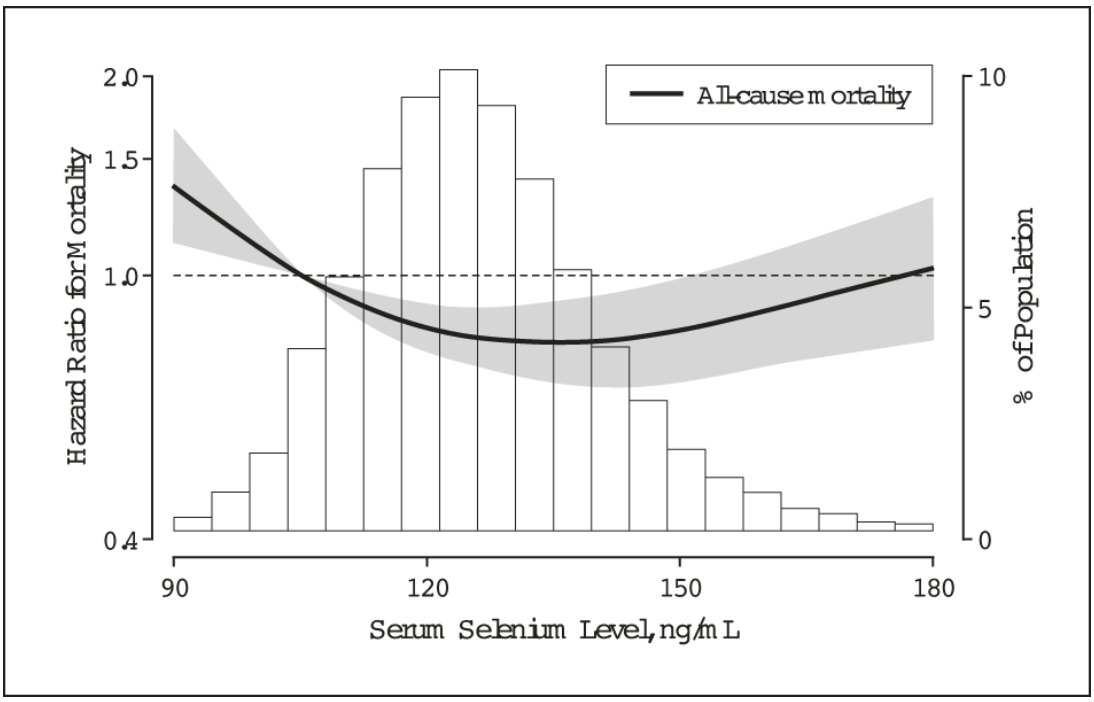

Figure 2*: Serum selenium levels and all-cause, cancer, and cardiovascular mortality among US adults. Bleys, J., Navas-Acien, A., & Guallar, E. (2008). Archives of internal medicine, 168(4), 404–410. https://doi.org/10.1001/archinternmed.2007.74*

Se deficiency in humans is considered with serum concentrations below 85 µg/L (Zwolak & Zaporowska, 2012) and linked to several severe health outcomes. Cai et al., published a comprehensive meta-regression analysis using 114 independent estimates from 69 studies worldwide, that linked Se deficiency to an increased risk in many cancers including breast, prostate, gastric, colorectal and lung (Cai et al., 2016).

Reproductive dysfunction occurs in men and women with low levels of Se, such as higher rates of spontaneous abortion (Abdulah et al., 2013). In men, a selenoprotein called Glutathione Peroxidase 4 (GPX4) is uniquely expressed in the testes, playing roles in antioxidant activity and structural support to mature sperm. Low Se concentrations affect the functionality of this enzyme and are linked to fertility issues, along with other selenoproteins including Thioredoxin-Glutathione Reductase (TXNRD), Selenoprotein P (SELENOP), and Selenoprotein V (SELENOV) (Qazi et al., 2019).

Regions with naturally low selenium bioavailability (e.g., central Poland, plasma levels average 50-55 µg/L) demonstrate heightened vulnerability to chronic Se deficiency-related conditions. The most extreme manifestation is Keshan disease, a cardiomyopathy endemic to selenium-deficient areas in China (Lei et al., 2011).

High doses of Se, whether acute or chronic, can cause significant toxicity in humans, leading to both non-fatal and fatal symptoms. Symptoms of acute Se toxicity include abdominal nausea, vomiting, pain, cardiac issues, and the characteristic “garlic breath”. Acute Se toxicity is linked to high oral intake, with doses of 1 – 100 Se mg/kg of body weight, which can result in fatalities. Blood or plasma levels of 300 – 30,000 µg/L are associated with mortality; however, there have been reported cases with similar levels that did not lead to death (Hadrup & Ravn-Haren, 2020).

Chronic Se poisoning symptoms include hair loss, discoloured and brittle nails, pains, weakness, gastrointestinal issues, and the characteristic garlic breath. Chronic toxicity levels have previously been linked to intakes of around 5 mg/day, with the daily upper tolerable

intake levels (UL) set at 300 µg/kg and 400 µg/kg of body weight (*Dietary Reference Intakes for Vitamin C, Vitamin E, Selenium, and Carotenoids*, 2000; *Essential-Trace-Elements-in-Human-Health-a-Physician-s-View_124_fr_0*, n.d.; *Vitamin and Mineral Requirements in Human Nutrition*, 2005). The most recent findings from the European Food Safety Authority, based on reviews of trials and scientific literature, set the adult daily UL at 255 µg from all Se sources. Although these findings are based on worldwide data, their recommendation is aimed at the general European population, and only regular users of supplements or those consuming large amounts of Brazil nuts are likely to exceed this dose (Turck et al., 2023). Therefore, maintaining selenium levels within its precise physiological range is crucial, as both deficiency and excess pose considerable health risks.

1.4.4 Forms of Selenium

Selenium is seldom found in its pure form, so selenium species are grouped into two categories: organically bound selenium forms (e.g., selenomethionine, selenocysteine) and inorganic forms (e.g., selenate, selenite). Organic and inorganic selenium species serve to follow separate biotransformation's within the human body but ultimately either end as selenoproteins or waste (Figure 3). Often, selenium compounds partially replace sulphur, such as in metal sulphide ores for inorganic selenium species and in proteins for organic ones. The vast majority of human Se intake consists of organically bound selenium, which can be transformed into selenoproteins present in most living organisms. Inorganic forms can be converted into organically bound species when crops are grown, e.g., yeast in an inorganic selenium-enriched medium, resulting in selenium that is organically bound, with a high proportion of selenomethionine (Rayman, 2004).

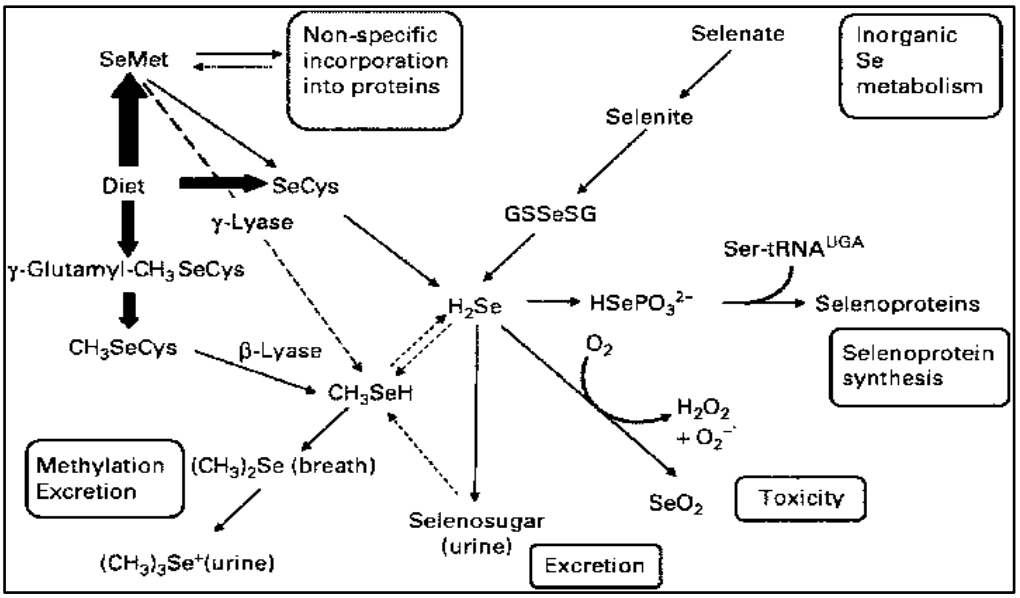

Figure 3: *Metabolic pathway of dietary selenium in humans. Se, selenium; SeMet, selenomethionine; SeCys, selenocysteine; GSSeSG, selenodiglutathione; c-glutamyl-CH 3 SeCys, c-glutamyl-Se-methylselenocysteine; H 2 Se, hydrogen selenide; HSePO 3 Selenium bioavailability: Current knowledge and future research requirements - Scientific Figure on ResearchGate. Available from: https://www.researchgate.net/figure/Metabolic-pathway-of-dietary-selenium-in-humans-Se-selenium-SeMet-selenomethionine_fig*

Se concentrations in the environment directly result from rock types within them, as the leaching of rock formations is the primary source of Se in soil and natural waters. The majority of Se entering the food chain is due to its content in soils, which is influenced by the underlying geology. Acidic igneous rocks produce low-concentration Se soils averaging 0.05 mg/kg, whereas soils with native sulphide and sulphur deposits can have concentrations up to 200 mg/kg (Sobolev et al., 2020). The bioavailability of Se to plants, and therefore its ability to move through the food chain, is highly variable. Bioavailability depends on soil pH, redox conditions, competition with other ionic species, and organic matter.

1.4.5 Selenium Supplementation

There is no comprehensive global database or review that details the average Se intake or Se reservoirs in land masses worldwide. As a result, individual countries must either conduct their own studies or rely solely on recommendations from other authorities. This has created a substantial market for lifestyle Se supplements, whether taken independently or as part of daily multivitamins. The increase in daily Se intake from lifestyle supplements is often observed in developed nations, where access is easier, and it includes those whose diets would otherwise stay within acceptable intake levels. Se biofortification strategies have been utilised with varying success to boost Se intake to optimal levels in countries with low environmental Se. Bio-fortification strategies include Se enrichment of soils or foliage for plants, genetic engineering of plants, additives in animal feed or specific microbes for yeast (Hu et al., 2021). For example, in New Zealand, which imports large amounts of Se-rich Australian wheat, Se fertilised soil has shown promise in increasing Se in home-grown wheat and reduces the need for importation or Se additives in bread which has been implemented in the past (Winkel et al., 2015).

Se supplements have been used medically in both trials and observational studies for therapeutic purposes with varying effects. Supplementation of 50–200 μg/day has boosted immunostimulant effects in individuals with both high and low Se levels. It enhances immune responses by increasing the proliferation of activated T-cells, natural killer cell activity, cytotoxic effects, and cell-mediated immune responses, which help slow disease progression. A supplementation of 200 μg/day for HIV patients, based on two randomised controlled trials, showed reductions in AE, and other studies suggest it may help lower viral loads and slow disease progression. Supplements of 80 μg/day sodium selenite and 200 μg/day selenomethionine have been found effective against the autoimmune disease Hashimoto's thyroiditis. A few smaller studies suggest that Se supplementation can reduce childhood seizures and improve sperm motility at 100 μg/day. (Rayman, 2012; Zhang et al., 2018).

1.4.6 Evaluating Selenium Levels

Assessing Se levels in humans is difficult because Se cannot be pooled within the body. Therefore, estimations are usually made in studies by using peripheral biomarkers of exposure, such as plasma/serum, toenail, urine, tissue, and SELENOP levels. While not entirely precise and subject to limitations, these levels have demonstrated a moderate correlation with average dietary intake, with this correlation strengthening as Se intake levels increase.

In general, plasma/serum and urine Se concentrations better reflect low to moderate exposure conditions than other biomarkers due to their biotransformation pathways. Toenail samples and possibly some tissue samples are more suitable for assessing moderate to long-term exposure, as their half-life is generally longer than that of their liquid counterparts. However, these methods reflect total Se in the body and do not account for overall Se exposure, because different selenium species have specific organ or tissue affinities. Some studies also indicate that factors affecting selenium levels include increasing age, gender, and smoking; however, these findings are inconsistent and may be related to initial Se exposure through dietary intake through dietary intake (Algotar et al., 2013; Reid et al., 2008; Reid et al., 2006).

1.5 Selenoproteins

Selenoproteins are a class of proteins that contain selenocysteine (Sec), one of the 22 known genetically coded (proteinogenic) amino acids found in humans. Selenoproteins are made from metabolised organic and inorganic Se that is not methylated i.e. selenocysteine, selenate, selenite (Figure 4). Selenomethionine (SLM) is able to be synthesised into sec where it continues the selenoprotein cycle. Selenocysteine is present in several important enzymes in humans and appears across all three domains of life and readily substitutes regular cysteine in proteins (Kryukov et al., 2003). It has a lower reduction potential than

sulphur-cysteine, making it more suitable for proteins involved in antioxidant pathways. Unlike other amino acids, there are no free pools of selenocysteine in cells. Because of its high reactivity, it is stored in a less reactive oxidised form known as selenocysteine, or more commonly as a tRNA-bound serine residue (Ser-tRNA(Ser)Sec) (Minich, 2022). These are then involved in a multi-mechanism biosynthesis process to produce the necessary Se selenoproteins. Selenocysteine is incorporated via a nucleotide sequence called the SECIS element in both eukaryotes and prokaryotes (Romagné et al., 2014).

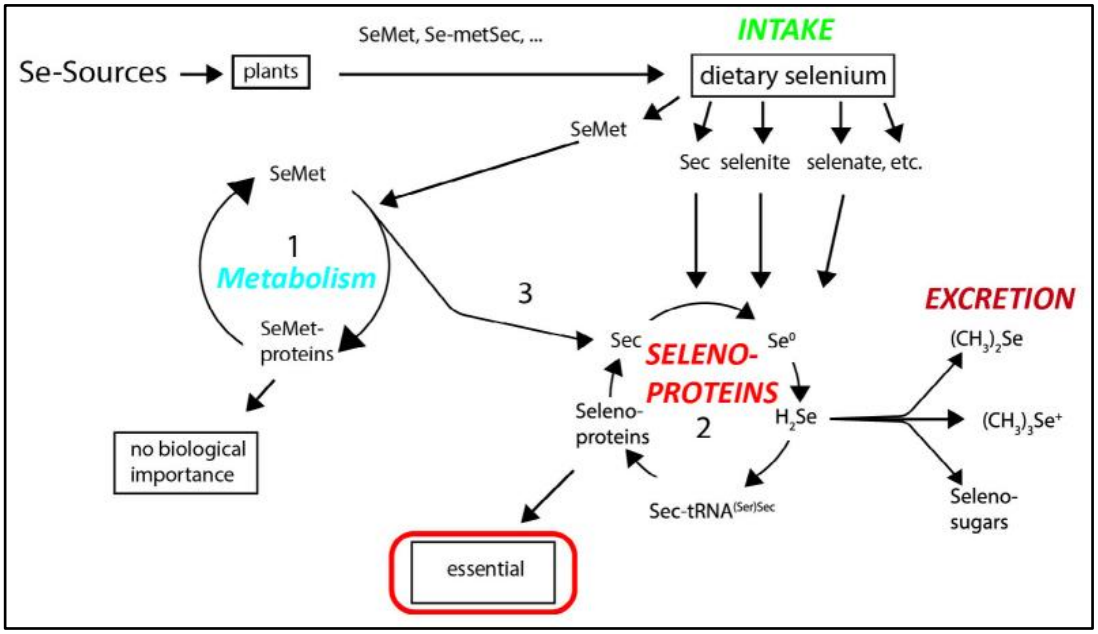

Figure 4: *Metabolism of Se-containing compounds in human body. Plant-derived SLM (SeMet) is incorporated into proteins (metabolism) or converted into Sec for selenoprotein synthesis. Hydrogen selenide (H_2Se) is an intermediate in Sec-tRNA$^{(Ser)Sec}$ formation. Excess Se is excreted as trimethylselenium ion, dimethyl selenide, and selenosugars. Used with permission under creative commons licence. Original work attributed to authors https://www.ncbi.nlm.nih.gov/corecgi/tileshop/tileshop.fcgi?p=PMC3&id=365255&s=134&r=3&c=4*

1.5.1 Selenium-containing Proteins

Only proteins containing sec are classed as selenoproteins, so proteins containing SLM or other methylated Se compounds such as MSC, are separate (Minich, 2022). SLM is an analogue similar to selenocysteine that replaces the sulphur in methionine with selenium and can subsequently replace be used in place of methionine in proteins. SLM is metabolised in humans via the food chain as it is commonly found in both plants and animals. It can remain in the body as SLM as a readily available methionine replacement as it is absorbed in the body by methionine transporters(Marshall et al., 2017). SLM can undergo the methylation pathway which primarily results in excretion in urine or exhalation. If needed, SLM can be biosynthesised into selenoproteins (Figure 5) (Letavayová et al., 2006).

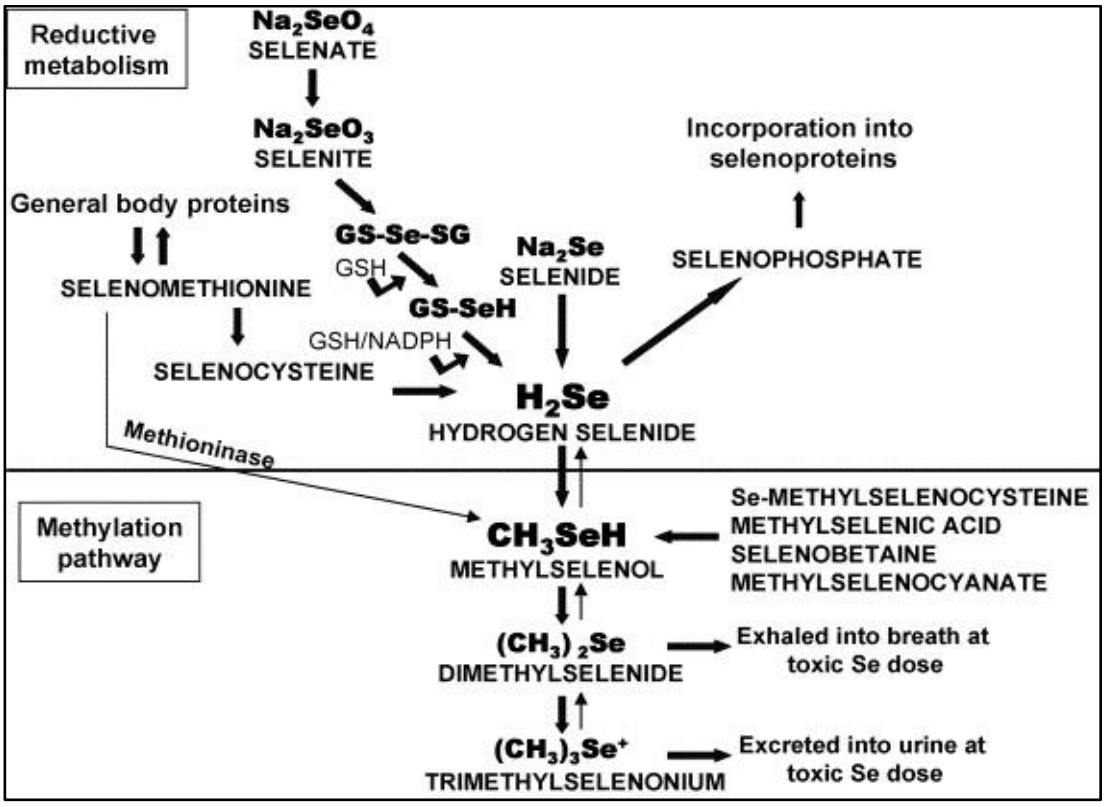

Figure 5: *Schematic representation of the Se methylation and metabolic pathways. Copyright: https://doi.org/10.1016/j.tox.2006.07.017 License number: 6093721312746*

Recent studies suggest that SLM can disrupt protein function, particularly under oxidising conditions. SLM readily replaces methionine in protein translation when in abundance but due to the dramatically higher redox properties, SLM mis-incorporation causes a higher rate of detrimental effects on protein function. The higher redox of SLM requires the increased use of intracellular antioxidants which in turn dramatically increases reactive oxygen species (ROS) which can damage nucleic acids, proteins and lipids. Additionally, oxidised selenium products catalyse unnatural di-sulphide and di-selenide bridge formation which leads to protein aggregation and protein inactivation (Hussein et al., 2022).

1.5.2 Selenoproteins in Humans

A total of 136 selenoproteins have been identified in humans, with twenty-five located in human cells; however, the exact function of all remains unresolved (Brigelius-Flohé & Arnér, 2018). Selenoproteins contribute to diverse biological processes, including antioxidant defence, thyroid hormone metabolism, DNA synthesis, and fertility. Specific selenoprotein families mediate these roles, each associated with distinct functions. For instance, Glutathione Peroxidases (GPX) and Thioredoxin Reductases (TXNRD) primarily facilitate antioxidant activity, while Iodothyronine Deiodinases (DIOX) regulate thyroid hormone activation. Thioredoxin Reductases also participate in DNA synthesis, and SELENOP serves as a selenium transporter and redox regulator. Additional selenoproteins, such as Methionine-R-Sulfoxide Reductase B1 (SEPX1), Formate Dehydrogenases, and Glycine Reductases, which are implicated in metabolic and reproductive processes (Gladyshev et al., 2016).

Decreased selenium intake is causative of an inability to synthesise these selenoproteins. Selenoprotein synthesis is biologically efficient and uses a variety of pathways and initial Se-compounds for synthesis (Figure 6). This allows the body to maintain

adequate levels of selenoproteins in the body allowing homeostasis for the important processes they are a part of. The lack of one or more specific selenoproteins is thought to be the cause of negative health effects as outlined in 1.1.3. The selenoproteins SELENOP, GPX1, GPX2 and GPX4, have been shown to be essential in mouse knockout experiments (Weeks et al., 2012). The deletion of GPX4 in the mice experiments showed cell death like that seen in Parkinson disease, GPX1 knockout were found to be susceptible to colonic abnormalities and GPX2 showing affinity to gastrointestinal cancers and SELENOP showed neurodegeneration (Pei et al., 2023). In vitro studies further support Se's anti-proliferative effects by showing its main role in maintaining genomic stability, promoting apoptosis in healthy and malignant cells, and regulation of oxidative stress (Fernandes & Gandin, 2015).

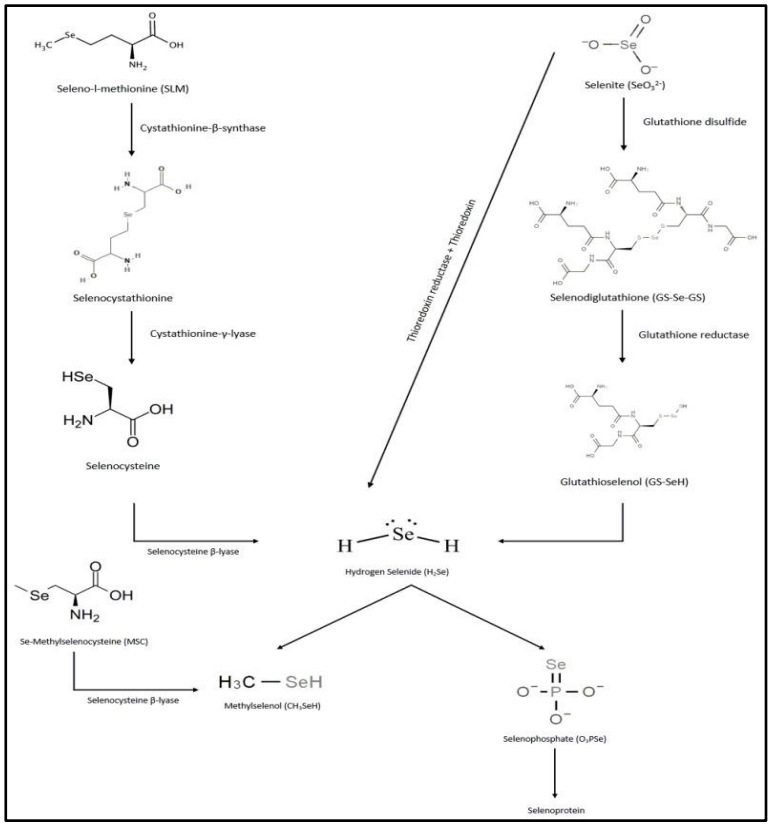

Figure 6*: Pathways of organic and inorganic Selenium forms and the pathways to Selenoproteins. Used under creative commons licence. Original image source: https://pmc.ncbi.nlm.nih.gov/articles/PMC887.*

1.5.3 Selenoprotein-P (SELENOP)

Selenoprotein-P (SELENOP) is an extracellular glycoprotein that is the most abundant selenoprotein in plasma and accounts for over 50% of plasma selenium reserves. It is a 318 amino acid (aa) (31.84 kDa) protein molecule which plays important roles in cell homeostasis, selenium transport to tissues and extracellular antioxidant activity including neutralising peroxynitrite which is a reactive product of inflammation (T.-J. Lee et al., 2022). SELENOP contains multiple selenocysteine (Sec) residues, forming two hairpin structures that are essential for Sec insertion, and is one of the few selenoproteins with multiple functions. Its concentration strongly correlates with selenium intake and can be directly measured in blood, serum, or plasma, making it a useful biomarker in medicinal studies (Schomburg, 2022b).

SELENOP binds to heparin, potentially protecting the endothelium and blood vessels, and exhibits enzymatic activity that may complement other protective GPX functions in circulation. SELENOP's primary role involves selenium transport, recycling, and storage, particularly in the liver and testes, where it is essential for GPX4 biosynthesis and protection during secretion. Additionally, SELENOP protects lipoprotein particles from oxidation and has been shown to prevent oxidative damage in gastrointestinal tissues, which is consistent with findings from the EPIC cohort regarding colorectal cancer (Hughes et al., 2015; Outzen et al., 2021).

1.5.4 Glutathione Peroxidase (GPX)

Glutathione Peroxidases (GPX) are a family of crucial selenoenzymes in mammals, present in most cellular processes throughout the human body. There are eight members of the GPX family (GPX1 – GPX8), but only GPX1 – 4 and GPX6 contain selenocysteine in their structures and are therefore classified as selenoproteins (Table 1). These selenoproteins typically use Se as a catalyst for vital biological functions, such as maintaining homeostasis

and combating oxidative stress. Their antioxidant properties enable GPX to neutralise hydrogen peroxides and organic hyperperoxides within cells, thereby reducing ROS and limiting its toxicity (Herbette et al., 2007). GPX enzymes utilise Se and sulphur as catalysts for essential biological processes. The enzymatic activity of GPX enzymes generally increases with supplemental selenium, while deiodinase 1 (a thyroid hormone-metabolising enzyme) exhibits tissue-specific selenium preferences (Brigelius-Flohé & Arnér, 2018). For these selenocysteine-based enzymes, evidence suggests their activity depends on selenium intake levels. Additionally, this reinforces the link between oxidative stress and selenium deficiency in animals (Pei et al., 2023).

Table 1: *Overview of the five GPX selenoproteins found in humans, their sites in the human body and other relevant information.*

Protein	Size from Uniprot	Primary Site in Humans	Function	References
GPX1	203aa 22,088 Da	Erythrocytes, liver, kidneys, lungs	Whole Body	(Brigelius-Flohé, 2018; Pei et al., 2023; Rayman, 2012; Weeks et al., 2012)
GPX2	190aa 21,954 Da	Gastrointestinal tissue and liver		
GPX3	226bp 25,552 Da	Extracellular fluid and plasma	Liver, kidneys, heart, lungs, thyroid, gastrointestinal tract, breasts, placenta, and the male reproductive system	
GPX4	197bp 22,175 Da	Ubiquitous in cells, Testes (high)	Whole Body	
GPX6	221bp 24,971 Da	Unknown	Unknown	

1.5.5 Thioredoxin Reductase (TXNRDX)

The Thioredoxin system is a crucial antioxidant system in humans and comprises of Thioredoxin (TXN), Nicotinamide Adenine Dinucleotide Phosphate (NADPH) and Thioredoxin Reductases (TXNRDx). TXN removes reactive oxygen species in cells and then TXNRD's use NADPH in order to maintain TXN's reduced state where it can then donate electrons to proteins which then activates these critical cellular pathways (Figure 7). Notably, TXN binds with Ribonucleotide Reductase (RNR) which is critical for DNA replication and repair, it binds with Apoptosis Signal-Regulating Kinase (ASK1) which regulates apoptosis, cellularly regulates transcription factors such as p53 and HIF-1α as detailed in Section 1.5. Modulation of TXN such as TXRND inhibition can cause pathological states leading to conditions such as cancer and chronic inflammatory diseases (Sudhadevi & Harijith, 2024).

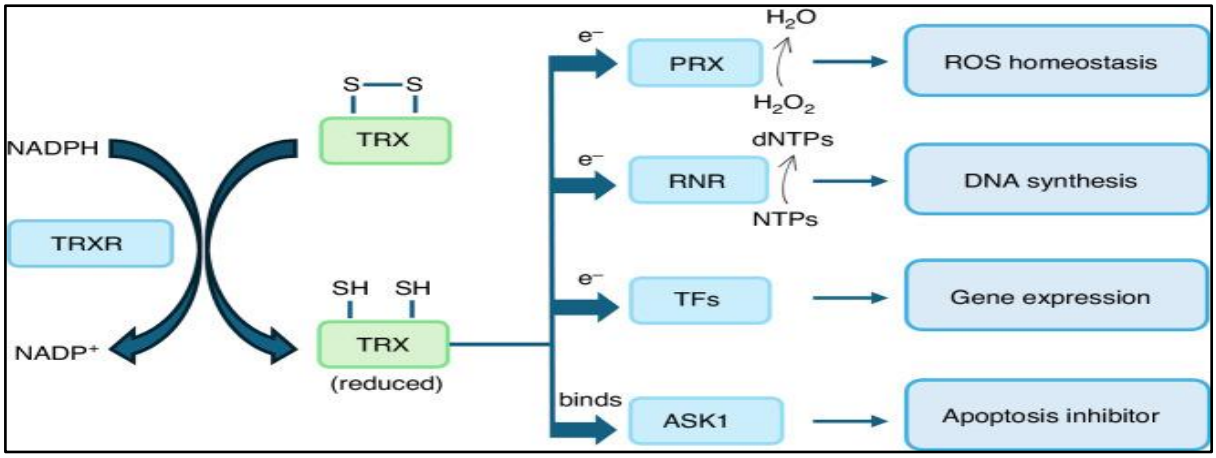

***Figure** 7: Thioredoxin pathway showing the reduction of TRC/TXN by TRXR/TXNRD through the binging of other proteins such as Peroxiredoxins (PRX) maintaining homeostasis by reducing reactive oxygen species (ROS). This pathway can generate dNTPs using RNR, modulates transcription factors (TF) to regulate gene expression and binds to ASK1 which prevents apoptosis. (Image from Sudhadevi & Harijith, 2024 and used with permission under creative commons licence 4.0)*

The TXRND family comprise of three enzymes (TXRND1, TXRND2, TXRND3). TXNRD1 is found intracellularly, TXNRD2 is prominent in the mitochondria but is widespread throughout the cell and TXNRD3 is specific to the testes. All three antioxidant enzymes involve a sec structure which make them susceptible to Se status in the body (Saccoccia & Bellelli, 2018). Notable, TXNRD1 is required in p53 activation which is a tumour suppressor and conversely is over-expressed in tumour cells; as well as the aforementioned roles in DNA transcription, DNA repair and cell proliferation. Cancer cells are shown to be highly sensitive to a selenite toxicity which is reduced by TXNRD1 into selenide which can then be used in the Selenium metabolism cycle. Deficiency of TXNRD1 causes selenite to remain in cells promoting cancer and thus the bespoke balancing of having usable Se in the body for TXNRD1 to use while not having an abundance of selenite which promotes cancer growth occurs (Tobe et al., 2012).

1.5.6 Iodythyronine Deiodinases (DIOX)

The Deiodinase family consists of three selenoproteins that are found in the thyroid, liver, kidneys and brown fat and they have a significant role in thyroid hormone metabolism. Deiodinases Type 1 (DIO1) converts inactive thyroxine into the active form of triiodothyronine. Deiodinase Type 2 (DIO2) engages in thyroid hormone activation while deiodinase Type 3 (DIO3) aids in deactivating thyroid hormones (Köhrle & Frädrich, 2022). While this family is mainly focused on the thyroid, DIO3 is both increased and has shown to be elevated in inflammatory cells while DIO2 and DIO1 is decreased in chronic illness such as cancer; marking it as a potential target for disease therapy (Schweizer & Braun, 2013).

1.5.7 Other Selenoproteins

Table 2 below is a non-exhaustive list of other selenoproteins in humans, including their main location and functions (in brief) based on the same list fromGladyshev et al.,.

***Table 2**: Non- exhaustive list of the known human selenoproteins, their abbreviation, main location and function in humans.*

Protein Name	Abbreviation	Main Location	Main Functions
Selenoprotein F	SELENOF	Endoplasmic reticulum (ER)	Plays a role in protein folding. Implicated in cancer protection
Selenoprotein H	SELENOH	Brain, nucleus, spleen	Gene regulation of the glutathione synthesis, transcription factor, increasing of cell viability
Selenoprotein K	SELENOK	ER, Immune cells, and spleen,	Antioxidant and development activity
Selenoprotein M	SELENOM	ER, neuronal cells	Protein folding, antioxidant activity
Selenoprotein N	SELENON	Most tissues, transmembrane glycoprotein associated with ER	Proper muscle development. Cell proliferation, redox signalling, calcium homeostasis
Selenoprotein R	SELENOR	Kidney, liver,	Antioxidant, methionine metabolism and proteins repair. Reduction of sulfoxymethyl group
Selenoprotein S	SELENOS	ER, Plasma membranes	Elimination of misfolded proteins from the ER, regulation of inflammation
Selenoprotein W	SELENOW	Brain, colon, heart, prostate and skeletal muscle	Antioxidant in human lung cancer cells, protect the developing myoblast Calcium-binding
Mitochondrial capsular selenoprotein	MCSeP	Sperm mitochondrial capsule	GPX4 storage
Selenophosphate synthetase-2	SEPHS2	Kidney, liver, testis	Synthesis of selenophosphate for selenoprotein synthesis

1.6 Hypoxia and Apoptosis

1.6.1 Hypoxia Response Pathway

Oxygen is a vital component in mammalian cells because it participates in key biological and physiological functions, including the synthesis of Adenosine Triphosphate (ATP), which provides energy for cells. Therefore, maintaining a proper oxygen balance in cells is crucial for homeostasis, as even minor fluctuations can lead to significant downstream effects. Reduced oxygen levels (hypoxia) cause cellular stress, activating pathways such as Hypoxia-Inducible Factor (HIF), autophagy, endoplasmic reticulum (ER) stress pathways, apoptosis, and alterations in energy metabolism. The HIF pathway is central to the cell's response, involving HIF transcription factors that detect hypoxic conditions and trigger all other responses. However, this pathway is also strongly associated with diseases like cancer, inflammation, cardiovascular issues, and metabolic disorders (Ostapowicz et al., 2024).

Hypoxic conditions inhibit the post-translational modifications of HIF's by EGLN1-3 which stabilises it within the cell, allowing for activation of genes. These genes allow for cellular adaptation to low-oxygenated environments and include promotion of glucose uptake, Krebs cycle inhibitions, stimulation of angiogenesis and regulation of apoptosis. Hypoxia is linked to the inappropriate accumulation of free radicals, which cause additional stress on proteins and DNA in the cell (F. S. Lee & Percy, 2011).

1.6.2 HIF-1α

Hypoxia-Inducible Factors (HIF) are recognised as key regulators in the transcriptional response to hypoxic stress. There are three isoforms of HIF: HIF-1α, EPAS1 (formerly HIF-2α), and HIF-3α (formerly IPAS). HIF-1α is expressed in all cells, while EPAS1 and HIF-3α are selectively expressed in certain tissues (Majmundar et al., 2010). Figure 8 illustrates that when oxygen is present in the cell, HIFs are hydroxylated on proline

residues by EGLN1, EGLN2, and EGLN3 (Strocchi et al., 2022). This modification enables HIFs to interact with the von Hippel-Lindau ligase, which subsequently targets them for degradation via the ubiquitin-proteasome pathway. When HIF-1α is not hydroxylated, it undergoes heterodimerisation with HIF, forming a transcriptionally active complex. This complex, along with co-factors, can then attach to a hypoxia response element (HRE) on the regulatory domain of target genes, leading to downstream effects such as activation or silencing (Liu et al., 2024). This response is a conservation mechanism to maintain cellular energy, blood flow, and oxygen transport to the cell, as decreased oxygen shifts cellular processes from a mitochondrial ATP energy basis to a more conserved glycolysis basis (Hirota, 2021). There have been many studies showing a strong association between elevated expression of HIF-1α in many cancer lines and poor prognosis. Notably, the effect of regulation in HIF target genes has shown to be key of tumour development and growth in solid tumours as well as metastasis (Luo et al., 2022).

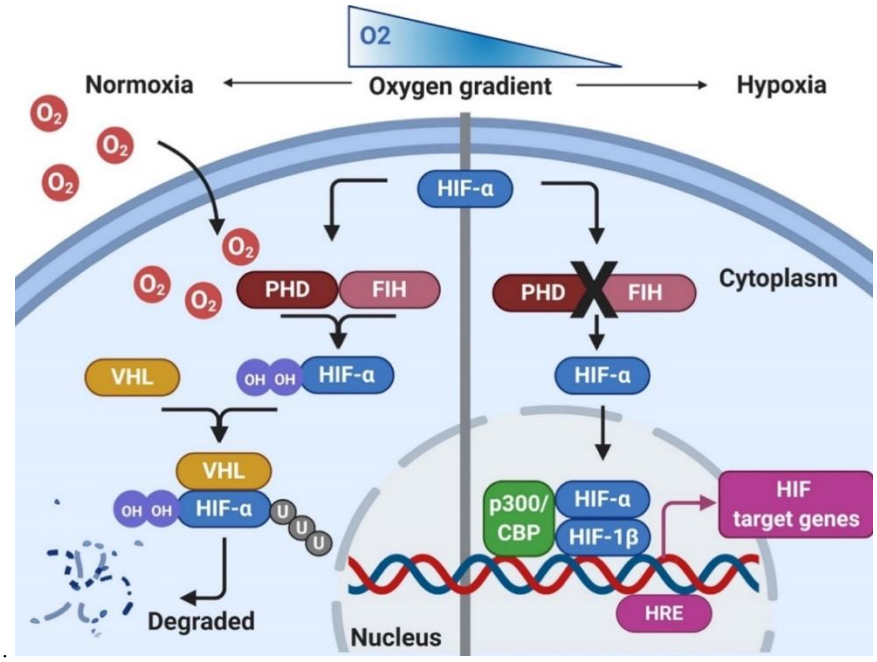

Figure 8: *Oxygen-dependent regulation of HIF-1α by PHD/EGLN in normoxia and hypoxia conditions.. Image used under creative commons licence*

1.6.3 EGLN1

Egl-9 Family Hypoxia Inducible Factor 1 (EGLN1) formerly Prolyl Hydroxylase 2 (PHD2) is the main oxygen sensor in the family of prolyl hydroxylases that regulate hypoxia in cells. EGLN1 selectively regulates HIF-1α at the transcript level, but not HIF-2α (Fujita et al., 2012). Studies have shown that silencing *EGLN1* using 21 nucleotide siRNA on HEK293 (kidney), and U-2 OS (bone) cells increases HIF-1α levels under normoxic conditions (To & Huang, 2005). Reduced levels of EGLN1 in tumour samples has shown a general positive correlation with higher grade tumours and poorer patient outcomes in a range of tumours. There are a few outlier tumour lines that have shown increased EGLN1 corresponding to increased tumour size (Ostapowicz et al., 2024).

1.6.4 EGLN3

EGLN3 is another PHD that can act on HIF-1α but shows preferential hydroxylation for EPAS1 over HIF-1α and HIF-3α. EGLN3 has shown higher rates of induction in certain cells under hypoxic conditions than of the other EGLN family (Appelhoffl et al., 2004). In low abundance, it can induce stabilisation of EPAS in the cell which leads to glucose tolerance improvement without toxicity in knockout mice (Taniguchi et al., 2013). However, like EGLN1, increased levels have been detected in primary tumours of patients with head and neck squamous cell carcinoma (HSNCC) compared to normal tissue cells. EGLN3, EGLN1 and HIF-1α all show significantly increased levels in metastatic cancer cell lines compared to both non-metastatic cancer cell lines and control cell lines (non-cancerous/tumorous) (Ostapowicz et al., 2024).

1.6.5 Apoptosis

The term “apoptosis” has been used since 1972 to describe a specific mode of cell death with unique characteristics separating it from other cell death pathways. Apoptosis is a highly regulated and intrinsic pathway that occurs from both physiological and pathological cell stress and signals. It involves activation of the cysteine-aspartic acid protease (CASPASE) family and extended members of the BCL-2 family that regulate apoptosis as a response to these endogenous signals. The CASPASE family of proteases forms a cascade type response pathway either through extrinsic or intrinsic pathways (Wyllie, 2010).

The extrinsic pathway involves the formation of a Death-Induced Signalling Complex (DISC) by a cytokine receptor binding to the cell membrane via a member of the Tumour Necrosis Factor Receptor Superfamily (TNFRSF), which activates Caspase-8 (CASP8) and Caspase-10. The intrinsic pathway involves changes in an organelle’s microenvironment, leading to mitochondrial outer membrane permeabilisation (MOMP), which causes the release of proteins such as Cytochrome C and second mitochondria-derived activator of Caspases (SMAC) into the intermembrane space. This protein release results in the activation of Caspase-9, initiating the formation of the apoptosome and subsequent caspases (Tummers & Green, 2017).

Activation of these initiator caspases is from the cleavage at specific target sites, which then “set off” effector Caspases, Caspase-3, Caspase-6 and Caspase-7, which in turn cleave an array of other proteins in the cell. The activation of these caspases creates the morphological changes that are specific of apoptosis: blebbing, loss of substratum contact, nuclease release from cytoplasm, unfolded nuclease, release of nucleotides (Wyllie, 2010).

The Tumour Suppressor p53 is a key pathway in apoptosis signalling. The p53 protein is a nuclear transcription factor that controls the expression of various genes involved in apoptosis, growth arrest, or senescence in response to genotoxic or cellular stress. E3 Ubiquitin Ligases, including MDM2 negatively regulate levels of the p53 protein. These

ligases facilitate the ubiquitination and subsequent proteasome-dependent degradation of p53. During stress conditions such as DNA damage, nucleolar stress, metabolic stress, and oncogenic stress, p53 protein levels are stabilised. The p53 gene can also trigger apoptosis through interactions with BCL-2 family proteins in the cytoplasm (Shiah et al., 2007).

1.6.6 Caspase-8

Cysteine-Aspartic Acid Protease 8 (Caspase-8) is a protein formed after cleavage of proteolytic sites on its precursor molecule, Pro-Caspase-8, which is activated when the DISC complex attaches (Zhao et al., 2010). It's main function in biological organisms is the primary mediator of extrinsic apoptosis, a genetically programmed cell death response. Induced *Caspase-8* gene knockout in mice shows increased development of bone marrow failure under inflammatory and infectious conditions indicating its essential nature in the cell death pathways.

Caspase-8 is synthesised as an inactive 55 kDa pro-enzyme (Pro-Caspase-8), which undergoes cleavage into the two active subunits p18 (18 kDa) and p10 (10 kDa) during apoptosis initiation. The persistent detection of the 55 kDa precursor in some samples suggests incomplete activation, potentially indicating suppressed apoptotic signalling or compensatory survival mechanisms in these patients. The 10 kDa band may represent a further cleavage product or alternative splicing variant, as reported in (Zhao et al., 2010).

1.7 Research Aims and Objectives

The aim of this research is to contribute to the evaluation of safety and pharmacodynamics of three Se compounds (SS, SLM and MSC) at two different daily dosages in nine cancer patients within a Phase Ib clinical trial run at Waikato Hospital, New Zealand. The specific aims of this research are:

1. To modify and validate molecular biology-based methods to measure genomic and mitochondrial DNA damage with the objective of assessing genotoxicity of compounds.
2. To evaluate pharmacodynamics (PD) pathways:
    a. The hypoxia response pathway
    b. The apoptosis pathway

The overarching hypothesis this body of work aims to support is that therapeutic high-dose Selenium may improve the effectiveness of anti-cancer treatments. This is achieved by inducing apoptosis in cancer cells, evidenced by an increase in Caspase-8, and by reducing hypoxia, as indicated by HIF-1α, EGLN1, and EGLN3, which normally inhibit apoptosis. The aim of this research is to gather evidence to validate this hypothesis, upon which future studies may be based. The first aim will be achieved using the LORD-Q PCR assay, and the second aim using western blot methodologies, which will be explained in more detail in Chapter 2.

2 Methods

2.1 Selenium Trial Participation and Sample Collection

2.1.1 Human Ethics Approval

The Health and Disability Ethics Committee (HDEC) approval for the study can be found under the Ethics committee reference 13/NTA/172/AM07 and was approved by the Northern A HDEC through the Expedited Review pathway. The study title under this amended approval is "*Phase 1b, randomised, double-blind, dose-escalation study to identify the safest, most effective selenium compound for use in cancer patients*." Copies of the HDEC approval and the participant information sheet and consent form are included in Appendix 1. The trial is registered in the Australian and New Zealand Clinical Trials Registry, number ACTRN12613000118707. The University of Waikato Human Ethics Committee also endorsed this study.

2.1.2 Study Design and Conduct

This randomised Phase Ib trial recruited two patient cohorts, the first consisting of 18 participants (9 with cancer and 9 with chronic lymphocytic leukaemia) who took Se 400 μg/day for 8 weeks as MSC, SLM or SS, and the results have been published (Evans et al., 2019, 2020). The second cohort of 9 participants (all with cancer), which is the subject of this research, were recruited from June 2023 to March 2024. These participants were randomised to take Se 1600 μg/day for 4 weeks then 6400 μg/day for 4 weeks, as one of three compounds: MSC, SLM or SS. The trial protocol was pre-determined before this thesis commenced and was unable to be altered. The protocol schedule (Figure 9) details the participant visits for blood samples and other study assessments, and the periods of study medication dosing.

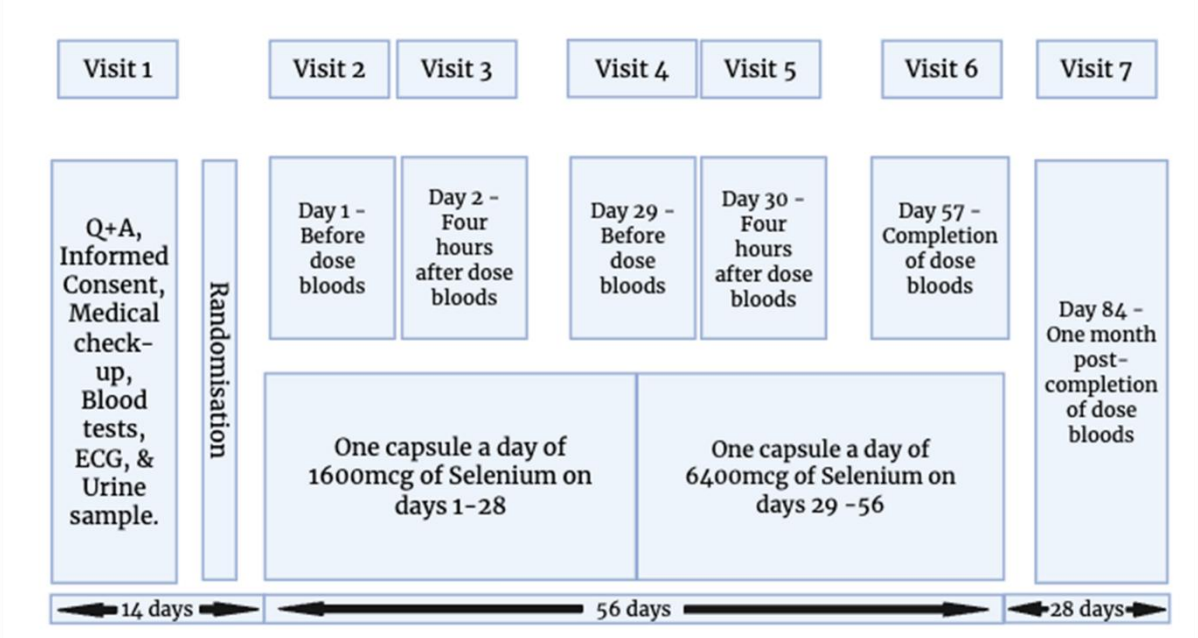

Figure 9*: Trial schema of time points including bloods drawn, pre-trial information from patients and visit numbers. Note mcg = µg.*

Patient consent was necessary for participation in this study. In summary, patients were invited to join the trial, and a participant information sheet was provided to give them comprehensive details along with a liaison to discuss the information and answer any questions about the study. The information sheet outlined the study itself, instructions for their participation both generally and during each of the seventh visits, including recording adverse events (aes) and medications in a study diary. Other details included the purpose of analysing all samples collected, potential benefits and risks- such as reproductive or sexual risks- guidance on whom to contact with health concerns during the study, procedures after the study, payment information, and how data gathered would be used and published. The consent form was then signed to confirm their agreement to participate and understanding of the information provided; however, patients could withdraw consent at any time.

The requirements for participant eligibility for the second cohort of this study are:

- *age 18 years and over*
- *have metastatic cancer, in whom the use of chemotherapy is not anticipated in the next 3 months*
- *not pregnant or breast-feeding*
- *no recent chemotherapy*
- *not taking more than 100 mcg of selenium supplements each day*
- *not allergic to any selenium compounds*
- *must be able to swallow capsules*
- *must have adequate liver, renal and bone marrow function*

2.1.3 Collection of Blood Samples

Patient blood samples were collected at Waikato Hospital with each patient having a maximum of seven visits. Figure 9 showed the initial samples were taken up to 14 days before the first day of treatment and then a second sample taken before treatment on the first day. These two pre-treatment samples were used to aid in identifying intrapatient variation in both DNA lesions and pathway regulation. Two samples were then taken for the 1600 µg and 6400 µg doses (4 hours and 28 days into dosing) to aid in determining the immediate and long-term changes. The last sample was taken a further 28 days after the last dose which helped in determining accumulation and longer-term changes due to treatment.

Samples were collected in 4 mL heparin vacutainer tubes and kept at room temperature (RT) during transportation to the UoW Physical Containment Level II (PC2) laboratory (#12236) in a biohazard-labelled secondary container. PBMCs were started within 6 hours of blood being drawn to limit haemolysis. All blood manipulation was conducted in a biohazard safety cabinet in PC2, and all blood and blood products were disposed of in

accordance with the UoW safety operating procedure "*Working with Human Blood, Tissue, and other Body Fluids: HESC-HS-S-0154.*"

2.1.4 Plasma Samples Extraction

Whole blood was transferred from the heparin tubes and trace element tubes to a sterile 15 mL Falcon® tube and centrifuged for 10 minutes at 1000 g at 4 – 8°C. The plasma phase was extracted from the tube using a sterile pipette and two 500 µL samples were aliquoted into sterile 2 mL screw capped tubes. The plasma tubes were stored immediately in a -80°C freezer until required for external immunoassays.

2.1.5 Whole Blood Samples Extraction

Patients' blood samples were transferred from the heparin into a 15 mL Falcon® tube and then made up to a final volume of 15 mL with RT sterile phosphate-buffered saline (1X PBS) solution at pH 7.4 (37 mM NaCl, 2.7 mM KCl, 10 mM Na2HPO$_4$, and 1.8 mM KH_2PO_4). These samples were mixed via pipetting and then added to 15 mL of Histopaque-1077 in a 50 mL Falcon® tube at RT and centrifuged at 400 g at RT for 30 minute with the brake off. The opaque interface containing mononuclear cells was carefully removed with a Pasteur pipette and transferred to a new 15 mL Falcon tube. The peripheral blood mononuclear cell (PBMC) were washed with 10 mL cold PBS and centrifuged at 250 g for 10 minutes at 4 – 12°C, repeated three times. After the third wash, cells were suspended in either 2.5 µL (V1, V3, V5 and V7) or 3.5 µL (V2, V4 and V6) of cell media in frost-resistant 2.0 mL centrifuge tubes according to Table 3. Cell concentration was obtained using 20 µL of a 1:1 ratio of 20 µL trypan blue and 20 µL cells in media mix. Concentration was counted using Countess™ Automated Cell Counter Slides by Invitrogen (CT# C10283) on the Countess™ 3 FL-Automated Cell Counter (CT# A49866). Cell concentration was considered

acceptable ≤ $5x10^6$ cells/mL and aliquoted into designated quantities and cryopreservation tubes as highlighted in Table 3.

Table 3: *Sample collection schedule for patients of each designated PBMC or plasma aliquot and volumes required.*

Visit number	Cryopreserved PBMCs (1mL)	Plasma (SEPP1) (2x 500µL)	Western blots (3x300µL)	Glutathione (1x300µL)	LGC Speciation (3x200µL)	Plasma speciation (3x300µL)	DNA rep Surrey (1x300µL)
1 (B), 2 (D1), 4 (D29). 6 (D57)	✓	✓	✓	✓	✓	✓	✓
3 (D2), 5 (D30), 7 (D84)	✓	✓	✓	✓	-	-	-

2.2 In vitro Mammalian Cell Culture

2.2.1 Reviving THP1 Cells

THP1 (ATCC TIB-202) is a monocyte suspension cell line obtained from peripheral blood from a patient with acute monocytic leukaemia. For this project, the DNA and protein extracted from this cultured cell line served as a positive control for the molecular assays. THP1 was selected since it was used in the previously published LORD-Q assays for DNA damage via UV-C (ultraviolet-C) radiation at 254 nm (Evans et al., 2016).

The cell line THP1 was initially obtained from the American Type Culture Collection (ATCC) and the passages (P) used for optimisation and later experiments were P100 – 110. A 1 mL aliquot of THP1 P100 at $1x10^6$ cells/mL was taken from cryopreservation in liquid

nitrogen and transferred to thePC2[1] facility in an ice bucket to remain frozen. The cryotube was quickly thawed in a 37°C water bath and then slowly diluted in a Biological Safety Cabinet Class II (Airstream® Gen 3 by ESCO) with THP1 complete growth medium and then placed into a non-treated Greiner Bio-One T-25 cell flask.

During the passages used for this experiment, the cell lines were incubated in at 37°C with 5% CO_2 levels, following ATCC guidelines and common practice (ATCC, 2024). THP1 complete growth media was made up into a 50 mL CellStar® Tube from Greiner Bio-One (CT# 227261) prior to cell culturing. The media contained 44.45 mL ATCC-formulated RPMI-1640 base medium + GlutaMAX™ media (Invitrogen 61870036), 5 mL 100% FBS, 500 µL 100X Penicillin/Streptomycin (PenStrep™) and 50 µL 14.3 M β-mercaptoethanol. The pre-made complete media contained all ingredients except for β-mercaptoethanol which was added to the desired media amount in a fresh container before feeding cells or sub-culturing at a ratio of 1:1000 (1 µL β-mercaptoethanol added to every 999 µL of media).

Cells received a full media change every 7 days or were sub-cultured when confluence reached approximately 80%. Subculturing of suspension THP1 cells involved transferring the flask contents into a 50 mL Falcon tube and centrifuging at 400 g for 10 minutes at RT until the cells pelleted and the supernatant was removed. The cell pellet was then resuspended in the appropriate amount of media before transfer to a cell flask.

2.2.2 Cell Culturing and Sub-Culturing

THP1 cells were grown in T-25 and T-75 Greiner Bio-One non-treated cell culture flasks filled with complete growth media (RPMI-1640 base medium + GlutaMAX™ media, 5% FBS, 1X Pen/Strep, 0.05 mM β-mercaptoethanol).

---

[1] THP1 can be cultured in Physical Containment Level 1 but the UoW Tissue Culture Room runs at Level 2.

THP1 cells were fed an additional 2 – 3 mL of complete media every 2 – 3 days and were resuspended at least once per week. Sub-culturing involved removing THP1 cells into a separate 15 mL CellStar® Tube and spinning down in Herafuge centrifuge. Supernatant was removed; cell pellet was resuspended in cell media and an aliquot of 20 µL was taken for cell analysis. Once resuspended cells are transferred to a new cell flask, the passage number increased by a factor of 1. Cells were considered for harvesting at a concentration of $1x10^8$ viable cells as determined by hemocytometry using Bio-Rad TC10™ Automated Cell Counter (CT# 145-0001).

2.2.3 DNA and Protein Extraction

THP1 cells were centrifuged at 200 g for 8 minutes to form cell pellets, after which the supernatant was removed and the pellet was resuspended in growth media to a concentration of $1x10^6$ viable cells/mL. The cells were then spun again in a 2.0 mL sterilised centrifuge tube (Tarsons, CT# 500020-N) at 200 g to establish the desired concentration. A total of twelve aliquots of THP1 cells at this concentration were prepared; four aliquots were allocated for protein analysis and the remaining eight for DNA extraction.

For protein extraction, the supernatant was removed, and 400 µL of laboratory-made lysis buffer containing protease inhibitors (50 mM Tris-HCl, 150 mM NaCl, 2 mM EDTA, 0.5% Triton X-100, 1X cOmplete ULTRA tablet (Roche: Cat. No. 05 892 970 001) was added to the pellet.

The samples were then stored at -80°C overnight to the lyse cells and prevent protein degradation. Protein levels were then measured using the Bradford assay outlined in Section 2.3.2. For DNA extraction, the cells were spun down and extracted using the Zymo DNA extraction kit from Zymo Research to concentrations between 20 and 200 ng/µL. Aliquots of 10 ng/µL of THP1 cell DNA were then prepared.

2.2.4 Mycoplasma Testing

Mycoplasma contamination is a major concern in cell culture, as these bacteria alter cell behaviour by disrupting nucleic acid synthesis, inhibiting proliferation, and causing chromosomal aberrations. Mycoplasma causes cell stress and can alter metabolism, cell growth, and induce DNA damage. Contamination often stems from poor lab practices (e.g., reused pipette tips) or equipment failures, and mycoplasmas resist standard antibiotics like penicillin. To ensure integrity, routine testing is critical as *M. pneumoniae* and other species thrive on lab surfaces and human skin, making them pervasive consistent threats (Dobrovolny & Bess, 2011).

Mycoplasma cell culture contamination was tested on THP1 cells using the Universal Mycoplasma detection kit (ATCC, CT# 30-1012K™), which tests for over 60 mycoplasma species. Briefly, THP1 samples were prepared at a 10^5 cell concentration and either underwent no UV-C damage, 20mJ UV-C damage or 100 mJ UV-C damage as elaborated in 2.2.7. Prepared cells were then transferred to tubes and centrifuged at 13,000 g at 4°C for 3 minutes after which supernatant was discarded. Cells were resuspended in lysis buffer (Kit), then incubated in a thermomixer at 37°C for 15 minutes, heated in another thermomixer at 95°C for 10 minutes and then centrifuged at 13,000 g at 4°C for 5 minutes. The PCR used 20 µL of universal primer PCR mix and 2.5 µL of universal primers (both from the kit) with an added 2.5 µL of prepared cells, cell growth media only or kit provided positive and negative controls with conditions set out in Table 4. The PCR samples were then run on a 3% agarose gel (2.2.4) where a positive band is seen at ~450 bp.

Table 4: *Cycling conditions for mycoplasma detection PCR as taken from the kit protocol.*

	Cycle Step	Temperature	Time	Repeats
Cycle 1	Initial Denaturation	94°C	15 minutes	-
	Denaturation	94°C	30 seconds	X 20
	Annealing	70°C-65°C (-0.5°C/cycle)	30 seconds	
	Elongation	72°C	45 seconds	
Cycle 2	Denaturation	94°C	30 seconds	X 12
	Annealing	60°C	30 seconds	
	Elongation	72°C	45 seconds	
	Final Elongation	72°C	4 minutes	
	Rest	4°C	15 minutes	-

2.2.5 Agarose Gel Electrophoresis

A 50 mL, 10 cm x 12 cm agarose gel was prepared with Le Agarose, Hyagarose powder (CT# R9012LE-500g), and lab-made 1X Tris-Acetate-EDTA (TAE) buffer to a 3% concentration. Five microliters of 10,000X SYBR™Safe Redstain from Invitrogen was added for visualisation of the amplified DNA. The agarose solution was poured into a level 10 x 10 cm cast with an eight-well comb. Once set, the combs were pulled out and the gel was placed into the horizontal electrophoresis tank (OWL™ Scientific, Inc), covered with 1X TAE and then connected to a Lighting VOLT™ OSP-250L power supply. PCR reaction with 10 µL of product was mixed with 1.5 µL of 6X loading dye (0.25% xylene cyanol FF, 0.25% bromophenol blue, and 30% glycerol) and loaded onto a 3% TAE agarose gel, along with an iNtRON siZer™ 100 bp DNA marker (CT# 24037). The agarose gel was run at 100 V for 30 minutes and then analysed on the iBright CL1500 Imaging system under UV light by Invitrogen (CT# A44240).

2.2.6 UV-C Damage

It was determined that UV-C damage at a concentration of 20 mJ and 100 mJ would be sufficient in inducing DNA damage at similar levels caused by cancer based on Lehle et al., 2014.Where 20 mJ would be considered moderate DNA damage and 100 mJ as high damage allowing further implications for results and analysis and to ensure that all PCR tests had accurate controls for experiments.

To induce DNA damage, 1 mL of $1x10^8$ cells were placed into five of the 6-well culture non-treated plates with one well containing 1 mL of complete growth medium as a control. The culture plates were placed into the DNA cross linker (BLX-254, Life Technologies) where conditions were set to 20 mJ or 100 mJ and took 30 second to a minute, respectively. The cells then underwent the same DNA extraction method as outlined in Section 2.2.3 and 2.4.1.

2.3 Western Blotting

2.3.1 Protein Extraction

One of the three whole blood PBMC aliquots for western blotting was chosen at random for each patient visit. Aliquots were then defrosted and lysed with 200 µL lysis buffer (Chapter 2.3.1). These were subsequently re-frozen at -80°C to undergo proteolysis, dephosphorylation, and denaturation. The samples were later transferred to an -18°C freezer for 1 to 4 weeks until required for Bradford assay and SDS-PAGE gel electrophoresis. An initial western blot, used for validation of the technique (2.3.5), was performed before patient samples due to their limited quantities and to maximise efficiency. The cell lines selected (Table 5) were readily available as protein, contained cancer, and had reported interactions with Glyceraldehyde-3-phosphate dehydrogenase (GAPDH), which was used as the loading control in this study (Iida et al., 2024; Wu et al., 2012).

***Table 5**: Cell lines used for validation of western blot protocol and primary antibodies of interest.*

Cell Line	Cancer Type	ATCC Identification
HeLa	Cervix	CCL-2 ™
MDA-MD436 (1)	Breast	HTB-130 ™
MDA-MD436 (2)	Breast	HTB-130 ™
A549	Lung	CCL-185

2.3.2 Bradford Assay

Bradford protein assay is a colorimetric protein assay that measures the absorbance of standards and samples to estimate protein sample concentration. The Bradford assay was carried out on a 96-well non-treated flat-bottomed plates (Greiner, CT# 655101) in triplicates with 10 Bovine Serum Albumin (BSA) standards ranging from 0 – 10 mg/mL including negative (0 BSA) and positive (0.1 – 10 BSA) control. Standards were made up to 100 µL from a 2.5 mL aliquot of 10 mg/mL concentration of BSA by Sigma Aldrich (CT# A7906-100g, Permit #2010041700) with the remaining quantity being 1X PBS with a pH 8 (Table 6).

***Table 6:** BSA standard concentrations and quantities used for Bradford assay prepared with 1X PBS and 10 mg/mL BSA stock solutions.*

	BSA Concentration (mg/mL)									
Reagent	**0**	**0.1**	**0.25**	**0.5**	**1.0**	**2.0**	**4.0**	**6.0**	**8.0**	**10.0**
1X PBS pH 8.0	100 µL	99 µL	97.5 µL	95 µL	90 µL	80 µL	60 µL	40 µL	20 µL	0 µL
10 mg/mL BSA	0 µL	1 µL	2.5 µL	5 µL	10 µL	20 µL	40 µL	60 µL	80 µL	100 µL

Bradford Protein Assay Reagent (Bio-Rad, CT# 5000006) was diluted with ultra-pure water (UP-H_2O) to a 1X concentration and stored at 4°C in the fridge. Once protein samples and BSA standards were ready, 100 µL of the Bradford protein assay reagent was added to

each of the 96 wells. BSA standard or patient sample (1 μL) was added to each well. Each standard and patient sample was done in triplicates with a reasonable amount of mixing from the pipette to ensure homogenous mixing.

The 96-well plates allowed a full set of standards and three patients to be analysed in a single assay (Figure 10), greatly reducing the time and resources required. A new assay was performed if any of the negative BSA samples (BSA 0) changed colour, indicating the presence of protein and potential contamination. To ensure confidence in the concentrations, a secondary BSA 1 triplicate was placed in each 96-well plate after loading the samples. If the difference in absorbance between the initial BSA 1 standard and the secondary BSA 1 standard exceeded 0.05, a new Bradford assay was conducted.

Plate: EXAMPLE

	1	2	3	4	5	6	7	8	9	10	11	12
A	BSA 0	BSA 0.1	BSA 0.25	BSA 0.5	BSA 1.0	BSA 2.0	BSA 4.0	BSA 6.0	BSA 8.0	BSA 10.0	Patient A Visit 1	Patient A Visit 2
B	BSA 0	BSA 0.1	BSA 0.25	BSA 0.5	BSA 1.0	BSA 2.0	BSA 4.0	BSA 6.0	BSA 8.0	BSA 10.0	Patient A Visit 1	Patient A Visit 2
C	BSA 0	BSA 0.1	BSA 0.25	BSA 0.5	BSA 1.0	BSA 2.0	BSA 4.0	BSA 6.0	BSA 8.0	BSA 10.0	Patient A Visit 1	Patient A Visit 2
D	Patient A Visit 3	Patient A Visit 4	Patient A Visit 5	Patient A Visit 6	Patient A Visit 7	Patient B Visit 1	Patient B Visit 2	Patient B Visit 3	Patient B Visit 4	Patient B Visit 5	Patient B Visit 6	Patient B Visit 7
E	Patient A Visit 3	Patient A Visit 4	Patient A Visit 5	Patient A Visit 6	Patient A Visit 7	Patient B Visit 1	Patient B Visit 2	Patient B Visit 3	Patient B Visit 4	Patient B Visit 5	Patient B Visit 6	Patient B Visit 7
F	Patient A Visit 3	Patient A Visit 4	Patient A Visit 5	Patient A Visit 6	Patient A Visit 7	Patient B Visit 1	Patient B Visit 2	Patient B Visit 3	Patient B Visit 4	Patient B Visit 5	Patient B Visit 6	Patient B Visit 7
G	Patient C Visit 1	Patient C Visit 1	Patient C Visit 1	Patient C Visit 2	Patient C Visit 2	Patient C Visit 2	Patient C Visit 3	Patient C Visit 3	Patient C Visit 3	Patient C Visit 4	Patient C Visit 4	Patient C Visit 4
H	Patient C Visit 5	Patient C Visit 5	Patient C Visit 5	Patient C Visit 6	Patient C Visit 6	Patient C Visit 6	Patient C Visit 7	Patient C Visit 7	Patient C Visit 7	BSA 1.0	BSA 1.0	BSA 1.0

Figure 10: *Layout of protein samples on a 96-well plate Bradford assay, with 10 BSA standards, three patients and their visits in triplicates. Uncompleted visits were skipped and left blank.*

Absorbance of each were measured by a plate reader (Thermo Multiskan GO, ThermoFisher) at a wavelength of 595 nm. Absorbance of the BSA 0.0 standard was subtracted from total absorbance of each standard and sample. It was assumed that the

BSA 0.0 contained only the coloured Bradford dye and by removing this reading from the others it would provide more accuracy on the concentration of the proteins. The absorbance of each standard was plotted on a graph and aligned with a linear and polynomial trendline to create a standard curve and used only if $R^2 \geq 0.97$. While linear trendline is a more rigorous and exact trendline, both were done as polynomial as this was used previously in this trial. Patient samples were then plotted against the standard curves to calculate their approximate protein concentration in µg/µL. The equation used below was then used to make 20 µL aliquots of 15 µg/µL for each sample to create standardised concentrations and even loading for western blots.

$$C_1 \times V_1 = C_2 \times V_2$$

Equation 1: *Dilution calculation used for all concentration standardisations.*

2.3.3 SDS-PAGE Gel Electrophoresis

Protein samples for SDS-PAGE gels were made up of 20 µL reactions with a final protein concentration of 15 µg/µL. They were made in a 1.5 mL boil-proof centrifuge tube from Eppendorf (CT# 15178) with 5 µL of Laemmli 4X dye (a final concentration of 1X) with protein sample amount equal to 15 µg/µL and the remaining made of lab-made 1X PBS solution. Heating of the sample after Laemmli dye and PBS is added ensures sufficient denaturing of proteins by boosting the process. This in turn allows proteins to reliably segregate from each other and ensure accurate molecular weights are seen. All samples were run at a final volume of 20 µL consisting of 5 µL Laemmli dye, sample DNA equivalent to 15 µg/µL and PBS (remaining volume). Heating temperatures of 70, 90 and 100 for 2 – 10 minutes were used during optimisation leading to a final denaturation step of 70°C for 8 minutes prior to SDS-PAGE loading.

All 20 µL of the protein samples were loaded onto a pre-made BioRad™ 10% SDS-PAGE gel (CT# 4561035) on a BioRad™ electrophoresis machine for 40 – 60 minutes at 160 V (2024). Membranes were run on the NuPAGE® 10% Bis-Tris methane (Bis-Tris) Mini Gels (CT# NP0316) using the Xcell SureLock™ Mini-cell machine for 80 minutes at 120 V at RT. Both sets of gels were run until the blue dye front was 1 cm from the bottom, indicating sufficient separation of the protein ladder. Each gel had the first lane containing 5 µL of Precision Plus Protein™ Dual Colour Standards protein ladder from Biorad™. Each sample represented a different patient, with each lane corresponding to a different visit in ascending order from left to right.

2.3.4 PVDF Membrane Transfer

Loaded SDS-PAGE gels were then transferred into a western blotting transfer machine, EBlot™ from GenScript, where proteins were transferred onto a PVDF membrane (0.45 µM Immobilon®-FL, Millipore). EBlot™ had its own single-use transfer kits, including anode pad, cathode pad, transfer buffer, and gel window, which were used with the gels. Preparation for transfer involved estimating the area of the proteins on the gels by assuming the blue loading dye at the bottom marked the end of the protein run and that the bottom of the loading wells was at the start. This area was measured with a ruler, and a PVDF membrane was cut to that size and transferred into a clean container in the fume hood. Two plastic containers (12 cm x 12 cm) were also placed in the fume hood with; 1) 20 mL HPLC-grade methanol in container 1 and 2) 100 mL transfer buffer (EBlot™ kit by BioRad) in container 2.

PVDF membranes have two blue protective sheets on either side. The membranes were carefully extracted from the sheets using flatbed tweezers and clean gloves to minimise the risk of damage. The white PVDF sheet was activated in methanol for 20 seconds, in container 1. After activation, it was immediately transferred to container 2 with the transfer

buffer from the kit. Care was taken to ensure that the transfer buffer covered the entire membrane.

Once the membrane was activated and placed in the transfer buffer, the SDS-PAGE gel's plastic casing was cracked open to expose the gel inside. The gel was then cut so that only the protein portion remained, and the rest of the gel was discarded. The EBlot™ was then layered on top of the system's graphene pads in this order: the anode pad (kit), activated PVDF membrane, SDS-PAGE gel, a gel window, and finally the cathode pad (kit). The gel window was positioned between the pads but not in contact with the SDS-PAGE gel or the PVDF membrane to minimise interference with electron conduction. The gel window size was one of two options supplied with the kit (small and large) and was chosen based on the size of the membrane, with a preference for greater coverage between the pads.

Once the individual components were in place, the lid of the EBlot™ was clamped down, reducing the space between the components. The system was then set for a 6 or 7 minute transfer according to manufacturer instructions; the membrane was immediately removed into a clean container with Ponceau stain upon completion.

The Ponceau stain incubates the membrane for approximately 60 minutes or until sufficient bands are visible, indicating successful protein transfer. At this point, the membrane undergoes de-staining before the western blot protocol as outlined below. After the initial Ponceau staining of a single membrane from each patient (data not shown), it was not repeated unless results indicated the possibility of incomplete transfer; otherwise, membranes were directly placed into 10% blocking buffer, and the western blot protocol was started.

2.3.5 Western Blotting Protocol

Freshly transferred membranes were blocked with 10% blocking buffer containing 10% skim/trim milk powder (Woolworths, NZ) and 1X TBST (20 mM Tris; 150 mM NaCl; 0.1% Tween 20) for 1 hour at RT. The membranes were washed three times with 1X TBS (20 mM Tris; 150 mM NaCl) before being blocked overnight at 4°C with a primary antibody of interest (Table 7) added to the blocking buffer. The membranes then underwent another washing step, this time for three 15-minute washes in 1X TBST, before adding a secondary antibody in blocking buffer and incubating for 2 hours with shaking at RT. Primary antibody concentrations ranged from 1:100 to 1:500, while secondary antibody concentrations were 1:5,000 and 1:10,000 (Table 7).

The membranes then underwent three additional washes in 1X TBST for 15 minutes each, followed by a final wash with 1X TBS. Two different kits were used for chemiluminescent signal development, including WesternBright™ Quantum™ (Advansta) and SuperSignal™ West Pico PLUS Chemiluminescent substrate (ThermoFisher). This involved mixing equal parts of luminol/enhancer and peroxide to approximately 1 mL per membrane, then incubating for 4 to 8 minutes. The chemiluminescent signal was detected as bands using the iBright system by Invitrogen. All western blot membranes were probed for the house-keeping gene GAPDH to confirm appropriate protein transfer and to check for degradation, ensuring higher confidence in the results.

Table 7: *Anti-rabbit antibodies used in western blot analysis. Shown; recommended concentrations, optimised concentrations, brand, and catalogue number. Secondary antibody used was horseradish peroxidase (HRP)-conjugated goat anti-rabbit. Product information for all antibodies used, states that band size may be 10 – 20 kDa higher-than-expected band size due to post-translational modifications.*

Primary Antibody	Recommended Concentration	Optimised Concentration	Expected Band Size	Brand	Catalogue Number	Secondary Antibody
CASPASE 8	1:100-1:1000	1:200	18 kDa (55 kDa precursor & 10 kDa subunit)	Santa Cruz	SC-7890	HRP goat anti-rabbit 1:15,000 (Abcam) ab97051
HIF-1α	1:1000-1:2000	1:200	~115 kDa	Novus Bio	NB100-479	
	1:500-1:3000	1:200	~93 kDa	GeneTex	GTX127309	
PHD2/EGLN1	1:1000	N/A	~46 kDa	Abcam	ab4561	
	1:500-1:3000	N/A	~46 kDa	GeneTex	GTX132293	
PHD3/EGLN3	1:1000	N/A	27 kDa, 18 kDa	Abcam	ab30782	
GAPDH	1:2,000-1:10,000	1:15,000	36 kDa	Antibodies	A92899	

2.4 DNA Damage

DNA damage occurs naturally every day due to internal and external factors, and the body repairs it to protect genomic integrity. If DNA damage is too severe from acute or chronic sources, or if the DNA repair systems are impaired, it can lead to diseases such as cancer. When new compounds or dosages are considered for therapeutic purposes, it is standard practice to assess their genotoxic properties, which could cause or worsen diseases. This trial examines three different compounds and two dosages to identify the most effective and least genotoxic option for further testing with cancer patients, as an adjunct to various therapies. Additionally, the literature indicates that Se may have a protective role against genotoxicity, potentially detectable at specific dosage levels (Evans, 2019; Hernandez et al., 2026). Determining DNA damage in patients as a result of therapeutic interventions is a key aim in preventing and understanding potential genotoxic effects. The long run qPCR

technique for DNA damage quantification (LORD-Q PCR) was developed to accurately represent the changes in DNA lesions over the course of treatment in a practical and reliable way for researchers which is why it is used in this study (Evans et al., 2016).

2.4.1 DNA Extraction

DNA extraction of patient samples was extracted using PureLink® Nucleotide DNA Kit by Invitrogen (CT# K1820-01). The cells were thawed and spun down in Eppendorf centrifuge 5425-R at 250 g for 5 minutes at RT and then supernatant removed and replaced with 200 µL 1X PBS. Twenty µL of proteinase K and then 20 µL of RNase A was added before being vortexed and incubated at RT for 2 minutes. Two hundred µL of the PureLink® genomic lysis/binding buffer (kit provided) was added to the solution and vortexed before transferring to a thermomixer (Eppendorf thermomixer, model 5350) at 55 °C for 10 minutes to promote protein digestion. The lysate was then removed and added to a PureLink® spin column and centrifuged at 10,000 g for 1 minute at RT. The spin column was then washed with 500 µL of wash buffer 1 and spun at 10,000 g for 1 minute, then washed with 500 µL of wash buffer 2 and spun at ~19,000 g (maximum speed) for 3 minutes. After each spin, collection tube contents were discarded into 2% trigene and tube was discarded and replaced with a new one.

After the wash step, the spin column was transferred to a sterilised 2.0 mL centrifuge tube (Tarsons, CT# 500020-N). Twenty five µL of PureLink® genomic elution buffer was added to the column, incubated at RT for 1 minute and then centrifuged at maximum speed for 1 minute. A negative control (water instead of DNA) was made during the first protocol run to be used as a blank for DNA quantification.

2.4.2 Quantification of DNA

Sample DNA was quantified after extraction using the DeNovix DS-11DX spectrophotometer to meet requirements for continuation with the samples. A 1 µL aliquot of the negative control run through the extraction protocol was used as a blank for the machine to ensure more accurate results. After this, sample were briefly resuspended by the tube-flicking method and then 1 µL was placed on the machine pedestal. The results from the spectrophotometer included a graph showing a peak at 260 nm wavelength as well as A260, A_{260}/A_{280}, A_{260}/A_{230} and DNA concentration values. The values obtained from the nanodrop determined whether the sample needed cleanup or concentration e.g. DNA samples less than 12.5 ng/µL and A_{260}/A_{230} values below one and above 4.

Samples requiring cleanup were processed using the Nucleotide DNA Clean & Concentrator Kit by Zymo Research (CT# D4011). Briefly, DNA binding buffer (provided in the kit) was added to the sample at a 4:1 ratio, mixed briefly by pipetting, and then transferred to a spin-column with a discard tube (both provided in the kit). The mixture was centrifuged using an Eppendorf centrifuge 5425-R for 30 seconds at 15,000 g, and the flow-through discarded. Two hundred µL of DNA wash buffer (also provided in the kit) was added to the spin column, centrifuged for 1 minute at RT, then discarded, and this step was repeated once more. After the washing step, 25 µL of DNA elution buffer (supplied with the kit) was added to the spin column, incubated for one minute at room temperature, then transferred to a new sterilised 2.0 mL centrifuge tube. The tube and spin column were centrifuged at 15,000 g for 30 seconds at RT to elute the ultra-pure DNA before the quantification and evaluation step as described above. The cleaned samples were then analysed using a spectrophotometer under the same requirements as previously specified.

2.4.3 Traditional PCR

A two-step PCR was performed on the BioRad T100™ thermocycler to first identify the most suitable primer candidates for LORD-Q PCR in the trial (Table 8). The 20 µL PCR reaction (Table 9) was prepared in a 200 µL PCR tube using the selected primer pair and applied to patient DNA samples, a negative control, or an undamaged THP1 DNA positive control. The DNA used in this and future PCRs was standardised from original concentrations to aliquots of 25 ng/µL to ensure comparability. Cycling conditions for the PCR are outlined in Table 10. After cycling, the products were run on an agarose gel following the procedure described in Chapter 2.2.5.

***Table 8**: Human candidate primers tested in normal RT-qPCR conditions in order to identify candidates for LORD-Q analysis with patient samples. The primers are named according to a previous MSc(R) student in the lab, Annie Ko (KO). F = Forward Primer; R = Reverse Primer; mtDNA = mitochondrial; nDNA = nucleotide DNA*

Primer	Sequence (5'-3')	Size (bp)	DNA	Length	Tm (°C)	Gene Target
KO4F	GCAGGCCTAGGAGATGTGAG	3438	nDNA	20	59.61	POU domain class 5, transcription factor 1
KO4R	AAGAGGGTGGTGTTGAGTGG			20	59.53	
KO5F	CATAACCGCAAATGGGAAAC	45	nDNA	20	55.61	Tumour protein p53 (*TP53*)
KO5R	CGTCCTTTTGATGGCCTTT			19	56.1	
KO6F	CATAACCGCAAATGGGAAAC	3075	nDNA	20	55.61	
KO6R	CGGGACGTGAAAGGTTAGAA			20	57.56	
KO7F	GGCCACAGCACTTAAACACA	67	mtDNA	20	58.97	
KO7R	TGGTTAGGCTGGTGTTAGGG			20	59.01	
KO8F	ATCGTAGCCTTCTCCACTTC	3650	mtDNA	20	56.74	
KO8R	TGGTTAGGCTGGTGTTAGGG			20	59.01	
KO9F	GCTTTGAGGTGCGTGTTTGT	247	nDNA	20	59.9	*TP53*
KO9R	CTTCTTTGGCTGGGGAGAGG			20	60.03	
KO10F	ACGTCTGCAGTCAACTGGAA	251	nDNA	20	59.54	Kirsten rat sarcoma viral oncogene homolog (*KRAS*)
KO10R	GCTGTATCGTCAAGGCACTCT			21	60.13	
KO11F	AGACGGGACTCGAGTGATGA	300	nDNA	20	60.04	B-Raf proto-oncogene, serine/threonine kinase (*BRAF*)
KO11R	AGTCCCGACTGCTGTGAACA			20	61.4	
KO12F	GGGCAAATACCTTGGGTGGA	3446	nDNA	20	59.96	Beta-2-microglobulin (*B2M*)
KO12R	GACGCTTATCGACGCCCTAA			20	59.97	
KO13F	TGGGTCTGCCTGTCATGTTT	60	nDNA	20	59.52	
KO13R	AGTTTGGACTGCATCTGCCT			20	59.6	
SE1F (Large)	CGCCTCACACTCATTCTCAA	3723	mtDNA	20	63.6	mtDNA (NC_012920; 11492–15214bp)
SE1R (Large)	AATGTATGGGATGGCGGATA	3723	mtDNA	20	62.6	
SE1sR (Small)	CAAGGAAGGGGTAGGCTATG	55	mtDNA	20	62.9	
SE2F (Large)	GAGGCAGGACTCAGGACAAG	3129	nDNA	20	65.2	E2F transcription factor -1 (E2F1)
SE2R (Large)	CTCCTCACATGCAGCTACCA	3129	nDNA	20	65.2	
SE2sR (Small)	GGATGCCTCAGGGACCAG	164	nDNA	20	65.3	

Table 9: *Components of 20µL PCR reaction, in 0.2mL clear tubes from with concentration of UP-H_20 making up to 20 µL reaction. The PCR primers were from IDT Technologies and the PCR components from Solis BioDyne, Estonia.*

Components	**Final Concentration**
DNA	25 ng
10 mM Primers (F+R)	0.5 mM
10X Buffer (B1)	1X
25 mM $MgCl_2$	2.5 mM
5 U/µL Hot FirePol® Taq	0.05 U/µL
10 mM dNTP's	200 µM
UP- H_20	-
Total	20 µL

Table 10*: Cycling conditions for standard RT-qPCR.*

	Cycle Step	**Temperature**	**Time**	**Repeats**
Cycle 1	Initial Denaturation	95°C	15 minutes	-
	Denaturation	95°C	15 seconds	X 9
	Annealing	65°C (-0.5°C/cycle)	15 seconds	
	Elongation	72°C	4 minutes	
Cycle 2	Denaturation	95°C	15 seconds	X 34
	Annealing	60°C	15 seconds	
	Elongation	72°C	4 minutes	
	Final Elongation	72°C	10 minutes	
	Hold	20°C	15 minutes	-

2.4.4 LORD-Q PCR

LORD-Q PCR is an innovative technique that uses fluorescence detection of samples to quantitatively evaluate relative mitochondrial DNA (mtDNA) or nucleotide DNA (nDNA) damage. When a sample is subjected to PCR conditions with a primer set that covers a large region (large primer), usually over a single gene, it is assumed that the gene remains intact and minimal or no DNA damage has occurred. If the same sample undergoes PCR with a primer set for the same sequence but covering a much shorter region (short primer), its results can be compared to those from the large primer to assess DNA damage. The main idea here is that if there is no DNA damage, fluorescence will stay consistent between the two primer sets. However, if DNA damage occurs, the large primer set will produce a significantly lower signal than the short primer set, indicating the presence of DNA lesions, calculated using Equation 2 below.

$$\textbf{Lesion per 10 kb} = [(E_L^{\,CpL(Sample)} \times E_S^{\,-CpS(Sample)} / E_L^{\,CpL(Control)} \times E_S^{\,-CpS(Control)})^{1/a} - 1] \times 10{,}000$$

Equation 2*: E_L and E_S are the amplification efficiencies of large and short products, respectively. The crossover threshold (Cp) values for fluorescence are CpL and CpS, corresponding to large and short primers, respectively. Controls used were A549 for mitochondrial DNA and THP1 for nucleotide (p53) DNA as positive controls, or UP-H_2O as a negative control. Positive controls consisted of undamaged samples, 20 UV-C, and 100 UV-C THP1/A549 cell lines to characterise the approximate amount of DNA damage. The 'a' represents the number of base pairs in the long fragment of the DNA type (mitochondrial or nucleotide).*

Using both long and short primers on the same sample allows for comparison of their presence, which can assess the amount of DNA damage in the patient sample at a specific time-point. Intrapatient analysis compares DNA damage across different timepoints, highlighting individual responses to the dosages as well as long-term effects. Intracompound

analysis compares differences between compounds at various timepoints to identify emerging patterns.

The LORD-Q PCR protocol was optimised on traditional PCR machines (Chapter 2.4.3) before being tested, refined, and run on the Corbett Rotor-Gene 6000 (Qiagen). The protocol used 0.2 mL clear, thin-walled, flat cap PCR tubes from Axygen (CT# 321-02-051). These specialised real time quantitative PCR (RT-qPCR) systems were selected for their high accuracy and fluorescence detection capability. An additional advantage of this system is its ability to produce results with small samples, maximising DNA retention. The Rotor-Gene machine can accommodate 36 samples set out in a ring formation as shown in Table 11 resulting in each patient having a total of four sets of samples run over two reactions. SYTO82™ fluorescent orange dye was added to the PCR mix (Table 9) along with the equivalent of 12.5 ng/µL DNA to make a 10 µL reaction with ultra-pure H_2O (UP-H_2O, resistivity of 18.2 MΩ·cm) as the remaining component.

Table 11: *Typical LORD-Q PCR run on the Corbett Rotor-Gene including placement of controls and patients with intra-assay replicates.*

Slot	***Sample Description***	***Notes***
1	*Negative Control*	All PCR products, replaced DNA with UP-H_2O
2-4	*Positive Controls:* *THP1/A549 Undamaged DNA* *THP1/A549 20 J/m² UV-C Damaged DNA* *THP1/A549 100 J/m² UV-C Damaged DNA*	Only one set of cells were used per primer pair: THP1 with p53 nDNA and A549 with mtDNA
5-11	*Patient X Run 1*	7 visits
12-15;18-20	*Patient X Run 2*	Intra-assay replicate
21-27	*Patient Y Run 1*	7 visits
28-34	*Patient Y Run 2*	Intra-assay replicate
16,17,35 and 36	*Unoccupied*	Equal distance is required for balancing

3 Results

3.1 Participant Sample Collection and Processing

Seven visits were scheduled for each patient, including a pre- and post-dose, following the guidelines set out in Chapter 2.1.2. Patient tolerability during the trial was assessed using the 2010 Common Terminology Criteria for Adverse Events v4.0 (CTCAE) (http://ctep.info.nih.gov). However, due to scheduling conflicts and AE, three patients did not complete all seven timepoints, resulting in absent data; patient 25 missed visits 3, 5, and 6, patient 27 is missed visits 5 and 6, and patient 30 missed visit 3. Each of these patients is from a different Se compound cohort.

The AE, including severity, for this trial were patient-reported as well as any current medication that could impact data (Appendix 2). Patients were encouraged to keep a diary of symptoms and/or AE and to inform trial staff during visits if they were mild or moderate, or to contact immediately if more severe. No patients were removed from the trial due to AE, and two patients chose to withdraw voluntarily. The AE experienced were of grade 1 and grade 2, which are designated as mild and moderate, respectively. Most of the AE reported were gastrointestinal-related.

The collection of whole blood and plasma samples was conducted at the intervals specified in Figure 9. Patient PBMC and plasma samples were extracted from the whole blood as described in Chapter 2.1. Patients' PBMC samples then underwent protein extraction as outlined in Chapter 2.3.1 or DNA extraction as outlined in Chapter 2.4.1. Samples were stored for up to 18 months at -80°C and subsequently transferred to a -18°C freezer during analysis.

Researchers were unblinded to Se compound allocation on 26 June 2025 after all western blot and LORD-Q analyses were completed to reduce bias during experiments (Table 12). With nine patients and three selenocompounds, the even distribution between all groups helped increase confidence in the comparisons. The unblinding had no impact on the results themselves but assisted in forming comparisons and analysing each compound's outcomes.

***Table 12**: Patient groups for each selenium compound.*

Se-methylselenocysteine (MSC)	L- selenomethionine (SLM)	Sodium selenite (SS)
Patient 25*	Patient 27**	Patient 26
Patient 28	Patient 29	Patient 30***
Patient 32	Patient 33	Patient 31

*Only 4/7 trial visits. **Only 5/7 trial visits. *** Only 6/7 trial visits. .

3.1.1 Protein Samples

The protein concentration of patient PMBC samples, cultured A549 and THP1 cell lines was determined using a Bradford assay as outlined in Chapter 2.3.2. Analysis of the plates was performed on the Thermo Multiskan GO by Thermo Fisher, measuring absorbance at 595 nm. The absorbance was then compared to standards to determine the protein concentration of the samples using a standard curve with R^2 values, which were only accepted if the value exceeded 0.97. This threshold was agreed upon by the researchers as sufficient for the test, aligning with Bradford assay examples by ThermoFisher and Qiagen (TECH TIP #57, n.d.).

Protein concentration in patient PBMC samples ranged from 0.75 µg/µL to 12 µg/µL, with an average of 2.67 µg/µL (Figure 11). Samples and controls were then standardised with ultra-pure water to a concentration of 15 µg/µL of protein and stored in 100 µL aliquots in a -18°C freezer until required.

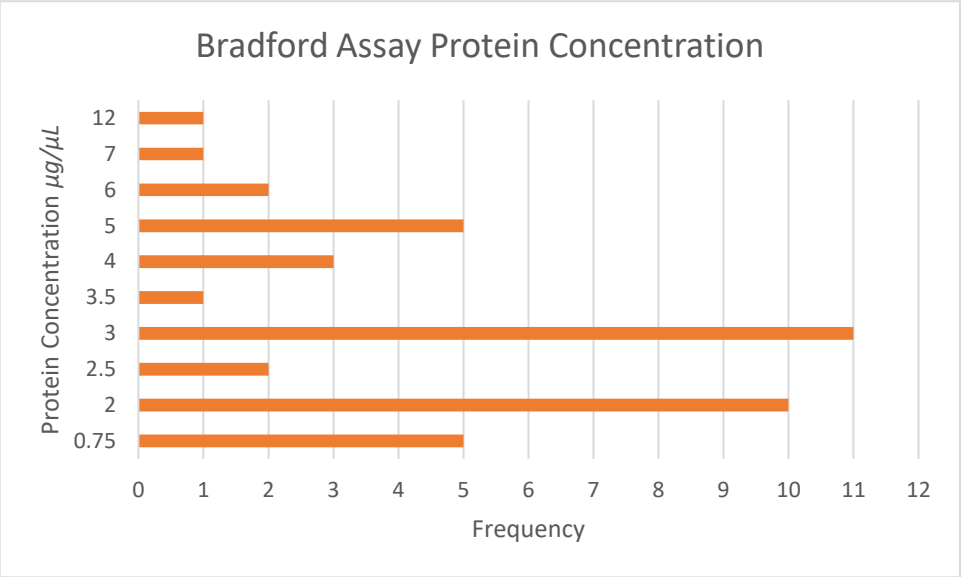

***Figure 11**: Frequency distribution of protein concentration in µg/µL across all 57 PBMC samples from trial patients.*

3.1.2 DNA Samples

Aliquots of nDNA were extracted from 1 – 2 samples that were frozen at -80°C using the PureLink® Nucleotide DNA Kits (CT# K1820-01, K1820-02, K1821-04) from Invitrogen. The extracted concentrations ranged from 1.391 ng/µL to 203.242 ng/µL, with the A_{260}/A_{280} ratio indicating quality values from 0.221 to 4.354. Extractions with concentrations below 12.5 ng/µL or outside the ideal quality A_{260}/A_{280} range of 1.75 – 2.25 were cleaned and concentrated using the Zymo Clean & Concentrate Kit. Once all patient samples were within the optimal range, concentrations were standardised into aliquots of 12.5 ng/µL.

3.2 In vitro Mammalian Cell Culture

3.2.1 THP1

THP1 leukaemia cells were chosen as a positive DNA damage control for LORD-Q PCR. A 1 ml aliquot of THP1 at P100 was frozen in liquid nitrogen in 2021 and thawed for use in this study, as detailed in Chapter 2.2.2. The THP1 cells were thawed at a concentration of 1×10^6 cells/mL and cultured with the recommended growth media over 10 weeks. The first aliquot of cryopreserved cells showed slow growth and was subsequently affected by facility contamination, leading to the destruction of all related flasks and cells. The second aliquot, thawed at the same concentration, reached the target P110 within 8 weeks under identical conditions. At the appropriate passage, the cells were first assessed for the desired confluency, as shown in Figure 12. The morphology of the cell is as expected; large, round, single-cell morphology. The concentration, exceeding 1×10^8 cells/mL, was then confirmed as suitable for proceeding with protein and DNA extraction, as well as UV-C treatment, as outlined in Chapter 2.4.1.

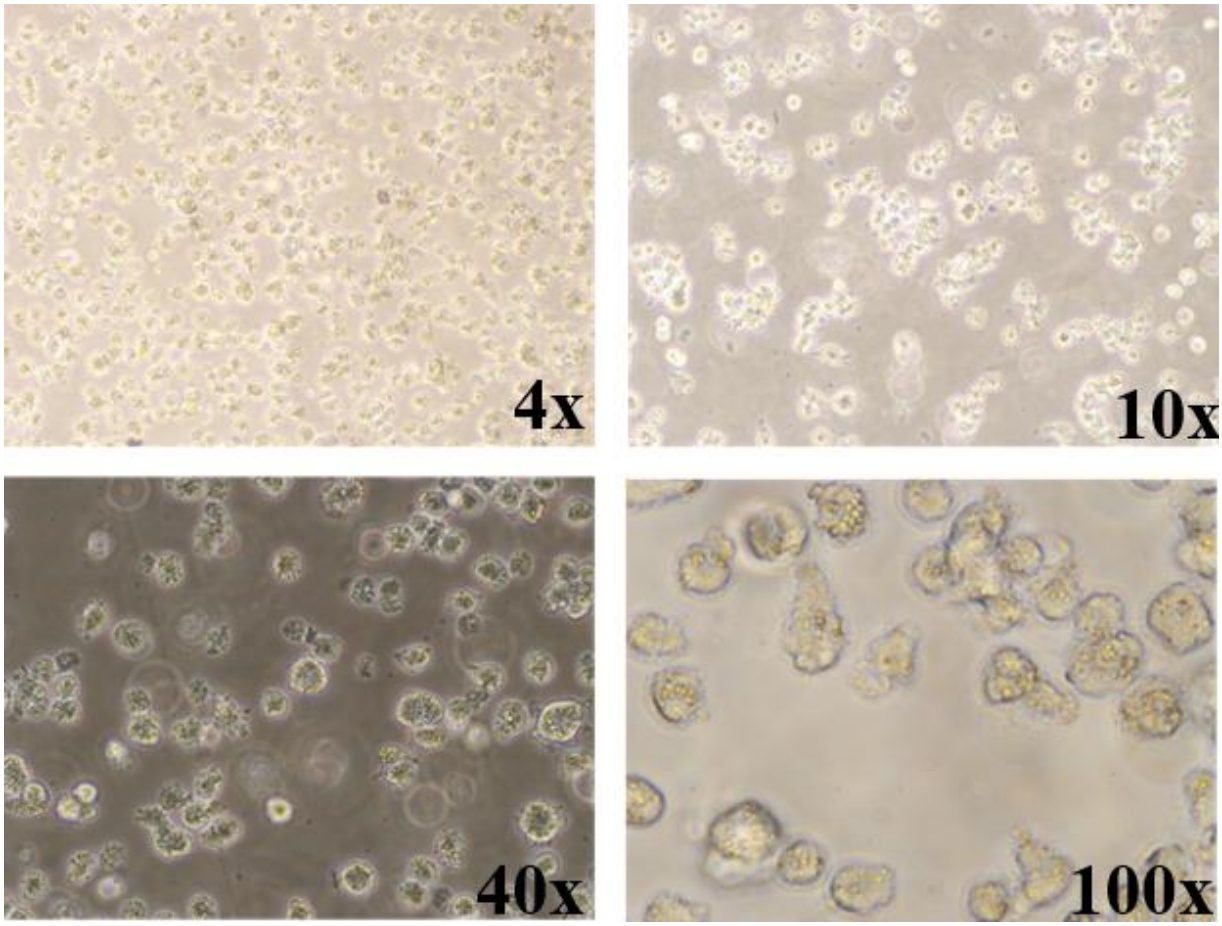

***Figure 12**: THP1 cells in growth media (T25) at 4X, 10X, 40X and 100X magnification under the Nikon Eclipse TS100 microscope. Images taken on the 11th September 2024 at p108 from p100.*

3.2.2 Mycoplasma

Mycoplasma cell culture contamination was excluded on 10/10/2024 using the Universal Mycoplasma Detection Kit (ATCC, CT# 30-1012K™), which tests for over 60 mycoplasma species. Briefly, THP1 cells and their growth media underwent standard PCR with the primers, positive control, and negative control provided by the kit (2.2.4). Mycoplasma contamination was evaluated in cell cultures using PCR before the DNA damage experiments outlined in 2.4 and 3.4. Since mycoplasma is a common issue in cell cultures and is not always visible under a microscope or to the naked eye, PCR amplification can help detect it. According to the detection method outlined in Chapter 2.2.4, mycoplasma should produce bands at approximately 450 bp on the agarose gel.

Figure 13 shows no bands the negative sample (lane 7), which had no cells or media, while the positive controls from the Mycoplasma testing kit displayed bands at the expected size of 500 bp (lanes 5 and 6). The test THP1 cell samples in lanes 1 – 3 showed no bands, smearing or primer dimers, indicating a low likelihood of incorrect results. Therefore, mycoplasma contamination was ruled out, and the cell culture samples obtained were used for LORD-Q PCR reactions.

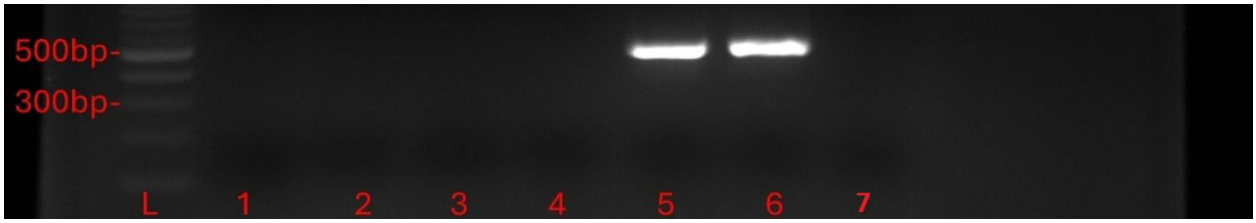

***Figure 13**: Agarose gel of PCR testing for presence of mycoplasma. Ladder is iNtRON SiZer 100bp; lane 1-3 is THP1 cells, undamaged, 20 J/mol UV-C, 100 J/mol UV-C respectively; lane 4 is THP1 growth media only and lane 5 and 6 are positive mycoplasma control, lane 7 is negative control.*

3.3 Western Blots

Western blotting was used to identify activated protein pathways in a patient sample through semi-quantitative analysis of the membranes. After transferring the proteins to the membrane, the western blotting protocol outlined in Chapter 2.3.5 was followed. The first primary antibody incubation involved the housekeeping gene GAPDH.

Over nine months, protein was collected from 9 patients across seven visits (Table 3; Figure 9), transferred onto PVDF membranes, and analysed using different primary antibodies. These antibodies were incubated on the membranes, then washed before applying a secondary HRP-conjugated goat anti-rabbit antibody, which binds to the primary antibody to enable detection. The target antibodies included CASP8, HIF-1α, EGLN3, and EGLN1. After detection, images were taken and analysed using semi-quantitative densitometry techniques which can be found in Appendix 3.

Band detection and intensity were compared between patients using data generated from the loading control GAPDH and test antibody, indicating differences in the selenium compounds used in the medications. Band intensity was also compared between visits within each patient to understand increases or decreases in pathway activation at different dosage levels. Detection at visit 1 was regarded as the patient's baseline before dosage interference. This detection was used to determine if pathways were present and at what levels before the dosage, serving as a baseline to assess whether the selenium dosage impacted the related pathways.

3.3.1 Antibody Validation

Four antibodies of interest were chosen for their relevance to pathways involving Se effects in the human body in the Phase 1 trial: CASP8, HIF-1α, EGLN3, and EGLN1. To ensure that these antibodies were recognising their specific molecular weight protein band on a SDS-PAGE gel, all four were run against four positive protein controls from cultured in vitro cancer cell lines to determine suitability and specificity prior to using the patient samples.

Protein concentrations of these cell lines were determined using a Bradford assay against 10 BSA Standards and then analysed via a spectrophotometer to measure absorbance at 595 nm. Protein was standardised to 15 µg/mL to ensure band intensity was due to increased pathway activation. The cell line proteins and a BSA 1 standard were run on a SDS-PAGE gel using the method outlined in Chapter 2.3.3 and transferred to a PVDF membrane using a transfer machine using the method in Chapter 2.3.4.

The control membrane was incubated with a primary antibody of GAPDH at a 1:20,000 concentration, and then with an HRP goat (anti-rabbit) secondary antibody at a 1:10,000 concentration using protocol from Chapter 2.3.5. Figure 14 shows membrane successfully transferred with a GAPDH band at the expected region of 36 kDa. The only two

proteins that did not show the GAPDH band was from protein extracted from HeLa which is seen in literature indicting user error or protein degradation and the BSA 1 protein (negative control protein) extract to test for non-specific antibody binding.

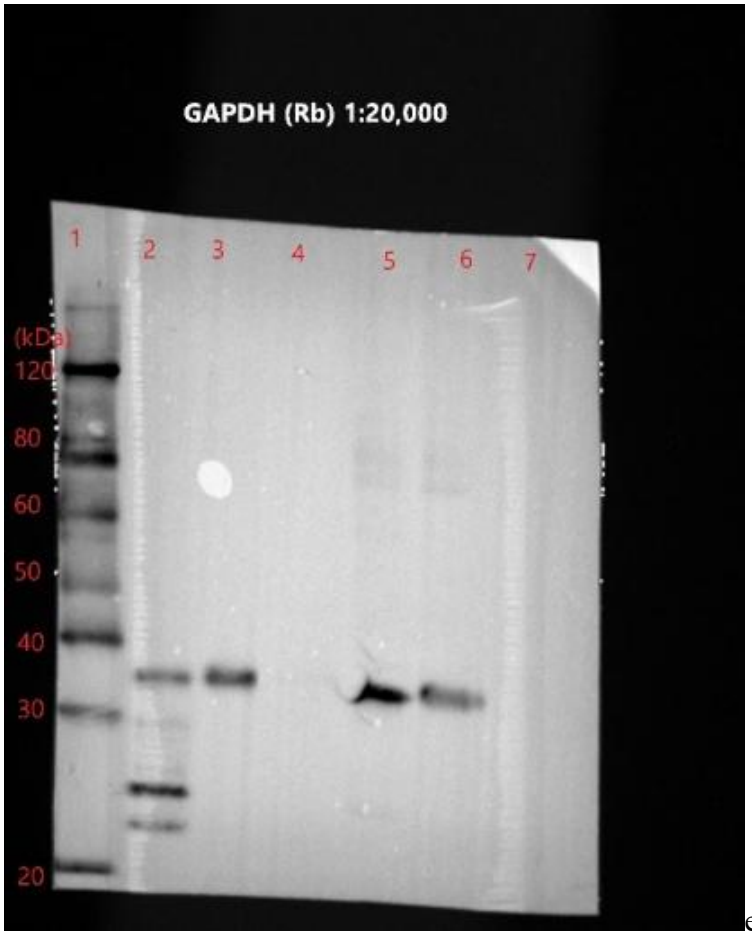

ethicsethics

Figure 14: *PVDF membrane of cell lines with GAPDH primary antibody at 1:20,000 concentration and secondary HRP goat anti-rabbit for validation of western blot method and materials. Lanes from left to right: 1) ladder, 2) A549, 3) A549, 4) HeLa, 5) MDA-MB 436, 6) MDA-MB 436, 7) BSA 1.*

The membrane was then stripped using the Abcam "Stripping for Reprobing" protocol and incubated with the antibodies of interest at the manufacturer's recommended dilutions initially. CASP8 was detected at the expected 18 kDa in most samples, with some showing a 10 kDa or 55 kDa precursor as well which are both seen in literature. HIF-1α was detected at the expected 93 kDa band and showed no alternative splices, which align with current

literature. EGLN-1 and EGLN-3 did not show bands on any of the controls. However, due to the age of the antibody being used, it was decided to purchase a new antibody from a different company and re-validate it using a patient sample that had positive GAPDH bands.

3.3.2 GAPDH

The antibody GAPDH was used as a housekeeping protein to ensure equal protein loading across all samples, as it is consistently abundant in protein expression and is unaffected by selenium or selenoprotein pathways. GAPDH was then employed as a baseline normalisation reference to determine whether the antibody of interest was upregulated or downregulated by comparing the differences in band intensities.

As expected, GAPDH was present in all patients, indicating that the protein was not fully degraded and that the results from other primary antibodies could reflect the presence or absence of the antibodies (Figure 15). Some patients, such as patient 30, did not consistently show GAPDH in every visit across a single membrane, resulting in their antibody data not being used. Overall results are displayed in Table 13 below. Specifically, one membrane showed visits 1–6 for patient 30, but not visit 7, while another membrane showed visits 1–4 and 6–7, but not visit 5 (data not shown). An argument could be made for combining results from multiple membranes to obtain a more comprehensive outcome; however, this would not be comparable to other results.

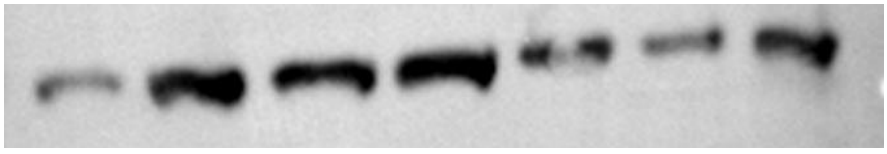

Figure 15: *Western blot of patient 32 showing the typical un-even loading and band intensities of GAPDH across visits 1-7 (left to right).*

***Table 13**: Western blot results obtained and presented in this research project.*

Patient #	Compound	GAPDH	CASP8	HIF-1α	EGLN1	EGLN3
Pt 25	MSC	✓	✓	✓	×	×
Pt 26	SS	✓	×	✓	×	×
Pt 27	SLM	✓	×	×	×	×
Pt 28	MSC	✓	×	✓	×	×
Pt 29	SLM	✓	✓	✓	×	×
Pt 30	SS	×	×	×	×	×
Pt 31	SS	✓	×	×	×	×
Pt 32	MSC	✓	×	✓	×	×
Pt 33	SLM	✓	×	×	×	×

.

3.3.3 EGLN3 & EGLN1

EGLN3 (previously PHD3) was initially excluded from the study after the validation step for 1) not producing any bands on any patients' samples or the THP1 protein, due to inactive antibody, and 2) another antibody for EGLN3 was unable to be purchased for this assessment due to availability and time constraints. EGLN1 (previously PHD2) was also inactive, but a replacement antibody was purchased for this assessment. It was thought that due to the interconnection in the pathway of EGLN1 and EGLN3, any results from EGLN1 would be a sufficient sign of the presence of EGLN3 in patients, which could later be explored more quantitatively when a new antibody was available.

EGLN1 was unsuccessful in obtaining any bands from any of the patient samples, including using different variations of the western blot methods outlined in Chapter 2.3.5. Variations included 2-hour primary antibody incubation rather than overnight, increasing the number of wash steps, decreasing the number of wash steps, reducing the 5% blocking buffer, and increasing primary and secondary concentrations.

3.3.4 HIF-1α

HIF-1α was used as a primary antibody at a concentration of 1:200 on all 9 patients but was only successful in 5. The success of the western blot was achieved when the antibody was shown to be present at each visit on a single membrane with a positive GAPDH band of ~36 kDa seen. During analysis, only 17 western blots were considered successful for HIF-1α over five patients (patient 25, 26, 28, 29 and 32). The other patient membranes had varying levels of HIF-1α present but were not considered successful due to GAPDH not being present, only some visits being present or no reaction seen.

The results obtained included all three MSC compound patients (patients 25, 28, and 32), as well as one patient each for SS (patient 26) and SLM (patient 29), making comparisons between compounds somewhat challenging and less precise. The relative density for each patient was calculated against GAPDH and normalised to baseline levels. The expression levels are adjusted against GAPDH, meaning a score of 1 indicates the same expression level in the cells as GAPDH. GAPDH has well-established expression values, allowing comparison with literature to determine whether HIF-1α is over- or under-expressed in cells due to treatment.

The patient data in Figure 16 shows that patient 29 had a large increase in HIF-1α expression levels throughout the trial. Visit 2 had no treatment and indicates a patient's intra-personal variation, which with patient 29 is far below the values obtained from analysis. The other four patients showed HIF-1α expression levels remain relatively low throughout the trial and were like pre-treatment levels. Visit 7 shows a small increase in almost all the patients (sans patient 32) showing that after treatment, hypoxic levels were increased. Indicating that the Se treatment and doses may have potentially decreased hypoxia.

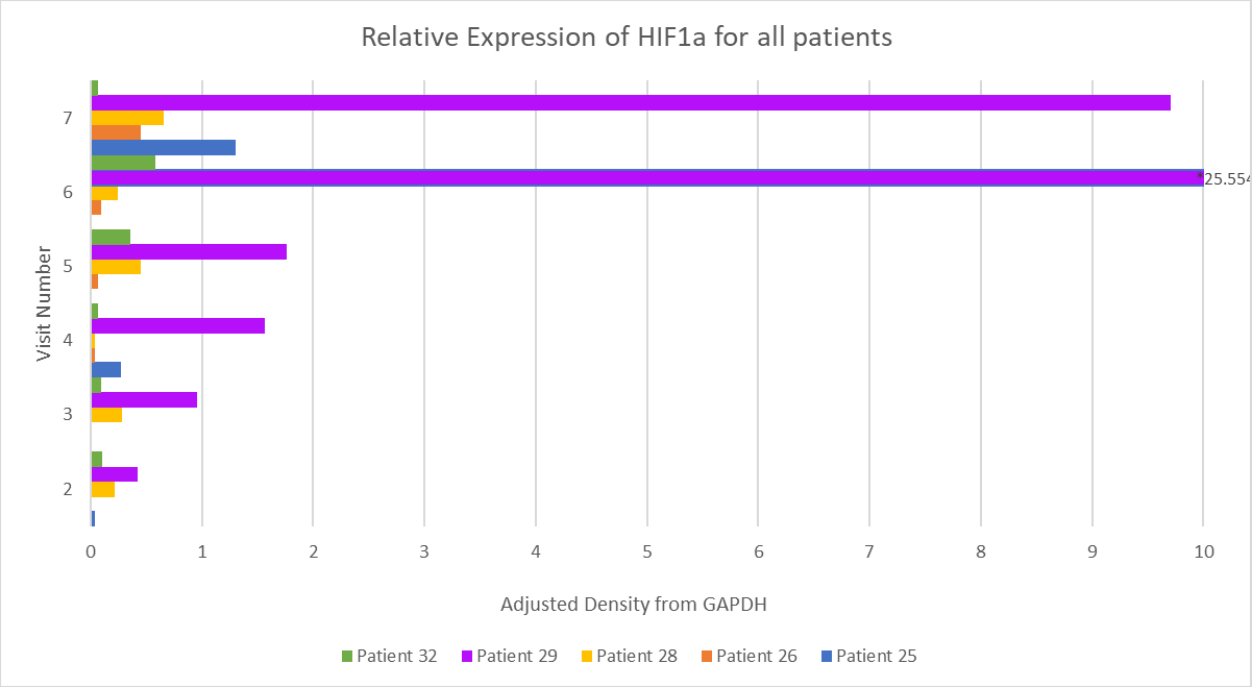

Figure 16: *Relative expression of HIF-1α for five patients using densitometry from western blots.*

Patients 25, 26, 28, and 32 (Figure 17) exhibited similar trends, showing increased HIF-1α expression during the trial. Visit 2 reflects the background fluctuation in expression, as no dose was administered at this point; for all four of the patients in Figure 17. Patient 28 showed a slight increase at the first 1600 µg dose (visit 3), while patient 25 and patient 26 showed a slight increase at two weeks on that dose (visit 4). Patient 25 did not have a visit 3 sample so it is unclear as to whether this increase was seen at the initial increase. Conversely, patient 28 and patient 32 showed decreased expression at visit 4 which may indicate tolerability of the compound and dose. While patient 25 does not have a visit 5 sample, all other patients showed an increase HIF-1α expression at the initial 6400µg dose of the compound. This expression increased after two weeks at this dose (visit 6) for patient 26 and patient 32 and decreased for patient 28. Post-treatment expression remained high for all 4 patients except for patient 32 which returned to pre-treatment.

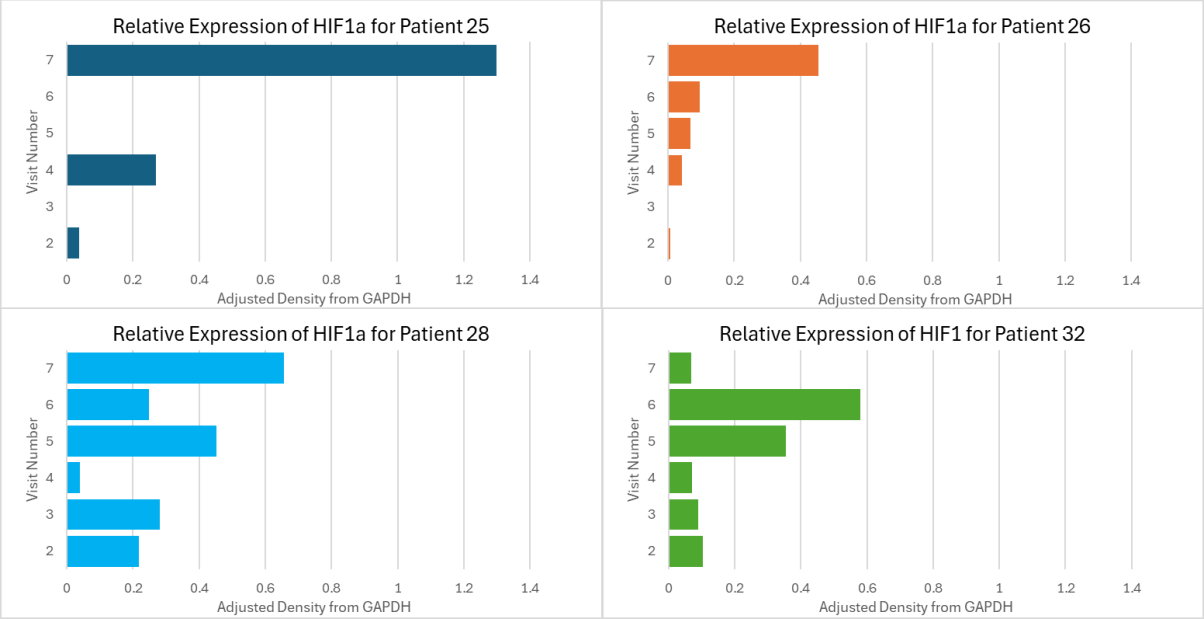

Figure 17: *Relative expression of HIF-1α for individual patients over the 7 timepoints. Top left: patient 25, top right: patient 26, bottom left: patient 28, bottom right: patient 32 (patient 29 in separate figure).*

Patient 29 showed a comparatively increased expression of HIF-1α in all trial timepoints with a large spike seen at visit 6, which corresponded to two weeks on the higher 6400 µg dosage (Figure 18). The average adjusted density showed HIF-1α expression for visit 6 was 25 times higher than GAPDH as calculated using 6 different membranes. This remained high at visit 7, post-treatment at nearly 9 times higher than baseline, even when factoring in intra-patient variation which sees visit 2 at ~0.5. While HIF-1α slowly increased during the 1600 µg dose (visit 3 and visit 4) and there was a small increase at visit 5 corresponding to the increased dosage, but these values remained under 2 which is more comparable to the other patients. Until the other results of the other two patients from the compound are calculated it is unclear as to whether this is a response to the treatment or specific to this patient. However, the increased dosage in this patient was not well tolerated as highlighted by the increased hypoxic response.

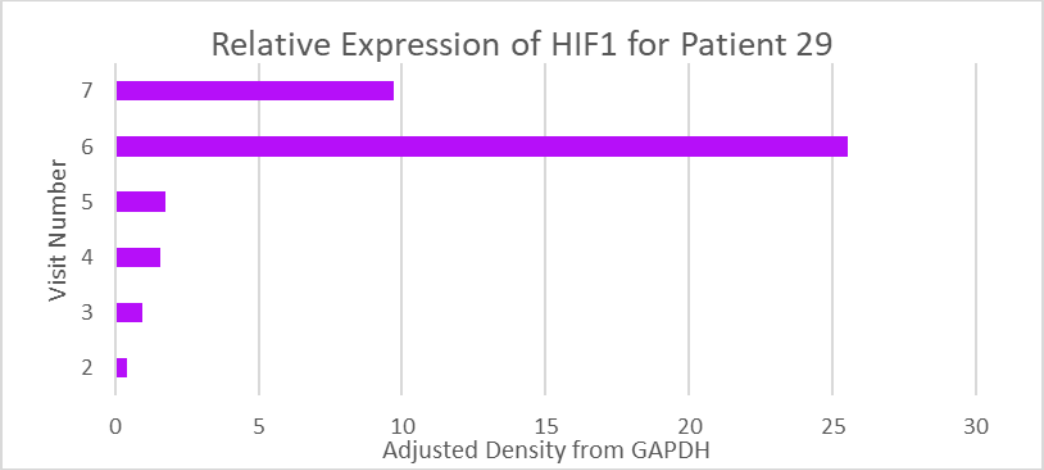

Figure 18: *Relative expression of HIF-1α for patient 29 on SLM.*

Patients 25, 26, 29, and 32 showed similar trends, with increased HIF-1α expression during the trial, while patient 28 exhibited a mixed response, notably with a decrease at visit 4. Patient 29 had high HIF-1α expression across most visits, which significantly increased the averages. Since this was the only patient on SLM included in the data and showed significantly different values, it was decided that the data analysis should be separated into all expression levels and expression levels excluding patient 29. Because all MSC patients were included, the data for this compound could be collated and analysed against the average. Table 14 shows that the average expression for patients on the MSC compound is around 0.321 with similar ranges, strongly indicating a compound-specific effect. This justifies grouping these patients into a separate cohort for comparative analysis against patients on other compounds.

Table 14: *Densitometry calculations for HIF-1α on each patient at each timepoint adjusted to baseline and relative to GAPDH expression. Average for each time points are also calculated for all 5 patients, all patients excluding patient 29 and for all three MSC patients.*

	MSC	***SS***	***MSC***	***SLM***	***MSC***	***All***	***MSC+SS***	***MSC Only***
	Patient 25	*Patient 26*	*Patient 28*	*Patient 29*	*Patient 32*	*Average*	*Average*	*Average*
Visit 1	1.000	1.000	1.000	1.000	1.000	1.000	1.000	1.000
Visit 2	0.038	0.006	0.219	0.425	0.104	0.158	0.092	0.120
Visit 3	-	0.003	0.281	0.959	0.091	0.333	0.125	0.186
Visit 4	0.269	0.041	0.038	1.563	0.070	0.396	0.105	0.126
Visit 5	-	0.069	0.453	1.761	0.355	0.659	0.292	0.404
Visit 6	-	0.096	0.247	25.554	0.581	6.620	0.308	0.414
Visit 7	1.299	0.454	0.655	9.703	0.068	2.436	0.619	0.674
Average	0.535	0.111	0.316	6.661	0.211	1.767	0.257	0.321

3.3.5 Caspase-8

Caspase-8 (CASP8) was detected using a Caspase-8 p18 rabbit polyclonal antibody from Santa Cruz Biotechnology, Inc. (SC-7890). The antibody had a recommended dilution of 1:100-1:2000, but after optimisation on membranes with the purchased antibody, it was determined that 1:200 yielded the optimal signal. The CASP8 active subunit p18 (18 kDa) was present in most patients, though some samples also presented with the pro-CASPASE-8 precursor at 55 kDa and the p10 precursor subunit at 10 kDa (Figure 19). While these bands may be present, the p18 subunit was the one chosen for this study so all future Caspase-8 results will be in reference to thus subunit.

***Figure 19**: Western blot of patient 25 showing the two lower CASP 8 Subunits 18 kDa and 10 kDa.*

Data for Caspase-8 was only achieved in patient 25 and 29 due to problems with loading, high background on membranes and band detection at the 55 kDa precursor or p10 subunit. Caspase-8 was seen to have some bands in all patients aside from patient 31 but were inconsistent between membranes of the same sample. The data obtained from the two patients showed the desired 18 kDa bands at all time-points. The band intensity was normalised to visit 1 (baseline) and adjusted for the calculated GAPDH intensity from the same membrane/samples.

Patient 25 showing consistent Caspase-8 expression throughout the trial at around 0.5, with an average of 0.48 and a range of 0.43 – 0.52 (Figure 20, A). Visit 2 expression level is pre-treatment, showing the patients intra-personal variation which is very similar to the rest of the trial. This suggests that the MSC treatment may have caused a small increase in the apoptosis pathway and was tolerated at both doses. Patient 29 showed an increase in expression at visit 2 (0.17), which was pre-treatment, and it remained relatively stable until visit 6, when it then increased to 6.24 (Figure 20, B). Visit 6 corresponds to two weeks of treatment at the higher 6400 µg dose. The increased expression may indicate reduced tolerability of prolonged exposure to the SLM compound at this dose.

A.

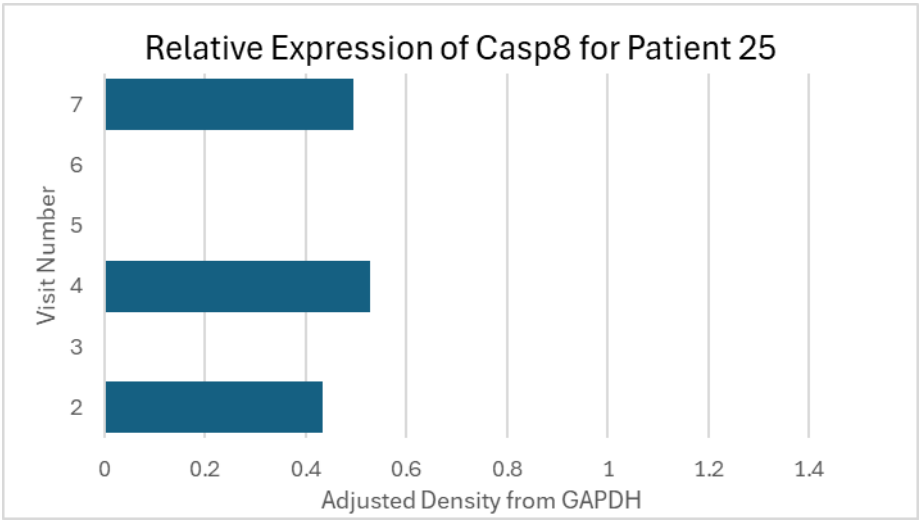

B.

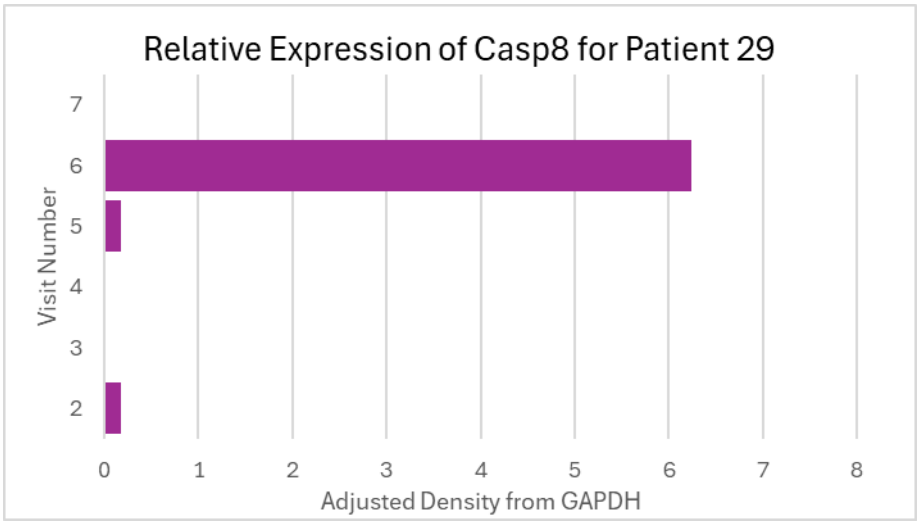

Figure 20: *Relative expression of Casp8 compared to GAPDH for patient 25 in A and patient 29 in B.*

3.4 DNA Damage

3.4.1 Primer Validation

Primer validation (Table 8) was performed using standard PCR and then the resulting amplicons were run on a 3% or a 1% 1X TAE agarose gel for short and long primers, respectively. Candidate primers were made to a 1:10 concentration in UP-H_2O, and 5 DNA samples used were from HeLa, THP1, MDA-MB431, MDA-MB456 and A549 at concentrations of 25 ng/mL. The requirements of the primer selection were: 1) there was one for mtDNA and one for nDNA, 2) clear bands at the expected size were identifiable on an agarose gel, 3) there was a primer pair with a large range and a small range within the same place on the DNA, 4) minimal or no primer dimers. From these requirements, Tumour protein p53 (*TP53*) gene earlier referred to as KO5 and KO6 was chosen for nDNA primer as previously published ((Yi-An Ko, 2016) The mtDNA primer pair was SE1 and chosen from the thesis based on the earlier Phase 1 trial (Evans, 2019). Both of the primer pairs were run through Geneious with current human DNA sequences and then new primers ordered so as to ensure quality and quantity throughout the trial.

3.4.2 LORD-Q PCR DNA Damage

Patient DNA samples of 9 patients over 7 visits/timepoints (3.1) were taken and analysed along with negative and positive control by LORD-Q PCR on the Rotor-Gene from Corbett using 0.2 mL Axygen clear-tubes as detailed in Chapter 2.4.5. Patient samples underwent two separate LORD-Q PCR runs per primer resulting in four technical replicates per primer. The negative control was UP-H_2O and three positive controls consisting of undamaged THP1/A549, 20 J/m² UV-C damaged THP1/A549, and 100 J/m² UV-C damaged THP1/A549. Where A549 cell line was used as the positive control for the mtDNA primers and THP1 cell line was used as the positive control for nDNA. Runs were between 3 and

5 hours long, with a total of four primer sets (mtDNA long and short, nDNA long and short). Since patients 25, 27, and 30 did not complete all 7 days, it was found that these three patients could be completed in duplicate in a single run (30 samples + 4 controls). In order of ease and potential cases of contamination, the other patients were paired as follows: patient 26 and patient 31, patient 28 and patient 32, and patient 29 and patient 33. It was hypothesised that if contamination occurred in a run, redoing the same two patients was more efficient than attempting to pair the patients with others that still needed to be done for the primer. Samples were run one primer at a time, starting with mitochondrial long, followed by mitochondrial short, nucleotide short, and then nucleotide long.

SYTO82™ fluorescence was monitored throughout each run using the Rotor-Gene PCR running software, collecting all relevant data such as fluorescence, amplification efficiency, C_t values, and melting temperatures. After the run was finished, the melt curve on the software (Figure 21) was used to assess whether contamination occurred; if no contamination was present, then raw data was transferred to an Excel spreadsheet for calculations (Appendix 4), where the raw data was refined. Raw C_t values were collected and averaged across four technical replicates per data point (two independent PCR reactions, each run-in duplicate). These average C_t figures, along with the average reaction efficiency and the bp of each primer, were put into the DNA damage equation (Equation 2) to obtain mtDNA damage and nDNA damage for each data point, as well as the efficiency values obtained from the Rotor-Gene software program.

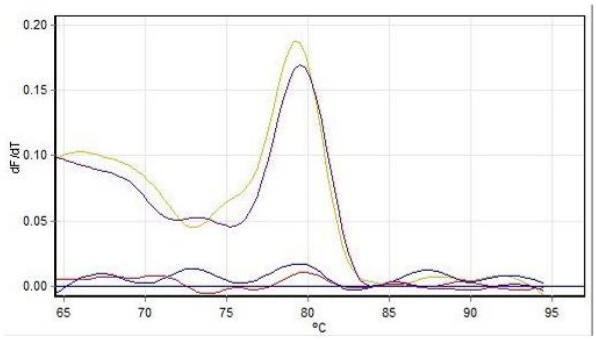

No.	Color	Name	Genotype	Peak 1	Peak 2	Peak 3	Peak 4
1		NEGATIVE		67.7	70.7	79.8	85.2
2		A549 UNDAM		66.0	79.3	87.8	91.7
3		A549 20UV DAM		67.3	73.0	79.5	87.3
4		A549 100UV DAM		73.2	79.5	85.5	92.7

Bin Name	Temperature	Sample No.	Sample Name	Peak

Figure 21: *LORD-Q PCR melt curve showing fluorescence detection in A549 control (olive) for mtDNA SE1 primer pair from table 8. Negative control (red) shows no peak above the 0.05 threshold indicating no contamination.*

The results seen in Figure 21, used the long mtDNA primer pair and high fluorescence peak indicates more “undamaged” DNA. The highest peak is from undamaged DNA; the second highest peak is from 20 mJ UV-C damage and the 100 mJ UV-C damage is extremely low. This indicates that the DNA damage is dose-dependent on damage stimuli as researched in (Lehle et al., 2014). For both A549 cells used with mtDNA and THP1 cells used with p53 nDNA primers, there were similar initial fluorescence detection. Data then showed that C_t values increased with UV-C dose for both control sets showing the same trend. Additionally, both control sets had similar lesion rates for long primers with A549 showing an average C_t value 19 – 21 and THP1 showing an average of 23 – 24. Notably, both control sets showed a small decrease from 20 J/UV-C to 100 J/UV-C which was not seen in Lehle et al., 2014. This may be due to the very high damage from the UV-C potentially killing cells at that level, cell tolerability as different cell lines were used than to that mentioned, the age of the UV machine and user error.

First-stage data analysis involved examining the melt curves immediately after run completion, specifically to ensure the samples functioned properly and that the negative control did not exhibit a peak, indicating contamination and necessitating a re-run. The second stage analysis involved downloading all the data from the software and onto an Excel spreadsheet, where the amplification efficiencies and C_t values could be scrutinised for each sample. Researcher discretion was used as to whether the run was considered for the end-stage analysis or whether the samples had to be redone. For this experiment, only those runs with contamination as identified in the negative control were redone, with all other data sets making it to the final data analysis.

Final data was then analysed by averaging the C_t values obtained for each sample. For instance, patient 25 V4 had four runs, so those four values were averaged. Once all the values were obtained, Equation 2 was used to determine the overall mitochondrial or nucleotide DNA damage for each patient, which was then presented in Figure 22. Figure 22 shows the average DNA damage between compounds with error bars, highlighting the patient-specific changes within each compound. Samples from visit 3 and visit 4 corresponded to the 1600 µg selenium dosage, while samples from visit 5 and visit 6 related to the 6400 µg daily dosage. Visit 7 was a sample taken 28 days after the final dose of 6400 µg (or 28 days after the patient ceased the trial).

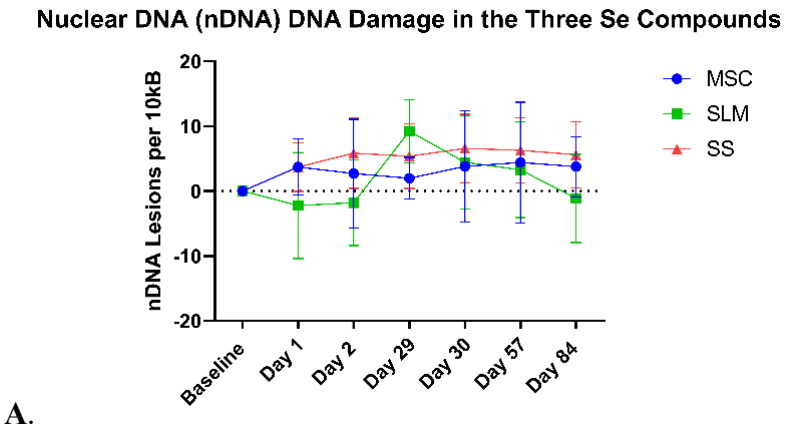

A.

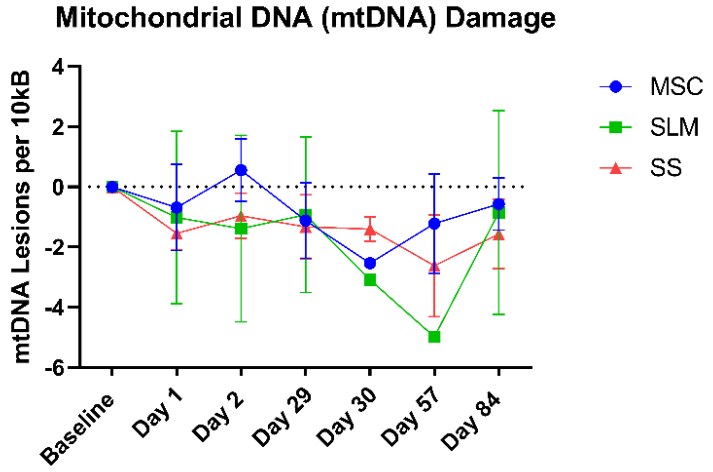

B.

Figure 22*: LORD-Q Assay. Means and ± SEM of the relative lesions of (A) the nDNA damage and (B) the mtDNA damage for each compound at each timepoint in the 84 day phase 1b clinical trial.*

The data shown is the calculated DNA lesions per 10kb (y-axis). DNA damage is plotted against "Days on Trial" for all seven major timepoints (x-axis), including baseline, dose escalation (1600 to 6400 µg at day 29), and post-trial assessment (day 84). This data shows the decrease/increase of DNA damage between sample timepoints with the assumption that a value of 0 would show that no DNA damage is calculated. The presence of negative values is theorised to be due to the controls used for the assay, as DNA damage is calculated against the undamaged control. The undamaged controls were cancer cell lines grown in the lab, which would be subject to mutation and a certain level of uncontrollable DNA damage

To accurately interpret the data and compare both between and within patient samples, DNA damage was normalised to baseline as shown in Tables 15 and 16 below. Relative DNA damage could then be attributed to the dosage and compound in the trial, with the change between visits 1 and 2 indicating the interpersonal variation in DNA damage among patients. While these results still showed negative values, they were less varied than before normalisation. Additionally, any negative values compared to baseline imply increased DNA repair or fewer lesions than before the trial, suggesting potential protective effects of the compounds. The post-trial sample (visit 7) then indicates any longer-acting effects of the dosage, including potential genotoxicity.

Table 15: *Calculated relative mtDNA damage lesions per 10kb for each patient at each visit. ND= no data.*

mtDNA Damage per 10kb							
Patients	V1	V2	V3	V4	V5	V6	V7
25	0.000	-1.802	ND	-2.399	ND	ND	-2.098
26	0.000	-2.573	-1.715	-3.254	-1.761	-6.002	-3.861
27	0.000	4.716	4.816	4.239	ND	ND	5.915
28	0.000	2.161	1.595	1.389	ND	0.433	0.899
29	0.000	-3.886	-4.492	-3.513	-3.084	-4.988	-4.243
30	0.000	-0.677	ND	0.446	-0.604	-0.692	-0.186
31	-0.001	-1.397	-0.212	-1.175	-1.856	-1.175	-0.660
32	-0.001	-2.415	-0.484	-2.360	-2.540	-2.870	-0.510
33	0.000	-3.886	-4.492	-3.513	-3.084	-4.988	-0.303

Table 16*:Calculated relative nDNA damage lesions per 10kb for each patient at each visit. ND= no data.*

nDNA Damage per 10kb							
Patients	V1	V2	V3	V4	V5	V6	V7
25	0.001	2.523	ND	0.045	ND	ND	1.086
26	0.000	11.121	11.279	15.266	16.826	16.113	15.469
27	0.001	-16.823	-8.684	15.576	ND	ND	-13.232
28	0.000	-3.144	-5.647	-2.386	-4.77	-4.898	-2.571
29	0.000	-1.303	-8.176	-0.302	-2.738	-4.070	-0.379
30	0.000	1.342	ND	1.367	3.690	3.086	3.027
31	0.000	-1.290	0.389	-0.486	-0.799	-0.323	-1.648
32	0.001	11.740	11.095	8.270	12.381	13.720	12.817
33	0.001	11.511	11.463	12.468	11.645	10.649	-0.323

3.4.3 SLM

Three patients, 27, 29 and 33 were on SLM. Mitochondrial and nuclear DNA damage were plotted on a graph (Figure 22) to show the calculated lesions per 10kb. The difference in the two graphs shows that the mtDNA damage remained relatively stable throughout the trial and at different dosages. Stability continued even after the end of the treatment, as indicated by day 84, which shows minimal changes in calculated lesions between the pre and post-trial. Nuclear DNA showed an extreme range in the rate of lesions, including a massive increase in patient 27 and patient 29 for visit 4 (day 29) and patient 33 on visit 2 (day 1). However, it also showed a significant decrease in lesion rates in patient 27 for visit 1 (day 1) and visit 7 (day 84) and patient 29 for visit 3 (day 2). All patients showed a relative increase in DNA lesions on visit 4 (day 29). After the initial increase from the initial dosage, patient 33 remained relatively stable throughout, even after the increased dosage, compared to the other patients,

3.4.4 SS

The three patients designated to the SS group were; patient 26, patient 30 and patient 31. Mitochondrial and nuclear DNA damage (Figure 22) remained relatively stable for all patients. mtDNA damage decreased for all three patients at the start of the trial (visit 2, day 1), where Se intake increased by 1600 µg. After dose escalation (visit 5, day 30), both patient 30 and patient 31 showed a decrease in mtDNA while patient 26 showed a slight increase. Patients 30 and 31 returned to similar levels as baseline at visit 7 (day 84), which was 28 days after the last dose. Patient 26 showed a massive decrease in mtDNA damage detected in visit 7 compared to that of baseline (pre-trial).

For the nDNA damage, patients 30 and 31 remained stable throughout the trial. There was a slight increase for patients 26 and 30 when the dosage increased to 6400 µg, while patient 31 had a slight decrease, but again, it remained relatively stable. The post-trial

damage (visit 7, day 84) showed patient 31 at approximately baseline levels of damage, patient 30 at slightly higher levels than baseline. Patient 30 showed a dramatic increase in nDNA damage between Visit 1 and visit 2 indicating a large range of background fluctuation. A similar change is seen between visit 3 and 4 which were both from the lower dosage, which could be the result of fluctuation or genotoxicity from accumulation. Considering the large changes in patient 30, the overall nDNA lesion rates seen throughout the trial were in line with the rest of the patients. The post-dosage bloods showed that nDNA damage is more like that seen at the first dose (visit 2, day 1) than that of the baseline indicating that the damage did return to pre-treatment levels.

3.4.5 MSC

The three patients designated with MSC were patient 25, patient 28 and patient 32. Mitochondrial DNA lesions reduced from baseline throughout the trial and did not increase at visit 4 (day 29) with the increased dosage indicating some protective qualities against mtDNA damage. While all three patients follow that general trend, there is a significant drop in DNA lesions detected for patient 28 at the start of the higher (6400 µg) dosage.

Nuclear DNA showed different trends for all three patients. Patient 25 remains relatively stable throughout the study, though it should be noted that three data points are missing (visit 3, visit 5 and visit 6). Patient 28 remained relatively stable with a slight increase at visit 4 (day 29) from visit 3, but both values were still lower than baseline damage. Day 84 also saw a slight increase after visit 6 (day 57) in nDNA damage, but the value itself is reflective of that of baseline, which indicates a lack of Se accumulation in the body. Patient 32 starts with a rapid increase in nDNA from baseline showing a large personal variance as no dose is administered within baseline and day 1 samples. The lesions then slowly decrease before another significant increase at visit 5 (day 30), which corresponds

with the increased dosage. Overall, with both mtDNA and nDNA, the lesions calculated followed a relatively stable curve.

3.4.6 MSC vs SS vs SLM

The calculated average mtDNA damage of all three compounds remains relatively stable throughout the patients. Figure 22 highlights how the compounds show a slight decrease in calculated lesions at visit 7 (day 84) compared to baseline. There is also a slight decrease in all three compounds at visit 5 (day 30), which is the day after the dosage. Sodium selenite shows an increase at visit 3, which is the day after the start of the trial, compared to the others. This could indicate an adjustment period for SS, causing a genotoxic effect.

The calculated nDNA damage for MSC and SS slightly increases throughout the trial, whereas SLM shows a very slight increase. This change can be seen in the difference in visit 1/ baseline to visit 7, which is 28 days post-trial. MSC and SS show an immediate increase in damage with the first dosage at visit 2 (day 1), whereas SLM shows a decrease on average. All compounds show an increase in lesion occurrence at the higher dosage as seen before visit 4 (day 29), compared to after. SLM has a high calculated lesion occurrence at visit 4 (day 29) compared to the other two; however, this is skewed by the extremely high damage for patient 27 seen at this visit compared to the other two patients.

The LORD-Q PCR was used to detect the mtDNA and nDNA lesions for patients throughout seven major timepoints of the trial. The aim of this was to determine the genotoxicity of each compound and each dosage. Additionally, it was used to assess the ongoing effects of high-dose Se in the body to aid in understanding genotoxic accumulation and potential mutagenicity. Figure 22 indicates that for mtDNA, the high dose Se can be flushed from the body, allowing systems to return to a similar state to that of baseline. The figure also highlights that on average, the addition of the high Se protected against DNA damage, particularly at the higher dosage. When comparing the error bars, SLM is identified

as having the highest inconsistencies between patients, which could be due to the compound itself not being as tolerable as the others.

Figure 22 also shows an increase in nDNA damage for all three compounds during the trial, which remains steady for SS and MSC even 28 days after the last dosage, whereas SLM shows damage returning to pre-trial levels. Like mtDNA, SLM has a higher spread of values for each of the visits, which again indicates that the effects of this compound are more patient-specific and have a higher chance of intolerability. There was a slight overall increase shown at the higher 6400 µg dosage compared to the 1600 µg for all compounds, but it did not show a significant overall change.

It is recommended that, moving forward with this trial, the SS and MSC compounds be used as they appear to be the least volatile of the three compounds, show protective capabilities against mtDNA damage, and while they did raise the nDNA damage level, it remained consistent throughout the trial. Regarding the dosage, the 1600 µg dose does not affect DNA damage as significantly as the 6400 µg dose in comparison to the patient's baseline. However, the overall aim of this trial was to determine the protective capabilities of the higher dosage. Given the minimal increase in nDNA lesions and considerable decrease in mtDNA lesions, indicating protective capabilities at the higher dosage, the 6400µg dose is recommended for the next phase of the trial. Overall, the data strongly indicate that the SS and MSC compound does not accumulate in this system, causing genotoxic effects for both mtDNA and nDNA.

4 Discussion

4.1 Western Blotting

4.1.1 Western Blot Transference

The EBlot™ system from GenScript was successfully used to transfer proteins from the samples loaded on the 10% SDS-PAGE gels onto a PVDF membrane. This was shown using Ponceau staining and the evidence of 36 kDa band when incubated with a GAPDH primary antibody as the housekeeping reference loading control. All house-made solutions and protocols were shown to work in the early validation steps of the western blotting as seen in earlier images and continued to work throughout the protocol to varying degrees as further discussed in Chapter 4.1.3.

4.1.2 Housekeeping Gene

GAPDH was initially tested on a membrane with protein extracted from four mammalian cancer cell lines: HeLa, MDA-MB-231, HEK293, and THP1. The cell lysates underwent a Bradford assay to estimate their protein concentrations and were then standardised to a 15 µg/µL concentration. These proteins were subjected to SDS-PAGE electrophoresis and transferred onto a PVDF membrane. GAPDH was the first antibody used and was employed at a 1:20,000 dilution and was detected in most of the cell lines, except for HeLa which was unexpected and BSA protein (a negative control as expected), as shown in Figure 14. The GAPDH antibody purchased indicated that HeLa cells produced protein bands under similar conditions in their scientific validation data, suggesting that the HeLa cell line used was either degraded or had too weak a concentration for this protein detection technique.

GAPDH was used as a housekeeping reference gene for each patient, helping to visualise and ensure consistent equal protein loading. Although equal loading was not always achieved, calculations accounted for variability, and the decision was made to proceed with calculating antibody changes. An exception was when GAPDH was not visible in the sample, even at high exposure levels; in such cases, a new patient membrane was prepared. Throughout the experiment, every patient sample displayed a positive band at the expected size for GAPDH (36 kDa) after incubation. This confirmed that protein of an acceptable quality was present in each sample at least once during testing. Based on these findings, patient PVDF membranes then underwent primary antibody incubation with the antibodies of interest (Table 7). If a band appeared at the expected size following a positive GAPDH band, it provided sufficient evidence that the protein was present in the sample and, therefore, the pathway was activated.

4.1.3 Antibodies of Interest

The antibodies of interest were originally run at dilutions 1:500 (HIF-1α, EGLN3) or 1:1000 (CASP8 & EGLN1), which was the midpoint for their respective manufacturers' recommended ranges. Faint bands were observed for HIF-1α at 110 kDa and CASP8 at 18 kDa, whereas we were unsuccessful in obtaining any bands for EGLN3 and EGLN1. The antibodies used were purchased for the previous cohort (pre-2018) due to budget constraints, which could have factored into the lack of response by EGLN3 and EGLN1 or the diminished response from HIF-1α and CASP8. Optimised dilutions of 1:200 were then used for the remaining experiments as this showed the clearest band with minimal background interference.

To determine if the EGLN1 and EGLN3 antibodies were functioning correctly, a new membrane was created due to the extensive stripping that occurred. All antibodies of interest were re-run with concentrations of 1:100 with EGLN1 first, followed by EGLN3, CASP8,

HIF-1α and GAPDH. This allowed the researchers to determine which antibodies were working and which needed to be reordered, along with the remaining quantities. It was decided to reorder EGLN3 and EGLN1, as there was no signal received from any of the cell lines, which was determined as likely due to their age. A new aliquot of HIF-1α antibody was also ordered due to the dwindling stock.

It was decided that EGLN3 and EGLN1 antibodies would be validated using patient membranes upon the new antibody arrival. The research team was unable to locate a suitable antibody replacement for EGLN3 as the one ordered from (CT# a121914) failed internal quality control and was discontinued with no alternative. However, due to the pathway in which they both act and their relatively close functions and proximity within that cycle, it was determined that any data for EGLN1 would reflect that of EGLN3, so it was removed from this arm of the project.

4.1.3.1 EGLN1 and EGLN3

EGLN1 antibody from Sapphire Bioscience (CT# A12194-50) was purchased and arrived on the 15/11/2024. It was run on several active membranes over the next fortnight without any bands showing, even with a positive GAPDH band. To further solidify whether this antibody was working, it was run on a membrane containing the THP1 cell line, which also did not produce a band. EGLN1 was then moved to the last antibody run on a patient membrane due to the low chance of it working as it was unable to be validated on THP1 or earlier cell lines.

The absence of EGLN1 bands could be due to the antibodies themselves. The original antibodies used were purchased pre-2018, which, due to their age, could have had affected performance, especially as it was stored at 4°C rather than frozen. Conversely, a 2013 paper in Histopathology investigated the use of 12- to 26-year-old expired antibodies stored under the same conditions and found that some antibodies may have a half-life of 10 years or more

rather than the 1 – 2-year expiry date given (Argentieri et al., 2013). This idea received further validation in 2023 when Henwood examined the nominally expired antibodies in a hospital laboratory. The data suggested that most antibodies had at least 6 years of usability, with a few far exceeding this (Henwood, 2023). This corresponds with the other primary antibodies (CASP8 & HIF-1α) in this study that were still usable and purchased at the same time as the EGLN1 and EGLN3. Though these expiry dates, both manufacturer-given and experimental, are all antibody-specific, they require more thorough investigation for those in this study.

The absence of EGLN1 and EGLN3 bands could also be due to the lack of EGLN1/3 in the system of the patients. EGLN3 (CT# A12194) has been validated in the pancreatic cancer cell line BxPC-3 as well as mouse brain, mouse kidney, and rat stomach by the manufacturer (Datasheet for A12194: Anti-PHD3 Antibody). The original EGLN3 antibody (CT# ab30782) was validated in the cervical cancer cell line HeLa as well as embryonic fibroblast mouse tissue by Abcam, the manufacturer (Antibodies, Proteins, Kits and Reagents for Life Science | Abcam). However, review of the online Protein Atlas database (https://www.proteinatlas.org/ENSG00000129521-EGLN3/cell+line) indicates that no RNA transcripts are expressed in the THP1 cell line, thus, no protein would be translated. Therefore, out data is in agreement with no band being observed on the western blot.

Further experimentation by preparing new HeLa protein lysates i.e. culturing in vitro HeLa cells and extracting the proteins with fresh lysis buffer could be used to determine if these antibodies are working or perhaps, ordering a Alexa Fluor® 647 Anti-PHD3 antibody so you avoid having to use two antibodies for detection using HRP system and instead detect positive fluorescent signal. An enzyme-linked immunosorbent assay (ELISA) from My BioSource could also be used as an alternative method to western blotting. The advantage of ELISA is increased replicates and it is more sensitive, detecting proteins at much lower concentrations than that of western blot. The protein concentrations could also be increased

from 15 µg/µL to a 25 µg/µL concentration to investigated into the possibility that the proteins are there at minimal concentrations that detection is difficult. However, increasing to this concentration limits further changes as for most Bis-Tris electrophoresis gels this would hit the maximum loading/concentration capacity.

4.1.3.2 HIF-1α

The primary antibody HIF-1α was used at the higher end of the manufacturer's recommended concentration range (1:200). This could indicate that the presence of HIF-1α in the samples is low, which aligns with the results observed in patients 25, 26, 28, and 32. This finding would be consistent if the cells were under normoxic conditions, which correlates with the relatively low DNA damage seen in these patients. Alternatively, the amount of protein used in the western blots may not have been sufficient to accurately reflect the cell conditions. Future assays might benefit from increasing the loaded protein from 15 µg to 25 µg, which could enhance visual expression enough for analysis.

Patient 29 showed a much higher increase in HIF-1α compared to the other four patients who underwent densitometry. As this was the only SLM patient with western blot data, it indicates increased hypoxic environment for cells. Along with the DNA damage for SLM patients (4.2) that this compound has a large cytotoxic and genotoxic effect on the human body. While antibody results from the other patients in this study will make the data more robust, these combined results strongly indicate that SLM is not an effective compound for the aims of this trial.

The data from other patients in the trial was not shown due to inconsistent results and unsuccessful GAPDH indications. GAPDH was used as the reference gene in this experiment because it is generally stable in most cells. Due to the sensitive nature of the hypoxia antibody, it was incubated on the membrane before GAPDH to ensure the best quality results. Additionally, HRP, used as the secondary antibody, produces byproducts that cause self-

inactivation, which can irreversibly damage the membrane, proteins, and antibodies; this may be a reason why further probing with GAPDH did not produce results. The stripping protocol for western blots involves relatively harsh chemicals known to remove varying amounts of protein and antibodies (Taylor et al., 2022). Future studies should focus on stripping and reprobing protocols that maintain cost-effectiveness and efficiency, and if these continue to fail, consideration should be given to using single use membranes.

All five patients showed an increased HIF-1α at the 1600 µg dose (visit 3 and 4) and another increase at the larger 6400 µg dose (visit 5 and 6) indicating a dose-dependent relationship of Se on the hypoxic pathway. Patient 28 and 32 showed a decreased expression at visit 4 compared to visit 3, with patient 28's expression decreasing again at visit 6 compared to visit 5, indicating that tolerability increases over time for some patients.

HIF-1α expression increased at each visit across all five patients during the trial when compared to visit 1/baseline. However, when examining the averages for MSC+SS and MSC only, it appears that expression decreases slightly at visit 4. Additionally, there is only a small rise at visit 6, suggesting that MSC and SS patients were able to tolerate the dose after longer periods. This is further emphasised by the higher average expression at visit 3 and visit 5 compared to the previous visit, as these were taken four hours after the new dose. Patient 29 also shows a significant increase at visit 3 and 5 indicating that the initial dose response is not tolerated well and potentially increases hypoxia in cells. The differences between visit 2 and visit 7 (post-trial) showed increased expression in all patients, indicating a potential longer-term elevation of HIF-1α and possible hypoxic induction of cells in the three MSC patients, and potentially SS patients as well, though only patient 26 has data here.

4.1.3.3 Caspase-8

Caspase 8 was run at a 1:200 concentration as it was found to show the highest quality bands, though the recommended range was 1:100 and 1:2000. All nine patients had evidence of some CASP8 activity through their visits but due to western blot limitations discussed in 4.1.4, data was only obtained for patient 25 (MSC) and patient 29 (SLM). Patient 25 showed a low expression throughout the trial and was like that seen of visit 2 which was also pre-treatment. Patient 29 showed similarly low expression until visit 6 indicating increased toxicity from prolonged exposure at the higher dosage. This is further indicated in this patient when combined with the higher levels of HIF-1α and the DNA damage seen in SLM patients.

4.1.4 Western Blot Troubleshooting

Most of the elements of the western blot technique stayed consistent throughout the project; however, the new set of SDS-PAGE gels obtained from Invitrogen in 2025 caused some problems. The first membranes from these new gels were made, but some factors of the process were already apparent and were visually confirmed at the end of the first western blot run with GAPDH. Firstly, the SDS-PAGE gels required a different electrophoresis system from the one previously used. This system did not have water running through, and as a result, at the recommended voltage and time, the buffer and the gel were extremely hot to touch at the end. At this point, visually, the blue dye in the gel pooled at the bottom across all 15 lanes, even though only eight were used. During the transference step, the gel was dried, and the membrane was partially dried out in the middle, which was evident in the initial HIF-1α run. It was discovered that the new gels were best suited to wet and semi-wet transfers rather than the semi-dry transfer method of the EBlot™ system being used.

To combat these changes, the SDS-PAGE gels were run at a lower voltage of 120 V for 1.5 hours and used pre-chilled buffer to aid in system cooling. The transfer time in the EBlot™ was reduced to 6 minutes, and care was taken to ensure timing was as efficient as

possible to reduce the drying of the membrane and gel. Both combined saw an immediate increase in the usability of the new membranes, with the electrophoresis running smoothly and limited smearing and/or smiling, no noticeable drying of the gels or membranes and no smells indicating burning.

Even with these changes, the challenges of band detection on the membranes remained. GAPDH became increasingly difficult to obtain bands for all patients, even for those who had previously loaded before the new gels. Most of the membranes from the new gels were missing entire lanes seemingly at random. Avenues for optimisations include making fresh protein aliquots for the patients to limit freeze/thaw cycles and protein degradation. Changing to a semi-wet or wet western blot transfer system, which, due to time constraints and availability of the researchers and those trained in this, could not be explored in this project. While the semi-dry transfer worked to some extent, the system and its components are all expired. The anode and cathode pads and transfer buffer provided in the EBlot™ transfer kit had expired (Exp: Nov 2018), which could lead to problems or inaccurate data. Furthermore, the transfer system used is retired, and the company no longer makes the consumables for this product. For these reasons, it is noted that changing to a transfer system that is currently in use and using non-expired reagents would aid in future studies and/or western blot analysis.

Even loading was not achieved in most patients, even when the same protocol was used with the same quantities. This variance in protein loading was observed throughout the trial, despite numerous attempts to rectify it, which ultimately failed. Multiple Bradford assays were done for each patient; new standards were made, and a new aliquot of Bradford Dye was used to achieve more accurate results. Concerns were raised about the number of freeze-thaw cycles each western blot PBMC aliquot underwent, prompting the removal of a second aliquot from -80°C storage. This aliquot was then mixed with freshly prepared protease inhibitor and lysis buffer before being aliquoted into smaller 200 µL quantities.

However, after Bradford assays and western blots with these fresh samples, the difference obtained was minimal. Enforcing more rigorous experimental techniques included mixing the sample tube each time a quantity was removed, not just once after thawing. Pipetting up and down multiple times, ensuring the quantity is taken from the middle of the suspension every time, helps decrease variance between sample loadings. However, this was not reflected on the membrane.

Even loading of protein samples on PVDF membranes for each patient was not achieved, as shown by the different band intensities in Figure 15. This is likely due to several factors, including technician error, in complete cell lysis, high protein viscosity and sample/protein degradation. Technician error consists of pipetting errors, inexperience with the protocol and an unpolished protocol. Considering this, the extended freezing period of 3 months to 18 months potentially degraded the sample. Lastly, protein degradation was thought to occur due to the number of freeze/thaw cycles for each patient visit; however, results only mildly improved with newly processed samples.

The oldest samples, which consisted of baseline/visit 1 sample and the day 1/visit 2 sample, and all of patient 25, were the hardest consistent bands to achieve with GAPDH. Patient 25 completed their treatment in 2023, and all other patients finished their first two visits by 26th March 2024. Analysis began on 1st July 2024. Even loading for these was difficult to achieve, and bands or even loading were observed even after increasing the concentration predicted from the Bradford assays. It is possible that sample degradation occurred from extended freeze conditions. Although these samples were included in most patients, it is notable that the bands for GAPDH appear less intense to the eye compared to the others.

4.2 LORD-Q PCR

Due to the extreme sensitivity of the LORD-Q PCR technique with respect to DNA amplification, extreme measures had to be taken when making the samples to avoid DNA contamination in the negative control. This involved used autoclaved UP-H_2O into freshly autoclaved sterile 0.6 mL and 2.0 mL centrifuge tubes, yielding 10 µL and 700 µL aliquots, respectively, in a non-template-specific Biosafety cabinet. These tubes were then discarded after a single use. The primers, PCR mix excluding DNA were also handled in a template-free Bio-Safety Cabinet to avoid DNA contamination. All sample tubes were sterilised under UV light for two hours in the packet provided from the manufacturer (unopened) before being put in containers that held ~40 tubes each, ensuring that only one of these tubes was opened at a time. The tubes were removed from the containers, with their lids shut, and placed in a PCR rack within the template-free Bio-Safety Cabinet.

Additionally, a single PCR tube was prepared with 1 µL of the 10 µL UP-H_2O aliquots, serving as the negative control for the run. The samples themselves were made up to 10 µL from the concentrate, which allowed for 10 single reactions before a new aliquot was to be made. The aliquots were made from the purified DNA sample and a single 700 µL UP- H_2O aliquot that was dedicated to this endeavour. All reagents were then confined to a dedicated ice box on a dedicated RT-qPCR bench with its racks, pipettes, sterilised filtered PCR tips and gloves. The bench is a dedicated station for extremely sensitive RT-qPCR and is wiped after each use using 1% Trigene followed by 70% Ethanol.

4.2.1 LORD-Q Analysis

Patients were run on the Corbett Rotor-Gene using the Rotor-Gene software, which detected fluorescence, amplification efficiency, C_t values, melting temperature and a standard curve, computationally. The fluorescence detection quantitatively defined the amount of amplification of each sample, while the amplification efficiency showed how efficient the PCR conditions were at amplification. The Ct values indicate where fluorescent detection starts, while the melting temperature indicates the temperature at which half of the sample has amplified into double-stranded DNA.

Assessing between the two Se dosages, for both mtDNA and nDNA, there is evidence of DNA damage in some patients, while for some, it shows little to no change between dosages. The results indicate that mtDNA is more protected from DNA damage from high Se dosages than nDNA, as indicated by the abundance of negative values in Table 15 and 16. This aligns with the current literature, which suggests that Se may protect against DNA damage, particularly in mtDNA. Visit 7 shows the DNA damage 28 days after the last dosage, indicating how long it takes for a patient's DNA damage to return to baseline and whether the Se has accumulated in the body, which could have lasting effects. Again, there is a considerable variation in numbers for all the patients across the two tables for visit 7, but most patients returned to a state of less than one lesion per 10 kb, indicating minimal long-term damage. Patients were then separated into their specific compounds to determine which compound was the safest and most effective.

4.3 Future Directions

This thesis and the related body of work contribute to the existing knowledge on the effects of therapeutic dose selenium, including the pharmacodynamics and pharmacokinetics of the SLM, SS, and MSC. The Phase 1 trial in this study focused on apoptosis and hypoxic pathways, as well as mitochondrial DNA and nuclear DNA, specifically the *TP53* gene. The original aims (1.7) and conditions (2.1) for the trial were set in advance and could not be altered. One aim was to develop and validate methods for measuring genomic and mitochondrial DNA damage to assess potential genotoxicity. This was achieved using LORD-Q techniques (2.4), which effectively quantified DNA damage levels and enabled comparisons between patients, within the same patient, and across different compounds and doses.

Based on this research, future trials should investigate MSC and SS compounds, depending on cost and availability at the higher 6400 µg dosage. To further assess the efficacy and dose optimisation and genotoxicity (Aim 1), a Phase II double blind two-armed trial would allow further understanding of the pharmacodynamics and pharmacokinetics. A total of 60 patients on chemotherapy, split with randomisation determining Se compound treatment dose of 3200 µg, 6400 µg or placebo of 20 patients each (Vreman et al., 2020). This would ensure that there is a relevant control group and the change to 3200 µg lower dosage compared to the 1600 µg in this study, would narrow the optimum-dose level window. A review on Se trials of the past 48 years showed only 5.4% of trials with greater than 800 µg daily dose Se, which mostly focused on critically ill patients. By using the same patient parameters of the Phase I trial with these doses, it will further the current body of knowledge on Se in cancer patients (Wu et al., 2025). Additionally, an increase in timepoints for different doses due to chemo/radiotherapy regimes, allotting the trial to fit with a round and an additional post-treatment sample would be beneficial as mapped out in Figure 23 below. The results of a study using this design (or similar) would further ensure that the aim

of assessing genotoxicity for these compounds would be more robust and potentially increase the exposure and use of this method in other clinical trials. Furthermore, one of the overarching aims of the trial is to assess it's potential use as an adjuvant to chemotherapy and radiotherapy; by looking at it's effect against a placebo and narrowing the dose window it allows future research to more thoroughly assess its' suitability.

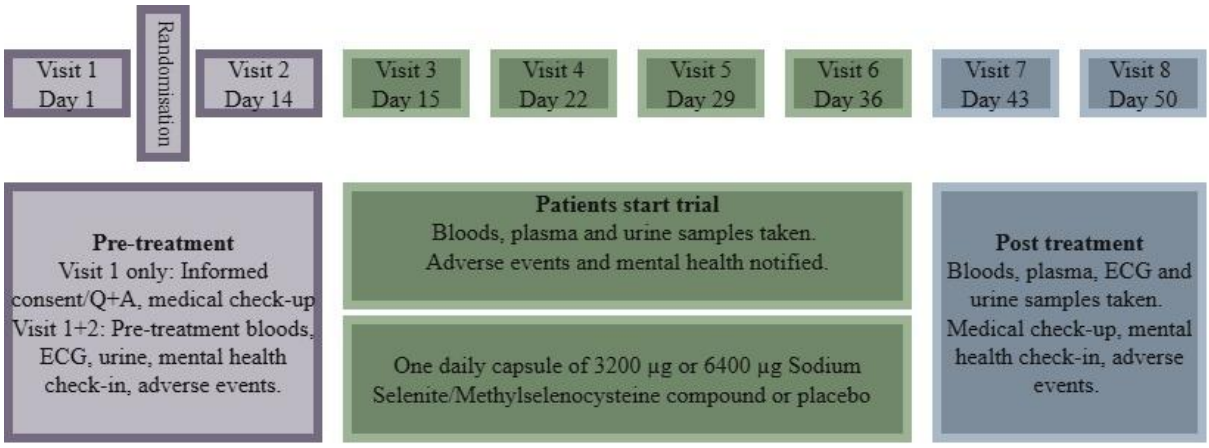

Figure 23: *Potential timepoints and mapped trial plan for future studies involving cancer patients and a dosage of Se compound to determine efficacy of adjuvant therapy use. Trial over 50 days (7 weeks) with 8 visits, including 2 pre and 2 post.*

The apoptosis pathway was investigated using CASPASE-8, which is an initiator protease that forms the complex protein formation that provides caspase activation/inhibition. However, there are two known executioner caspases (Caspase-3 and Caspase-7) that are cleaved by the initiators and then directly elicit apoptosis by cleaving substrates downstream from the initiators downstream from initiators (Sanmartín et al., 2012). Studies using apoptotic inducer D-501036 (novel selenophene derivative) and thioredoxin reductase inhibitors found increased Caspase-3 activity and induced apoptosis (Shiah et al., 2007; Xing et al., 2008). Using Caspase-3 antibodies for western blots in future studies would aid in validating whether Se dose/compounds only activated the apoptosis pathway or if apoptosis was induced.

The second aim for the trial was to evaluate the pharmacodynamics of the compounds and dose by specifically investigating the hypoxic and apoptotic pathways. By adding in the additional Caspase-3 antibody it would not only further validate the effects on the apoptotic pathway but potentially show insight into where in the pathway these therapeutic doses have the most effect. This could impact further research by solidifying its' use as a pharmacodynamic biomarker for similar studies, aid in understanding upstream and downstream effects of high-dose Se compounds by comparing the results to Caspase-8.

As mentioned in Chapter 4.1.3.1, the use of ELISA in conjunction with western blotting would provide valuable insight into these pathways. The advantage of increased patient replicates for a single plate would provide a more efficient way in determining semi-quantitative analysis of pathway regulations. The higher sensitivity of ELISA would indicate earlier whether an antibody was present in the sample and would add certainty in regards to antibody validation (Paulie et al., 2023). This would also aid in the aims set out as it would provide further validation on the potential absense of EGLN1/3 in patient samples and ensure the presence of HIF-1α and Caspase-8 in all visits which can then be further validated by western blots.

5 Conclusion

The Se Phase 1(b) trial conducted between 2023 and 2025 investigated the safety and efficacy of three Se compounds as a therapeutic dosage to aid in protection against DNA damage and genotoxicity. Further research conducted should use the MSC and/or SS compounds at 6400 µg dosage as these combinations have been shown as the least volatile with the highest level of protective properties. The SLM compound should not be used in further research as it is shown in this research and other studies including the NPC trial that there are little to no benefits. The 1600 µg starting dosage for patients was effective and showed some degree of protection but it was not as significant as the 6400 µg. Coupled with the lack of adverse events with the higher dosage it is hypothesised that this combination will produce the most promising results in further trials.

The western blot analysis also showed that the hypoxic (HIF-1α) and apoptosis (CASPASE 8) pathways were active in all patient samples during the trial, to varying degrees. However, only patients 25, 26, 28, 29 and 32 for HIF-1α and patients 25 and 29 for Caspase-8 achieved the semi-quantitative analysis stage. This found that the hypoxic pathway showed low expression in most patients throughout the trial, sans patient 29, showing minimal cytotoxic effects. Relative increases of expression were seen both over time and after the increased dose for patients; however in most patients this effect was still not significant. Additionally, most patients were able to reduce any increase to that reflective of pre-treatment levels after the trial. patient 29 was the only patient on SLM with data and showed high expression of both the hypoxic and apoptotic pathways, indicating this compound had high toxicity at the dosage used. patient 25 showed minimal to no change in apoptosis throughout the trial. Overall, these pathways indicate tolerability of cells to MSC and SS treatment.

References

Abdulah, R., Noerjasin, H., Septiani, L., Mutakin, Defi, I. R., Suradji, E. W., Puspitasari, I. M., Barliana, M. I., Yamazaki, C., Nakazawa, M., & Koyama, H. (2013). Reduced serum selenium concentration in miscarriage incidence of indonesian subjects. *Biological Trace Element Research*, *154*(1), 1–6. https://doi.org/10.1007/s12011-013-9701-0

Algotar, A. M., Stratton, M. S., Ahmann, F. R., Ranger-Moore, J., Nagle, R. B., Thompson, P. A., Slate, E., Hsu, C. H., Dalkin, B. L., Sindhwani, P., Holmes, M. A., Tuckey, J. A., Graham, D. L., Parnes, H. L., Clark, L. C., & Stratton, S. P. (2013). Phase 3 clinical trial investigating the effect of selenium supplementation in men at high-risk for prostate cancer. *Prostate*, *73*(3), 328–335. https://doi.org/10.1002/pros.22573

Appelhoffl, R. J., Tian, Y. M., Raval, R. R., Turley, H., Harris, A. L., Pugh, C. W., Ratcliffe, P. J., & Gleadle, J. M. (2004). Differential function of the prolyl hydroxylases PHD1, PHD2, and PHD3 in the regulation of hypoxia-inducible factor. *Journal of Biological Chemistry*, *279*(37), 38458–38465. https://doi.org/10.1074/jbc.M406026200

Arayici, M. E., Basbinar, Y., & Ellidokuz, H. (2023). High and Low Selenium Exposure and Cancer Risk: A Meta-Meta-Analysis. *Biology and Life Sciences Forum 2023, Vol. 29, Page 6*, *29*(1), 6. https://doi.org/10.3390/IECN2023-15798

Argentieri, M. C., Pilla, D., Vanzati, A., Lonardi, S., Facchetti, F., Doglioni, C., Parravicini, C., & Cattoretti, G. (2013). Antibodies are forever: a study using 12–26-year-old expired antibodies. *Histopathology*, *63*(6), 869–876. https://doi.org/10.1111/his.12225

Brigelius-Flohé, R. (2018). Selenium in human health and disease: An overview. In *Molecular and Integrative Toxicology* (pp. 3–26). Springer Science+Business Media B.V. https://doi.org/10.1007/978-3-319-95390-8_1

Brigelius-Flohé, R., & Arnér, E. S. J. (2018). Selenium and selenoproteins in (redox) signaling, diseases, and animal models - 200 year anniversary issue. *Free Radical Biology and Medicine*, *127*, 1–2. https://doi.org/https://doi.org/10.1016/j.freeradbiomed.2018.09.026

Cai, X., Wang, C., Yu, W., Fan, W., Wang, S., Shen, N., Wu, P., Li, X., & Wang, F. (2016). Selenium Exposure and Cancer Risk: an Updated Meta-analysis and Meta-regression. *Scientific Reports*, *6*, 19213. https://doi.org/10.1038/SREP19213

Clark, L. C., Combs Jr, G. F., Turnbull, B. W., Slate, E. H., Chalker, D. K., Chow, J., Davis, L. S., Glover, R. A., Graham, G. F., Gross, E. G., Krongrad, A., Lesher Jr, J. L., Park, H. K., Sanders Jr, B. B., Smith, C. L., & Taylor, J. R. (1996). Effects of Selenium Supplementation for Cancer Prevention in Patients With Carcinoma of the Skin: A Randomized Controlled Trial. *JAMA*, *276*(24), 1957–1963. https://doi.org/10.1001/jama.1996.03540240035027

Dietary Reference Intakes for Vitamin C, Vitamin E, Selenium, and Carotenoids. (2000). National Academies Press. https://doi.org/10.17226/9810

Dobrovolny, P. L., & Bess, D. (2011). Optimized PCR-based detection of mycoplasma. *Journal of Visualized Experiments*, *52*. https://doi.org/10.3791/3057

Duffield-Lillico, A. J., Dalkin, B. L., Reid, M. E., Turnbull, B. W., Slate, E. H., Jacobs, E. T., Marshall, J. R., & Clark, L. C. (2003). Selenium supplementation, baseline plasma selenium status and incidence of prostate cancer: An analysis of the complete treatment period of the Nutritional Prevention of Cancer Trial. *BJU International*, *91*(7), 608–612. https://doi.org/10.1046/j.1464-410X.2003.04167.x

Duffield-Lillico, A. J., Reid, M. E., Turnbull, B. W., Combs Jr., G. F., Slate, E. H., Fischbach, L. A., Marshall, J. R., Clark, L. C., & Group, for the N. P. of C. S. (2002). Baseline Characteristics and the Effect of Selenium Supplementation on Cancer Incidence in a Randomized Clinical Trial: A Summary Report of the Nutritional

Prevention of Cancer Trial1. *Cancer Epidemiology, Biomarkers & Prevention*, *11*(7), 630–639.

essential-trace-elements-in-human-health-a-physician-s-view_124_fr_0. (n.d.).

Evans, S. O. (2019). *Comparative Safety, Pharmacokinetic and Pharmacodynamic Evaluation of Three Oral Selenium Compounds in Cancer Patients*.

Evans, S. O., Jacobson, G. M., Goodman, H. J. B., Bird, S., & Jameson, M. B. (2019). Comparative Safety and Pharmacokinetic Evaluation of Three Oral Selenium Compounds in Cancer Patients. *Biological Trace Element Research*, *189*(2), 395–404. https://doi.org/10.1007/S12011-018-1501-0

Evans, S. O., Jacobson, G. M., Goodman, H. J. B., Bird, S., & Jameson, M. B. (2020). Comparison of three oral selenium compounds in cancer patients: Evaluation of differential pharmacodynamic effects in normal and malignant cells. *Journal of Trace Elements in Medicine and Biology*, *58*. https://doi.org/10.1016/J.JTEMB.2019.126446

Evans, S. O., Jameson, M. B., Cursons, R. T. M., Peters, L. M., Bird, S., & Jacobson, G. M. (2016). Development of a qPCR method to measure mitochondrial and genomic DNA damage with application to chemotherapy-induced DNA damage and cryopreserved cells. *Biology*, *5*(4). https://doi.org/10.3390/biology5040039

Fernandes, A. P., & Gandin, V. (2015). Selenium compounds as therapeutic agents in cancer. *Biochimica et Biophysica Acta (BBA) - General Subjects*, *1850*(8), 1642–1660. https://doi.org/10.1016/J.BBAGEN.2014.10.008

Fujita, N., Markova, D., Anderson, D. G., Chiba, K., Toyama, Y., Shapiro, I. M., & Risbud, M. V. (2012). Expression of Prolyl Hydroxylases (PHDs) is selectively controlled by HIF-1 and HIF-2 proteins in nucleus pulposus cells of the intervertebral disc: Distinct roles of PHD2 and PHD3 proteins in controlling HIF-1α activity in hypoxia. *Journal of Biological Chemistry*, *287*(20), 16975–16986. https://doi.org/10.1074/jbc.M111.334466

Gladyshev, V. N., Arnér, E. S., Berry, M. J., Brigelius-Flohé, R., Bruford, E. A., Burk, R. F., Carlson, B. A., Castellano, S., Chavatte, L., Conrad, M., Copeland, P. R., Diamond, A. M., Driscoll, D. M., Ferreiro, A., Flohé, L., Green, F. R., Guigó, R., Handy, D. E., Hatfield, D. L., … Zhang, Y. (2016). Selenoprotein Gene Nomenclature. *Journal of Biological Chemistry*, *291*(46), 24036–24040. https://doi.org/10.1074/jbc.M116.756155

Hadrup, N., & Ravn-Haren, G. (2020). Acute human toxicity and mortality after selenium ingestion: A review. *Journal of Trace Elements in Medicine and Biology*, *58*, 126435. https://doi.org/10.1016/J.JTEMB.2019.126435

Hanahan, D. (2022). Hallmarks of Cancer: New Dimensions. In *Cancer Discovery* (Vol. 12, Issue 1, pp. 31–46). American Association for Cancer Research Inc. https://doi.org/10.1158/2159-8290.CD-21-1059

Hanahan, D., & Weinberg, R. A. (2000). The Hallmarks of Cancer. *Cell*, *100*(1), 57–70. https://doi.org/10.1016/S0092-8674(00)81683-9

Hanahan, D., & Weinberg, R. A. (2011). Hallmarks of Cancer: The Next Generation. *Cell*, *144*(5), 646–674. https://doi.org/10.1016/j.cell.2011.02.013

Harris, H. R., Bergkvist, L., & Wolk, A. (2012). Selenium intake and breast cancer mortality in a cohort of Swedish women. *Breast Cancer Research and Treatment*, *134*(3), 1269–1277. https://doi.org/10.1007/S10549-012-2139-9,

Henwood, A. F. (2023). Validation of nominally expired antibodies for immunohistochemistry. *Biotechnic & Histochemistry*, *98*(2), 86–93. https://doi.org/10.1080/10520295.2022.2114609

Herbette, S., Roeckel-Drevet, P., & Drevet, J. R. (2007). Seleno-independent glutathione peroxidases: More than simple antioxidant scavengers. In *FEBS Journal* (Vol. 274, Issue 9, pp. 2163–2180). https://doi.org/10.1111/j.1742-4658.2007.05774.x

Hernandez, A., Goel, K., Hussain, S., & Gassman, N. R. (2026). DNA Damage, Repair, and Advanced DNA Damage Detection Technologies. *Reference Module in Biomedical Sciences*, 164–200. https://doi.org/10.1016/B978-0-323-95488-4.00179-0

Hirota, K. (2021). Special Issue: Hypoxia-Inducible Factors: Regulation and Therapeutic Potential. *Biomedicines*, *9*(12), 1768. https://doi.org/10.3390/BIOMEDICINES9121768

Hu, W., Zhao, C., Hu, H., & Yin, S. (2021). Food Sources of Selenium and Its Relationship with Chronic Diseases. *Nutrients 2021, Vol. 13, Page 1739*, *13*(5), 1739. https://doi.org/10.3390/NU13051739

Hughes, D. J., Fedirko, V., Jenab, M., Schomburg, L., Méplan, C., Freisling, H., Bueno-de-Mesquita, H. B., Hybsier, S., Becker, N., Czuban, M., Tjønneland, A., Outzen, M., Boutron-Ruault, M., Racine, A., Bastide, N., Kühn, T., Kaaks, R., Trichopoulos, D., Trichopoulou, A., … Hesketh, J. E. (2015). Selenium status is associated with colorectal cancer risk in the European prospective investigation of cancer and nutrition cohort. *International Journal of Cancer*, *136*(5), 1149–1161. https://doi.org/10.1002/ijc.29071

Hughes, D. J., Fedirko, V., Jenab, M., Schomburg, L., Méplan, C., Freisling, H., Bueno-De-Mesquita, H. B., Hybsier, S., Becker, N. P., Czuban, M., Tjønneland, A., Outzen, M., Boutron-Ruault, M. C., Racine, A., Bastide, N., Kühn, T., Kaaks, R., Trichopoulos, D., Trichopoulou, A., … Hesketh, J. E. (2015). Selenium status is associated with colorectal cancer risk in the European prospective investigation of cancer and nutrition cohort. *International Journal of Cancer*, *136*(5), 1149–1161. https://doi.org/10.1002/IJC.29071,

Hussein, R. A., Ahmed, M., Kuldyushev, N., Schönherr, R., & Heinemann, S. H. (2022). Selenomethionine incorporation in proteins of individual mammalian cells determined with a genetically encoded fluorescent sensor. *Free Radical Biology and Medicine*, *192*, 191–199. https://doi.org/10.1016/J.FREERADBIOMED.2022.09.019

Iida, M., Crossman, B. E., Kostecki, K. L., Glitchev, C. E., Kranjac, C. A., Crow, M. T., Adams, J. M., Liu, P., Ong, I., Yang, D. T., Kang, I., Salgia, R., & Wheeler, D. L.

(2024). MerTK Drives Proliferation and Metastatic Potential in Triple-Negative Breast Cancer. *International Journal of Molecular Sciences*, *25*(10). https://doi.org/10.3390/ijms25105109

Jenkins, D. J. A., Kitts, D., Giovannucci, E. L., Sahye-Pudaruth, S., Paquette, M., Blanco Mejia, S., Patel, D., Kavanagh, M., Tsirakis, T., Kendall, C. W. C., Pichika, S. C., & Sievenpiper, J. L. (2020). Selenium, antioxidants, cardiovascular disease, and all-cause mortality: a systematic review and meta-analysis of randomized controlled trials. *The American Journal of Clinical Nutrition*, *112*(6), 1642–1652. https://doi.org/10.1093/AJCN/NQAA245

Klein, E. A., Thompson, I. M., Lippman, S. M., Goodman, P. J., Albanes, D., Taylor, P. R., & Coltman, C. (2000). SELECT: The selenium and Vitamin E Cancer Prevention Trial: Rationale and design. *Prostate Cancer and Prostatic Diseases*, *3*(3), 145–151. https://doi.org/10.1038/SJ.PCAN.4500412;KWRD=BIOMEDICINE

Köhrle, J., & Frädrich, C. (2022). Deiodinases control local cellular and systemic thyroid hormone availability. *Free Radical Biology and Medicine*, *193*, 59–79. https://doi.org/https://doi.org/10.1016/j.freeradbiomed.2022.09.024

Krannich, F., Mücke, R., Büntzel, J., Schomburg, L., Micke, O., Hübner, J., & Dörfler, J. (2024). A systematic review of Selenium as a complementary treatment in cancer patients. *Complementary Therapies in Medicine*, *86*, 103095. https://doi.org/10.1016/j.ctim.2024.103095

Kryukov, G. V., Castellano, S., Novoselov, S. V., Lobanov, A. V., Zehtab, O., Guigó, R., & Gladyshev, V. N. (2003). Characterization of mammalian selenoproteomes. *Science (New York, N.Y.)*, *300*(5624), 1439–1443. https://doi.org/10.1126/SCIENCE.1083516

Lee, E.-H., Myung, S.-K., Jeon, Y.-J., Kim, Y., Chang, Y. J., Ju, W., Seo, H. G., & Huh, B. Y. (2011). Effects of Selenium Supplements on Cancer Prevention: Meta-analysis of

Randomized Controlled Trials. *Nutrition and Cancer*, *63*(8), 1185–1195. https://doi.org/10.1080/01635581.2011.607544

Lee, F. S., & Percy, M. J. (2011). The HIF pathway and erythrocytosis. *Annual Review of Pathology: Mechanisms of Disease*, *6*, 165–192. https://doi.org/10.1146/annurev-pathol-011110-130321

Lee, T.-J., Nettleford, S. K., McGlynn, A., Carlson, B. A., Kirimanjeswara, G. S., & Prabhu, K. S. (2022). The role of selenoproteins in neutrophils during inflammation. *Archives of Biochemistry and Biophysics*, *732*, 109452. https://doi.org/https://doi.org/10.1016/j.abb.2022.109452

Lehle, S., Hildebrand, D. G., Merz, B., Malak, P. N., Becker, M. S., Schmezer, P., Essmann, F., Schulze-Osthoff, K., & Rothfuss, O. (2014). LORD-Q: A long-run real-time PCR-based DNA-damage quantification method for nuclear and mitochondrial genome analysis. *Nucleic Acids Research*, *42*(6). https://doi.org/10.1093/nar/gkt1349

Lei, C., Niu, X., Ma, X., & Wei, J. (2011). Is selenium deficiency really the cause of Keshan disease? *Environmental Geochemistry and Health*, *33*(2), 183–188. https://doi.org/10.1007/s10653-010-9331-9

Letavayová, L., Vlčková, V., & Brozmanová, J. (2006). Selenium: From cancer prevention to DNA damage. *Toxicology*, *227*(1–2), 1–14. https://doi.org/10.1016/J.TOX.2006.07.017

Lippman, S. M., Klein, E. A., Goodman, P. J., Lucia, M. S., Thompson, I. M., Ford, L. G., Parnes, H. L., Minasian, L. M., Gaziano, J. M., Hartline, J. A., Parsons, J. K., Bearden, J. D., Crawford, E. D., Goodman, G. E., Claudio, J., Winquist, E., Cook, E. D., Karp, D. D., Walther, P., … Coltman, C. A. (2009). Effect of Selenium and Vitamin E on Risk of Prostate Cancer and Other Cancers: The Selenium and Vitamin E Cancer Prevention Trial (SELECT). *JAMA*, *301*(1), 39–51. https://doi.org/10.1001/JAMA.2008.864

Liu, X., Tang, J., Wang, Z., Zhu, C., Deng, H., Sun, X., Yu, G., Rong, F., Chen, X., Liao, Q., Jia, S., Liu, W., Zha, H., Fan, S., Cai, X., Gui, J. F., & Xiao, W. (2024). Oxygen

enhances antiviral innate immunity through maintenance of EGLN1-catalyzed proline hydroxylation of IRF3. *Nature Communications*, *15*(1). https://doi.org/10.1038/s41467-024-47814-3

Luo, Z., Tian, M., Yang, G., Tan, Q., Chen, Y., Li, G., Zhang, Q., Li, Y., Wan, P., & Wu, J. (2022). Hypoxia signaling in human health and diseases: implications and prospects for therapeutics. In *Signal Transduction and Targeted Therapy* (Vol. 7, Issue 1). Springer Nature. https://doi.org/10.1038/s41392-022-01080-1

Majmundar, A. J., Wong, W. J., & Simon, M. C. (2010). Hypoxia-Inducible Factors and the Response to Hypoxic Stress. *Molecular Cell*, *40*(2), 294–309. https://doi.org/10.1016/J.MOLCEL.2010.09.022

Marshall, J. R., Burk, R. F., Ondracek, R. P., Hill, K. E., Perloff, M., Davis, W., Pili, R., George, S., & Bergan, R. (2017). Selenomethionine and methyl selenocysteine: multiple-dose pharmacokinetics in selenium-replete men. *Oncotarget*, *8*(16), 26312. https://doi.org/10.18632/ONCOTARGET.15460

Minich, W. B. (2022). Selenium Metabolism and Biosynthesis of Selenoproteins in the Human Body. *Biochemistry. Biokhimiia*, *87*(Suppl 1), S168. https://doi.org/10.1134/S0006297922140139

Ostapowicz, J., Ostrowska, K., Rawłuszko-Wieczorek, A. A., Wojtera, B., Koczot, S., Golusiński, W., & Suchorska, W. M. (2024). Understanding Hypoxia-Driven Tumorigenesis: The Interplay of HIF1A, DNA Methylation, and Prolyl Hydroxylases in Head and Neck Squamous Cell Carcinoma. *International Journal of Molecular Sciences*, *25*(12), 6495. https://doi.org/10.3390/ijms25126495

Outzen, M., Tjønneland, A., Hughes, D. J., Jenab, M., Frederiksen, K., Schomburg, L., Morris, S., Overvad, K., & Olsen, A. (2021). Toenail selenium, plasma selenoprotein P and risk of advanced prostate cancer: A nested case-control study. *International Journal of Cancer*, *148*(4), 876–883. https://doi.org/10.1002/ijc.33267

Paulie, S., Perlmann, P., & Perlmann, H. (2023). Enzyme Linked Immunosorbent Assay. *Cell Biology: A Laboratory Handbook*, 533–538. https://doi.org/10.1016/B978-012164730-8/50065-4

Pei, J., Pan, X., Wei, G., & Hua, Y. (2023). Research progress of glutathione peroxidase family (GPX) in redoxidation. In *Frontiers in Pharmacology* (Vol. 14). Frontiers Media SA. https://doi.org/10.3389/fphar.2023.1147414

Qazi, I. H., Angel, C., Yang, H., Zoidis, E., Pan, B., Wu, Z., Ming, Z., Zeng, C. J., Meng, Q., Han, H., & Zhou, G. (2019). Role of Selenium and Selenoproteins in Male Reproductive Function: A Review of Past and Present Evidences. *Antioxidants*, *8*(8), 268. https://doi.org/10.3390/ANTIOX8080268

Rayman, M. P. (2004). The use of high-selenium yeast to raise selenium status: how does it measure up? *The British Journal of Nutrition*, *92*(4), 557–573. https://doi.org/10.1079/BJN20041251

Rayman, M. P. (2012). Selenium and human health. *Lancet*, *379*, 1256–1268. https://doi.org/10.1016/S0140

Reid, M. E., Duffield-Lillico, A. J., Slate, E., Natarajan, N., Turnbull, B., Jacobs, E., Combs, G. F., Alberts, D. S., Clark, L. C., & Marshall, J. R. (2008). The nutritional prevention of cancer: 400 Mcg per day selenium treatment. *Nutrition and Cancer*, *60*(2), 155–163. https://doi.org/10.1080/01635580701684856

Reid, M. E., Duffield-Lillico, A. J., Slate, E., Natarajan, N., Turnbull, B., Jacobs, E., Combs Jr., G. F., Alberts, D. S., Clark †, L. C., & Marshall, J. R. (2008). The Nutritional Prevention of Cancer: 400 Mcg Per Day Selenium Treatment. *Nutrition and Cancer*, *60*(2), 155–163. https://doi.org/10.1080/01635580701684856

Reid, M. E., Duffield-Lillico, A. J., Sunga, A., Fakih, M., Alberts, D. S., & Marshall, J. R. (2006). Selenium supplementation and colorectal adenomas: An analysis of the

nutritional prevention of cancer trial. *International Journal of Cancer*, *118*(7), 1777–1781. https://doi.org/10.1002/ijc.21529

Romagné, F., Santesmasses, D., White, L., Sarangi, G. K., Mariotti, M., Hübler, R., Weihmann, A., Parra, G., Gladyshev, V. N., Guigó, R., & Castellano, S. (2014). SelenoDB 2.0: annotation of selenoprotein genes in animals and their genetic diversity in humans. *Nucleic Acids Research*, *42*(D1), D437–D443. https://doi.org/10.1093/nar/gkt1045

Saccoccia, F., & Bellelli, A. (2018). Thioredoxin Reductase. *Encyclopedia of Signaling Molecules*, 5385–5399. https://doi.org/10.1007/978-3-319-67199-4_101928

Sanmartín, C., Plano, D., Sharma, A. K., & Palop, J. A. (2012). Selenium Compounds, Apoptosis and Other Types of Cell Death: An Overview for Cancer Therapy. *International Journal of Molecular Sciences*, *13*(8), 9649. https://doi.org/10.3390/IJMS13089649

Schomburg, L. (2022a). Selenoprotein P – Selenium transport protein, enzyme and biomarker of selenium status. In *Free Radical Biology and Medicine* (Vol. 191, pp. 150–163). Elsevier Inc. https://doi.org/10.1016/j.freeradbiomed.2022.08.022

Schomburg, L. (2022b). Selenoprotein P - Selenium transport protein, enzyme and biomarker of selenium status. *Free Radical Biology & Medicine*, *191*, 150–163. https://doi.org/10.1016/j.freeradbiomed.2022.08.022

Schwarz, K., & Foltz, C. M. (1999). Selenium as an integral part of factor 3 against dietary necrotic liver degeneration. 1951. *Nutrition (Burbank, Los Angeles County, Calif.)*, *15*(3), 255.

Schweizer, U., & Braun, D. (2013). Selenium and Iodothyronine Deiodinases. *Encyclopedia of Metalloproteins*, 1898–1904. https://doi.org/10.1007/978-1-4614-1533-6_475/FIGURES/187

Shamberger, R. J. (1984). Selenium. In *Biochemistry of the Essential Ultratrace Elements* (pp. 201–237). Springer US. https://doi.org/10.1007/978-1-4684-4775-0_9

Shiah, H. S., Lee, W. S., Juang, S. H., Hong, P. C., Lung, C. C., Chang, C. J., Chou, K. M., & Chang, J. Y. (2007). Mitochondria-mediated and p53-associated apoptosis induced in human cancer cells by a novel selenophene derivative, D-501036. *Biochemical Pharmacology*, *73*(5), 610–619. https://doi.org/10.1016/j.bcp.2006.10.019

Sobolev, O. I., Gutyj, B. V., & Soboleva, S. V. (2020). Selenium in natural environment and food chains. A Review. *Ukrainian Journal of Ecology*, *10*(4), 148–158. https://doi.org/10.15421/2020_182

Strocchi, S., Reggiani, F., Gobbi, G., Ciarrocchi, A., & Sancisi, V. (2022). The multifaceted role of EGLN family prolyl hydroxylases in cancer: going beyond HIF regulation. *Oncogene 2022 41:29*, *41*(29), 3665–3679. https://doi.org/10.1038/s41388-022-02378-8

Sudhadevi, T., & Harijith, A. (2024). Thioredoxin: an antioxidant, a therapeutic target and a possible biomarker. *Pediatric Research*, *96*(5), 1117. https://doi.org/10.1038/S41390-024-03370-6

Sung, H., Ferlay, J., Siegel, R. L., Laversanne, M., Soerjomataram, I., Jemal, A., & Bray, F. (2021). Global Cancer Statistics 2020: GLOBOCAN Estimates of Incidence and Mortality Worldwide for 36 Cancers in 185 Countries. *CA: A Cancer Journal for Clinicians*, *71*(3), 209–249. https://doi.org/10.3322/caac.21660

Taniguchi, C. M., Finger, E. C., Krieg, A. J., Wu, C., Diep, A. N., LaGory, E. L., Wei, K., McGinnis, L. M., Yuan, J., Kuo, C. J., & Giaccia, A. J. (2013). Cross-talk between hypoxia and insulin signaling through Phd3 regulates hepatic glucose and lipid metabolism and ameliorates diabetes. *Nature Medicine*, *19*(10), 1325–1330. https://doi.org/10.1038/nm.3294

Taylor, S. C., Rosselli-Murai, L. K., Crobeddu, B., & Plante, I. (2022). A critical path to producing high quality, reproducible data from quantitative western blot experiments. *Scientific Reports*, *12*(1), 17599. https://doi.org/10.1038/S41598-022-22294-X

TECH TIP #57. (n.d.). www.thermoscientific.com/pierce

The discovery of selenium. (2023). In *Jac. Berzelius* (pp. 61–63). University of California Press. https://doi.org/10.2307/jj.8500920.17

To, K. K. W., & Huang, L. E. (2005). Suppression of Hypoxia-inducible Factor 1α (HIF-1α) Transcriptional Activity by the HIF Prolyl Hydroxylase EGLN1. *Journal of Biological Chemistry*, *280*(45), 38102–38107. https://doi.org/10.1074/jbc.M504342200

Tobe, R., Yoo, M. H., Fradejas, N., Carlson, B. A., Calvo, S., Gladyshev, V. N., & Hatfield, D. L. (2012). Thioredoxin reductase 1 deficiency enhances selenite toxicity in cancer cells via a thioredoxin-independent mechanism. *The Biochemical Journal*, *445*(3), 423. https://doi.org/10.1042/BJ20120618

Tummers, B., & Green, D. R. (2017). Caspase-8: regulating life and death. In *Immunological Reviews* (Vol. 277, Issue 1, pp. 76–89). Blackwell Publishing Ltd. https://doi.org/10.1111/imr.12541

Turck, D., Bohn, T., Castenmiller, J., de Henauw, S., Hirsch-Ernst, K. I., Knutsen, H. K., Maciuk, A., Mangelsdorf, I., McArdle, H. J., Peláez, C., Pentieva, K., Siani, A., Thies, F., Tsabouri, S., Vinceti, M., Aggett, P., Crous Bou, M., Cubadda, F., Ciccolallo, L., … Naska, A. (2023). Scientific opinion on the tolerable upper intake level for selenium. *EFSA Journal*, *21*(1), e07704. https://doi.org/10.2903/J.EFSA.2023.7704

Vinceti, M., Filippini, T., Del Giovane, C., Dennert, G., Zwahlen, M., Brinkman, M., Zeegers, M. P. A., Horneber, M., D'Amico, R., & Crespi, C. M. (2018). Selenium for preventing cancer. In *Cochrane Database of Systematic Reviews* (Vol. 2018, Issue 1). John Wiley and Sons Ltd. https://doi.org/10.1002/14651858.CD005195.pub4

Vitamin and mineral requirements in human nutrition. (2005). World Health Organization.

Vreman, R. A., Belitser, S. V., Mota, A. T. M., Hövels, A. M., Goettsch, W. G., Roes, K. C. B., Leufkens, H. G. M., & Mantel-Teeuwisse, A. K. (2020). Efficacy gap between phase II and subsequent phase III studies in oncology. *British Journal of Clinical Pharmacology*, *86*(7), 1306. https://doi.org/10.1111/BCP.14237

Weeks, B. S., Hanna, M. S., & Cooperstein, D. (2012). *Dietary selenium and selenoprotein function*. http://www.medscimonit.com/fulltxt.php?ICID=883258

Winkel, L. H. E., Vriens, B., Jones, G. D., Schneider, L. S., Pilon-Smits, E., & Bañuelos, G. S. (2015). Selenium cycling across soil-plant-atmosphere interfaces: A critical review. In *Nutrients* (Vol. 7, Issue 6, pp. 4199–4239). MDPI AG. https://doi.org/10.3390/nu7064199

Wu, Y., Pei, J., Xu, Y., Yu, F., & Xu, S. (2025). Selenium: 48-year journey of global clinical trials. *Molecular and Cellular Biochemistry*, *480*(6), 3253–3265. https://doi.org/10.1007/S11010-024-05202-X/FIGURES/6

Wu, Y., Wu, M., He, G., Zhang, X., Li, W., Gao, Y., Li, Z., Wang, Z., & Zhang, C. (2012). Glyceraldehyde-3-phosphate dehydrogenase: A universal internal control for Western blots in prokaryotic and eukaryotic cells. *Analytical Biochemistry*, *423*(1), 15–22. https://doi.org/10.1016/J.AB.2012.01.012

Wyllie, A. H. (2010). "where, o death, is thy sting?" A brief review of apoptosis biology. In *Molecular Neurobiology* (Vol. 42, Issue 1, pp. 4–9). Humana Press. https://doi.org/10.1007/s12035-010-8125-5

Xing, F., Li, S., Ge, X., Wang, C., Zeng, H., Li, D., & Dong, L. (2008). The inhibitory effect of a novel organoselenium compound BBSKE on the tongue cancer Tca8113 in vitro and in vivo. *Oral Oncology*, *44*(10), 963–969. https://doi.org/10.1016/J.ORALONCOLOGY.2007.12.001

Yi-An Ko, by. (2016). *Differential effects of organic versus inorganic selenium species on BRCA1-mutated and non-mutated breast cancer cell lines*.

Zhao, Y., Sui, X., & Hong, R. (2010). From procaspase-8 to caspase-8: Revisiting structural functions of caspase-8. In *Journal of Cellular Physiology* (Vol. 225, Issue 2, pp. 316–320). https://doi.org/10.1002/jcp.22276

Zwolak, I., & Zaporowska, H. (2012). Selenium interactions and toxicity: A review. In *Cell Biology and Toxicology* (Vol. 28, Issue 1, pp. 31–46). https://doi.org/10.1007/s10565-011-9203-9